Molecular and functional characterization of biglycan during pathologic cardiac remodelling

Inaugural-Dissertation
zur Erlangung des Doktorgrades
Dr. rer. nat.

der Fakultät für Biologie und Geografie
an der

Universität Duisburg-Essen

vorgelegt von

Ariane Melchior-Becker

aus Lörrach

Supervisor: Prof. Dr. rer. nat. Jens W. Fischer
Review 1: Prof. Dr. rer. nat. Verena Jendrossek
Review 2: Prof. Dr. med. Bodo Levkau

Date of Disputation: 12.04.2011

Abbreviations

Bgn	biglycan
BMP	bone morphogenic protein
BSA	bovine serum albumine
CTGF	connective tissue growth factor
Dcn	decorin
ECM	extracellular matrix
ERK	extracellular signal regulated kinase
et al.	et alii
FAK	focal adhesion kinase
bFGF	basal fibroblast growth factor
g	gramm
GAG	glycosaminoglycan
kDa	kilodalton
kg	kilogram
l	litre
LDL	Low density Lipoprotein
MAPK	mitogen activated protein kinase
MI	myocardial infarction
µl	micro-litres
ml	milli-litre
µM	micro-molar
mM	mili-molar
MMP	matrix metalloproteinase
mRNA	messenger RNA
NFκB	nuclear factor kappa β
PARP	poly [Adenosine-diphosphate]-polymerase
PBS	phosphate buffered saline
PCR	polymerase chain reaction
PDGF	platelet derived growth factor
rpm	rotations per minute
SMAD	mothers against decapentaplegic homolog
SMURF	E2 ubiquitin ligase SMURF2

TAK1	transforming growth factor β associated kinase 1
TEMED	*N*,*N*,*N′*,*N′*-Tetramethylethan-1,2-diamin
TGF-β	transforming growth factor-β
TGF-β RI/II	transforming growth factor-β receptor type I/II
TLR	toll- like receptor
TBS	tris buffered saline
WT	wild-type

Directory

Figure directory

Table directory

1 Introduction

1.1 Cardiac Remodelling

Myocardial infarction (MI) occurs as the result of total occlusion of a pre-atherosclerotic coronary artery and leads to ischemia characterized by necrosis of cardiomyocytes (1). This event is followed by continuous changes within the myocardium. Granulation of tissue and scar formation both come along with molecular, cellular and extracellular adaptations. Cardiac remodelling manifests as changes in left ventricle size, shape, wall thickness and function. The cellular and extracellular response leads to wall thinning, dilation and infarct expansion as well as inflammation and necrotic resorption. Once cardiomyocytes disappear in the infarct zone, fibroblasts accumulate to form a scar by extracellular matrix (ECM) remodelling. Remodelling is influenced by a variety of aspects like inflammatory response, growth factor secretion but also by hemodynamic load and pressure. Adverse or pathological remodelling leads to fibrosis dilation and the loss of heart function (2). ECM remodelling appears during all stages of infarct healing and scar formation. Remodelling is characterized by *de novo* synthesis and degradation of ECM (3). Cardiac remodelling is best investigated in response to injury after MI and has been described also in response to pressure overload, volume overload, cardiomyopathy, infection or cardiotoxic agents as well (2).

1.1.1 Cardiac fibroblasts and their differentiation into myofibroblasts

Cardiac fibroblasts are the main non-myocyte population in the heart. In the adult murine heart approximately 45 % of the non-myocytes are fibroblasts the other non-myocyte hearts are cells of the vasculature, endothelial and smooth muscle cells (4). Cardiac fibroblasts maintain the chemical and biomechanical responsiveness of the heart tissue and preserve

the tissue structure via autocrine and paracrine action of secreted factors, cell-cell interactions or cell-matrix interactions (5). Fibroblasts maintain ECM homeostasis and thereby tissue integrity. In cases of injury, fibroblasts start remodelling to restore cardiac tissue and function. If this restoration of a functional tissue fails, it results in heart failure (6). Fibroblasts differentiate into myofibroblasts in response to injury. These differentiated myofibroblasts are the key cell type that reorganizes ECM to adapt to injury (6). Myofibroblasts act upon paracrine and autocrine secreted signalling molecules. Activated myofibroblasts express both isoforms of the cyclo-oxigenase, the constitutively expressed COX1 and the inducible COX2, and are capable of prostaglandin secretion (7-11).

Table 1-1 Myofibroblast secreted signalling mediators

Cytokines/ Chemokines	*Growth Factors*	*Inflammatory Mediators*	*Neurotransmitters & Paracrine Mediators*	*Receptors*	*Adhesion Proteins*
IL-1β	TGF-β	PLA_2 activating protein	acetylcholine	IL-1	ICAM-1
IL-6	CSF1	PGE_2	histamine	IL-1Rα	VCAM-1
TNF-α	GM-CSF	prostacyclin	serotonin	TNF-αR	NCAM
IL-10	PDGF-AA	HETES	bradykinin	IL-6R	MCP-1
IL-8	PDGF-BB	PAF	endothelin	IL-8R	$\alpha_1\beta_1$-integrin
MCP-1	bFGF	NO	ANF	IL-4R	CD18
GRO-1α	IGF-I & -II	CO	aldosterone	IL-11R	
MIP-1α	NGF	H_2O_2, O^-	ANG II	TGF-α/EGFR	
MIP-2	KGF			TGF-βR I & II	
RANTES	HGF			PDGF-α & β	
ENA-78	SCF			c-kit	
				FGFR I & II	
				IGF-R	
				Thrombin R	

IL, Interleukin; TNF, tumor necrosis factor; TGF, transforming growth factor; MCP, monocyte chemoattractant protein; CSF, colony stimulating factor; GM-CSF, granulocyte/macrophage-colony stimulating factor; PDGF, platelet derived growth factor; FGF, fibroblast growth factor; IGF, insulin-like growth factor; NGF, nerve growth factor; KGF, keratinocyte growth factor; HGF, hepatocyte growth factor, SCF, stem cell factor; MIP, macrophage inflammatory protein, RANTES, regulated upon activation of normal T-cell expressed and secreted; ENA, epithelial neutrophil activating peptide; PLA_2, phospholipase A_2; GRO, melanoma growth-stimulatory activity; HETES, hydroxyeicosatetraenoic acids; PAF, platelet activating factor; ANF, atrial natriuretic factor; PGE, prostaglandin E; EGF, endothelial growth factor; ICAM, intracellular adhesion molecule; VCAM, vascular cell adhesion molecule; NCAM, neural cell adhesion molecule; R,RI and RII receptor types (12)

Table 1-1 presents an overview on signalling molecules and receptors secreted and expressed by myofibroblast. This set of bioactive mediators clearly shows that myofibroblasts are highly active and able to influence a broad variety of other cell types.

Myofibroblast exhibit clearly defined functions. Myofibroblasts become activated and proliferate in response to cytokines, chemokines, growth factors, ECM molecules and tension. Upon activation myofibroblasts secrete an increasing amount of ECM molecules and additional signalling molecules. The disappearance of myofibroblasts after tissue repair and scar formation is regulated by apoptosis (fig. 1-1) (13-17).

TGF-β appears to be one of the most important mediators of myofibroblast differentiation, leading to the activated phenotype. In some tissues myofibroblasts have already been distinguished in activated myofibroblasts and transient myofibroblasts. The transient myofibroblast exhibits a stellate phenotype characterised by decreased proliferation (18,19)

As myofibroblasts are not present in the healthy myocardium, the differentiation of cardiac fibroblasts into myofibroblasts is a crucial event in infarct healing (21). Compared to normal fibroblasts, myofibroblasts are more motile and show higher proliferative and ECM producing activity. Myofibroblast express contractile proteins (22). Tissue contraction by myofibroblasts is a characteristic feature of the healing process. In the skin myofibroblasts undergo apoptosis after a normal status of a healthy re-established tissue is reached (23). After MI myofibroblasts will persist in the infarct area. The persistence of larger numbers of myofibroblasts in the heart could lead to fibrosis and thus to further impairment of cardiac function. Longer persistence of cardiac myofibroblasts might in part be explained by the mechanical load through heart contraction and relaxation. This shows that cardiac myofibroblasts have tissue specific characteristics (16,23).

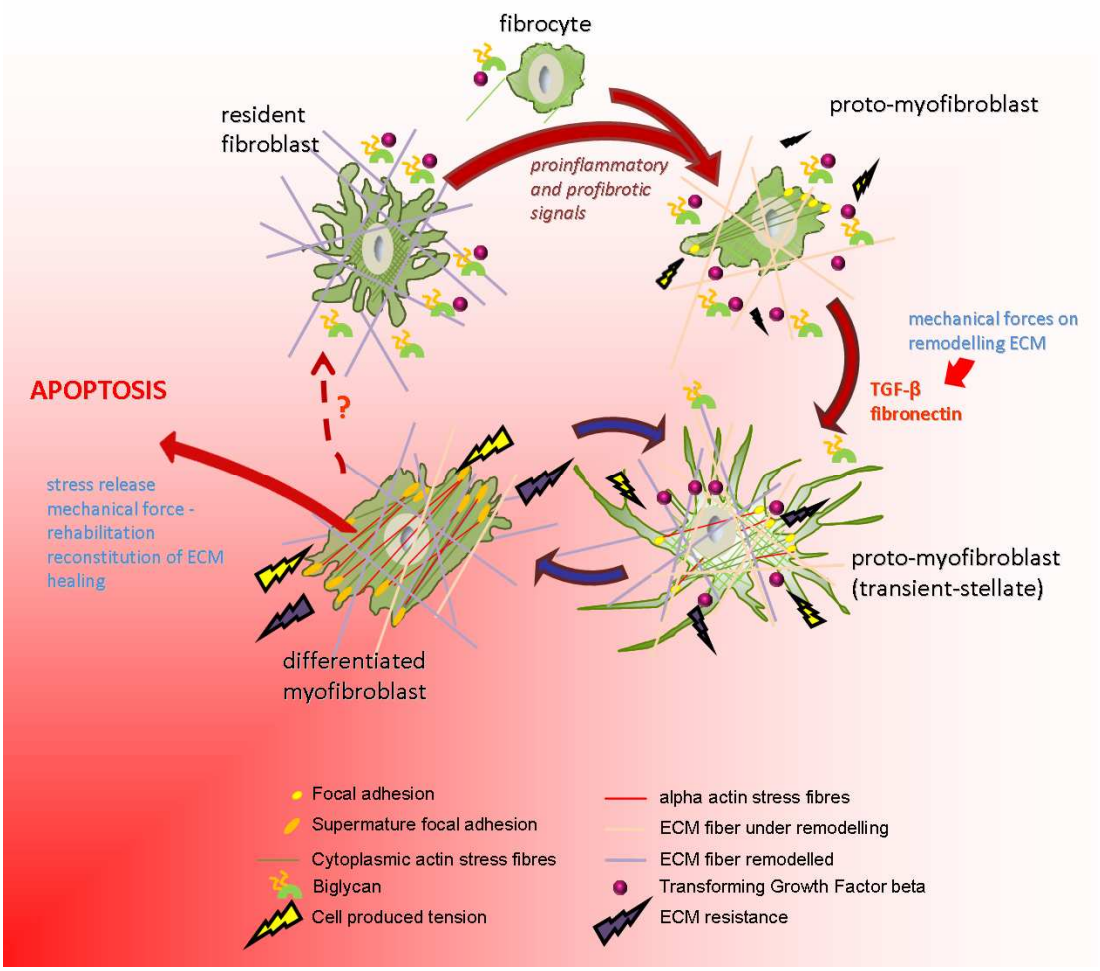

Figure 1-1 Differentiation of fibroblast to myofibroblast

Resident fibroblasts or fibrocytes differentiate into an active state through pro-inflammatory and/or pro-fibrotic stimulation, mechanical forces and ECM remodelling. Activated myofibroblasts secrete TGF-β as well as fibronectin fragment ED-A, both known to induce further differentiation characterized by incorporation of α-smooth muscle actin into stress fibres. Myofibroblasts are characterized by strong contractile abilities that are necessary for ECM remodelling. Once the tissue has achieved a functionally healed state, when stress releases and the tensile forces within the tissue reach a normal level, myofibroblasts undergo apoptosis and disappear. (Scheme adapted and modiefied from Hinz *et al.* (20)).

1.2 Small leucine-rich repeat proteoglycans: biglycan

Biglycan is a class II small leucine-rich repeat proteoglycan (SLRP). The gene encoding for biglycan is located on the x-chromosome and is conserved in mammalian species. The biglycan gene (*bgn*) consists of 8 exons and the exon structure has no obvious relation to the structural domains of the core protein. The gene structure is identical to the homologous SLRP decorin in length and position.

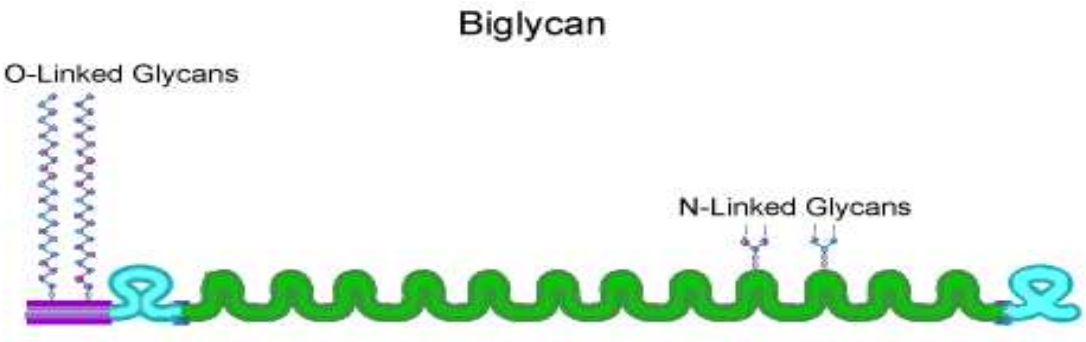

Figure 1-2 Schematic organization of biglycan proteoglycan

The protein core is dominated by the twelve tandem leucine-rich repeats (green) which are flanked by cystein-clusters (turquoise). There are two glycosaminoglycan attachment sites for O-linked glycans at the extreme amino terminus (lilac) and two more attachment sites for N-linked glycans near the c-terminal cystein-cluster.

The complete conservation of intron and exon organization of biglycan and decorin indicates that they may have evolved from a common ancestor gene (24). On protein level biglycan shows a high homology to decorin, fibromodulin and asporin (9,10).The protein contains twelve tandem leucine-rich repeats and two glycosaminoglycan attachment sites at the extreme amino terminus. Biglycan is classified as a dermatan- or chondroitin-sulphate proteoglycan whereas in most connective tissues chondroitin-sulphate is modified to dermatan-sulphate. Biglycan is synthesized as a pro-peptide and cleaved by BMP1 to its mature form (25,26). Biglycan also exists in non-glycanated forms that accumulate with age (13,14). These non-glycanated forms of biglycan are

results of proteolysis within the amino terminal region of the core protein for example after cleavage by MMP13 (27).
The functions of biglycan show a broad diversity and are cell type and tissue specific.

1.2.1 Biglycan interacts with growth factors, surface complexes, receptors and ECM proteins

Despite its structural functions biglycan is involved in growth factor signalling by sequestering growth factors into the ECM (28). Biglycan is a ligand to receptors in innate immunity via binding to toll-like receptors 2 and 4 and promotes pro-inflammatory signalling. Biglycan deficiency in mice causes a survival benefit in LPS- or zymosan-induced sepsis that is explained by lower concentrations of circulating TNF-α in blood and the reduced infiltration of mononuclear cells causing less end-organ damage. Furthermore, it has been shown that upon stimulation with LPS-induced pro-inflammatory factors, macrophages synthesize and secrete biglycan (29).
Recently it was demonstrated that biglycan acts as a ligand to CD44 and that it mediates leukocyte rolling by this interaction (30). CD44 is a cell surface receptor that is postulated to co-interact with TGF-β in myofibroblast differentiation (31). In addition biglycan is associated with the mechano-transducing dystrophin protein complex that is carefully regulated in the heart and plays an important role in maintaining heart function. Biglycan has been shown to regulate the expression of complex components such as dystrobrevins and syntrophins as well as it seems to play a role in localization of the dystrophin associated protein complex (DAPC) in the sarcolemmal lipid rafts (32,33). Biglycan and decorin are key regulators of lateral assembly of collagen fibres. Deficiency of one or more SLRPs leads to abnormal collagen fibre diameters and disturbed lateral association of fibres (34,35). Both proteoglycans, biglycan and decorin, interact with tropoelastin. Especially

biglycan binds the elastin core in elastic fibres (36). It has also been shown that biglycan can protect collagenous fibrils from cleavage by MMPs (37).

1.2.2 TGF-β signalling and regulation

TGF-β signalling has shown complex cross-talk to other signalling cascades, depending on genetic make-up, cell type, ECM environment and cellular origin. The canonical signalling by SMAD proteins involves different levels of regulatory mechanisms. The transcription of each component of the signalling pathway can be regulated. There is a variety of possible modifications like posttranscriptional regulation, posttranslational modifications, various interaction partners, as well as degradation by the proteasome (38).

TGF-β influences other signalling molecules like CTGF or WISP1, as well as transcription factors like β-catenin and NFκB, too. The differences in cellular outcome reveals that not yet all possibilities of cross talk nor all members of the cascades might be known and that the function of each player is still not understood in total.

Nevertheless TGF-β is the most important activator of myofibroblast differentiation. But it has been shown that other receptors like CD44 and signalling pathways like extracellular signal regulated kinase (ERK) are activated by TGF-β during differentiation (31,39).

TGF-β is secreted in a latent form bound to a large multi-protein complex. Mature TGF-β can be sequestered by ECM molecules such as biglycan (28,31,39). TGF-β binds to TGF-β receptor type II (TGF-βRII) at the surface membrane which leads to recruitment of TGF-βRI. TGF-βRII then activates TGF-βRI by phosphorylation. This active complex recruits the receptor regulated r-SMADs (SMAD2 and 3).

At the receptor complex r-SMADs become phosphorylated and thereby active. Phosphorylated r-SMADs can interact with common co-SMAD4 to build an active transcription factor-complex that translocates into the nucleus to induce transcription of TGF-responsive genes. Among these genes are cytoskeletal

components like α-SMA and adhesion molecules as well as various extracellular components like collagens and biglycan. Furthermore, active SMAD2 can interact with E2-ubiquitin ligase SMURF2, an interaction that leads to degradation of various transcription repressors like SnoN and c-SKI and thereby induces the transcription of further genes (40) . One of the responding genes is SMAD7 an inhibitory SMAD, localized in the nucleus. During TGF-β signalling SMAD7 leaves the nucleus, it interacts with SMURF2 in the cytosol and leads to degradation of TGF-βRI. This is a negative feedback loop to regulate TGF-β signalling (41). In addition SMAD7 interacts with the kinases TAK1, MKK3 and p38. Activation of this pathway induces phosphorylation of p53 leading to apoptosis. TAK1 also activates the transcription factor nuclear factor kappa B (NFκB), a pro-proliferative and pro-migratory factor. SMAD7 stabilizes β-catenin in the cytosol where it is localized at cadherin cell-cell adhesion sites. Upon TGF-β stimulation β-catenin accumulates in the cytosol as more adhesion sites are induced. This cytosolic accumulation of β-catenin is not only caused by induction of gene expression, it is also caused by a specific function of SMAD7. SMAD7 prevents ubiquitinylation and degradation of β-catenin. Accumulation of β-catenin can lead to active signalling as β-catenin translocates into the nucleus and induces transcription of genes associated with apoptosis. Furthermore SMAD7 interaction with β-catenin is required for TGF-β induced apoptosis (42-44).

The genes that are activated by TGF-β are predominantly encoding ECM molecules like collagens and the fibronectin ED-A fragment. Additionally TGF-β has been described to induce expression of plasminogen activator inhibitor 1 (PAI-1) (45). Genes corresponding to proliferation are differentially regulated depending on cell type and molecular environment. While various cell types, including endothelial cells and epithelial cells, are inhibited in growth, mesenchymal cells like fibroblasts are stimulated (46). Upon stimulation with TGF-β r-SMADs become phosphorylated, which is the so called canonical pathway. On the one hand the smad2/3/4 complex activates expression of several genes for example, cycline-dependent kinase (CDK) inhibitors p15 and p21.

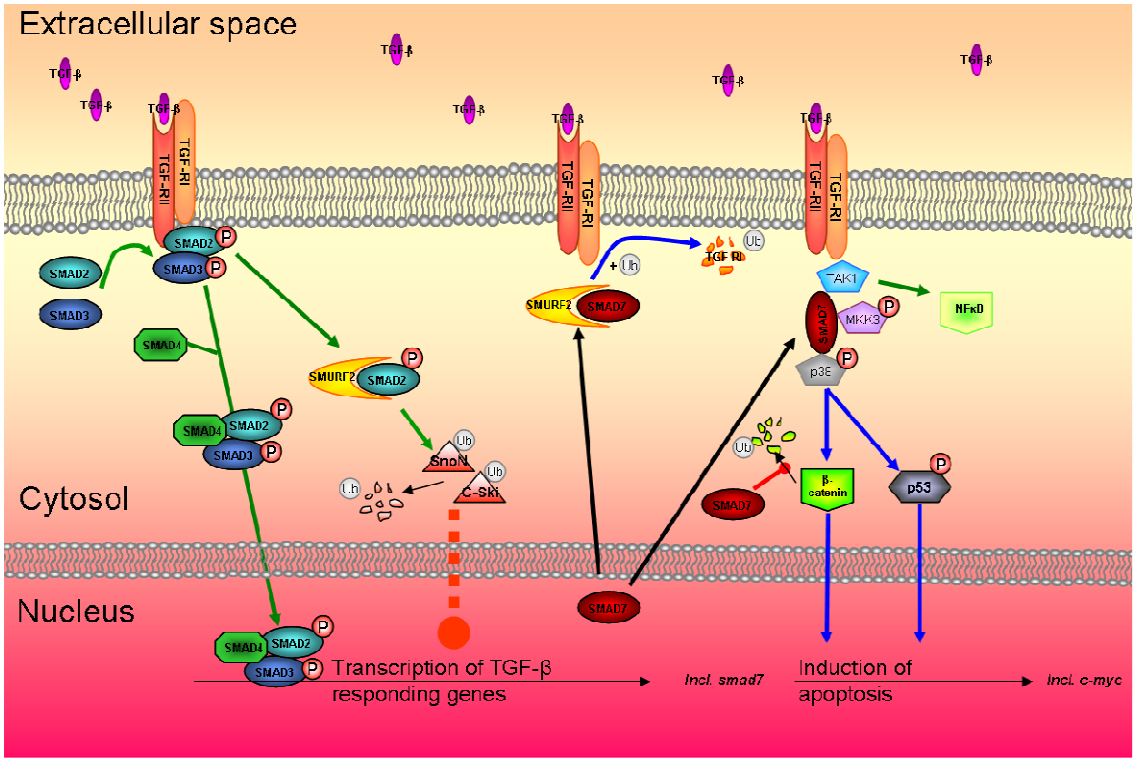

Figure 1-3 Simplified scheme of TGF-β signalling

TGF-β interacts with the receptor complex and leads to recruitment of r-SMADs to the receptor complex where r-SMADs become phosphorylated. Phosphorylated r-SMADs can interact with co-SMAD4 to build an active transcription factor complex that translocates into the nucleus to induce transcription of TGF-responsive genes. Furthermore active SMAD2 can interact with E2-ubiquitin ligase SMURF2, an interaction that leads to degradation of various transcription repressors like SnoN and c-SKI, thereby induces the transcription of further genes. One of the responding genes is SMAD7, an inhibitory SMAD, localized in the nucleus. Activated by TGF-β signalling SMAD7 leaves the nucleus. In the cytosol SMAD7 interacts with SMURF2 and leads to degradation of TGF-βRI receptor. This is a negative feedback loop to regulate TGF-β signalling. Furthermore SMAD7 interacts with TAK1, MKK3 and p38. Activation of this pathway induces phosphorylation of p53 leading to apoptosis. While TAK1 also activates the transcription factor NFκB. SMAD7 stabilizes β-catenin in the cytosol at cadherin adhesion sites. SMAD7 interaction with β-catenin has been shown to be required for TGF-β induced apoptosis.

On the other hand this complex of SMADs also represses the expression of genes such as cyclin-dependent kinases in coordinated function with transcription repressors like SnoN or Ski (38). Biglycan itself induces G1 arrest in pancreatic cancer cells by induction of p21 and p27 (47). These controversial effects of TGF-β demonstrate that its activity always depends on the cell type, environment and how the cell reads TGF-β signalling (48).

1.3 Biglycan and its role in cardiac system

Biglycan is ubiquitously expressed in the healthy heart. It is expressed by cardiomyocytes and non-myocytes (fibroblasts) and is differentially regulated in response to pathological changes (49,50). It was reported that both SLRPs biglycan and decorin are up-regulated during infarct healing (51,52).

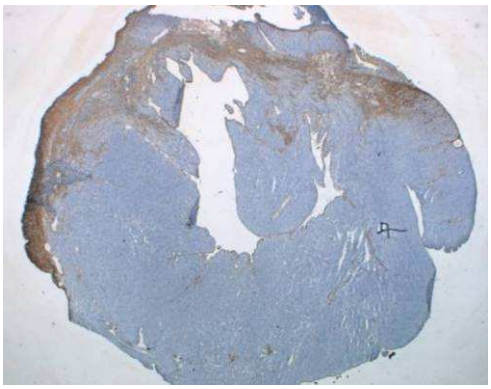

Figure 1-4 biglycan accumulation within the infarct area 7 days after experimental MI
Representative image shows an immunohistochemical staining for biglycan within the infarct zone 7 days after experimental myocardial infarction. Biglycan positive signal is stained as brown portion within the cross-section of the left ventricle from a WT mouse at 7 days after experimental myocardial infarction. 25 x magnification

Biglycan-deficient male mice ($bgn^{-/0}$) show increased mortality and impaired hemodynamic functions after experimental MI and a higher incidence for ventricular ruptures, as a stiff and hence fragile collagen scar is established in the absence of biglycan (52,53). Additionally it was shown that pro-hypertrophic and pro-fibrotic factors like WISP1 induce biglycan expression *in vivo* (49). It has been demonstrated *in vitro* that fibroblasts upon treatment with pro-fibrotic growth factors like TGF-β produce increasing amounts of ECM components, including SLRPs. Upon stimulation with pro-fibrotic growth factors the majority of fibroblast secreted SLRPs is biglycan (54).

Biglycan is importantly relevant in the vascular system, where it influences the proliferation of vascular smooth muscle cells (55). But not only vascular smooth muscle cells are influenced by biglycan, it has been demonstrated that biglycan is essential for vessel stability by it's presence in the adventitia. Because

biglycan deficiency in Balb/c mice leads to spontaneous aortic dissection and rupture, as the adventitia does not achieve normal functionality (56). In human aortic aneurysms a loss of biglycan has also been documented (57). Furthermore biglycan is up-regulated in pressure-overloaded rat hearts after aortic banding (58) which might contribute to biglycans function to stabilize the ECM. The biglycan expression increases in mesenchymal cells of the myocardial interstitium as well as in endothelial cells and smooth muscle cells of thickened coronary arteries as part of perivascular fibrosis. This indicates that biglycan contributes to both ventricular and vascular remodelling in response to pressure-overload (58).

1.4 Aim of Investigation

Small leucine-rich repeat proteoglycans (SLRPs) are components of the ECM in every tissue, that interact with structural molecules like collagens, elastin, fibronectin and provides stability and integrity of the matrix. Investigations of the last years have shown that proteoglycans exhibit more functions than just decorating and filling the matrix: It has been revealed that biglycan and decorin are important for lateral association of collagen fibrils. Furthermore, SLRPs are not only sequestering growth factors within the ECM but also modulate growth factor and signalling molecule presentation to their receptors. In addition it was shown that SLRPs are themselves ligands for various receptors (29,30).
Remodelling of ECM is a crucial process during hypertrophy and scar formation following ischemic myocardial infarction. About 70-80 % of non-myocytes in the heart are fibroblasts and these are the main source of scar forming molecules and thereby contribute to functionality of the tissue once the infarct has healed. Biglycan as well as collagens are induced in response to MI (52). Investigations of the role of biglycan for survival of mice after MI, showed that biglycan deficient mice die more frequently than WT-mice. As it turned out biglycan - deficient mice show increased incidence for ventricular rupture, which was attributed to perturbed collagen network formation.

The overall aim of the present thesis was to investigate the function of biglycan (bgn) regarding the phenotype of cardiac fibroblasts. For this purpose primary cardiac fibroblasts from $bgn^{-/0}$-mice were compared to fibroblasts from wildtype mice (WT; CL57BL/6J) with respect to the following questions:

(1) Do $bgn^{-/0}$-fibroblasts exhibit differences in cellular morphology and phenotypical features?
   - Fibroblasts were analysed with respect to cell shape, proliferation and apoptosis.
   - The contractile responses of cardiac fibroblasts will be analyzed.

- Effects on the cytoskeleton, focal adhesions and ECM modifying enzymes will be determined?

(2) What are the mechanisms of phenotypical differences between biglycan deficient and WT- fibroblasts?

- Does lentiviral overexpression of murine biglycan rescue the biglycan knock out phenotype and does myofibroblast differentiation depend on biglycan expression?
- Characterization of the TGF-β system will be performed and effects of neutralizing endogenous TGF-β will be analysed. Furthermore TGF-β canonical signalling will be addressed.

(3) Is the described phenotype of relevance for post MI remodelling in vivo?

- Myofibroblast phenotype of cardiac fibroblasts will be analyzed after experimental myocardial infarction in WT versus $bgn^{-/0}$-mice.

2 Material and Methods

This project includes molecular biological and biochemical procedures carried out in vitro by usage of a cell culture model of primary cardiac fibroblasts. To advance the relevance of the results translation to an *in vivo* model of myocardial infarction was included.

2.1 Material and Substances

In the following chapter, all materials and substances are listed with information of distributors. All substances were used at the highest analytical grade.

2.1.1 Mice

C57/BL6 mice were obtained by The Jackson Laboratory, Maine, USA, Tierversuchsanstalt, Heinrich-Heine University of Düsseldorf and Zentrales Tierlaboratorium, Universitätsklinikum Essen, University of Duisburg-Essen. Biglycan deficient ($bgn^{-/0}$) mice were kindly supplied by Marian F. Young (Craniofacial and Skeletal Diseases Branch, National Institute of Dental and Craniofacial Research, NIH, Bethesda, Maryland, USA). Mice were fed with normal chow with food and water *ad libitum* and housed with a constant 12 h day- 12 h night-rhythm.

2.1.2 Substances

Phosphate-buffered saline (PBS), Dulbecco's Modified Eagle Medium (DMEM), fetal calf serum (FCS), penicillin/streptavidin, L-glutamin, Minimum Essential Media (MEM) and trypsin-EDTA solution were from GIBCO® supplied by Invitrogen, Darmstadt, Germany. Growth factors, DEAE-Sephacel and

chemicals were purchased from Sigma-Aldrich, Munich, Germany. [^{3}H]-methyl-thymidine was from Hartman Analytic, Braunschweig, Germany. Rotiszint® eco plus was delivered by Carl Roth, Karlsruhe, Germany. Pure-Col™ collagen solution for oil-supported collagen retraction assay was obtained from nutacon, Leimuiden, the Netherlands. Ascorbate was obtained from Caesar & Loretz GmbH, Hilden, Germany.

Table 2-1 Buffers and Solutions

Buffers and Solutions	**Ingredients**
ABC-Buffer	0.60 g Tris 1.33 g sodiumacetate x 3 H_2O 0.30 g NaCl *ad* 100 ml Aqua dest. BSA 1 mg/ml pH 8.0
2-fold loading buffer	150 mM Tris pH7 4 % SDS 20 % glycerol 8 % β-Mercaptoethanol
Blocking buffer	2 mg/ml BSA in PBS
Running buffer for SDS-PAGE	25 mM Tris/HCL 0.19 mM Glycine 0.01 % SDS
Stacking gel (5 %)	0.5 M Tris pH 6.8 0.625 ml 10 % SDS 50 µl dH_2O 3.895 ml 40 % Acrylamide 375 µl Temed 5 µl 10 % APS 50 µl
Separating gel (10 %)	1.5 M Tris pH 8.7 1.85 ml 10 % SDS 75 µl dH_2O 4.545 ml 40 % Acrylamide 375 µl Temed 5 µl 10 % APS 25 µl
Transfer-buffer	1 x Running Buffer 20 % Methanol 0.01 % SDS
TBST	100 mM Tris HCl 1.5 mM NaCl 0.1 % Tween 20 pH7.4
PBS	137 mM NaCl 2.7 mM KCl 1.5 mM KH_2PO_4 8.3 mM Na_2HPO_4 pH7.4
Histoblock	2 % BSA 10 % FCS in 1 x PBS
Blocking solution for endogenous peroxidases	3 % H_2O_2 in 1 x PBS
Trisbuffer for immunohistochemistry	6.07 g Tris *ad* 1 l Aqua dest. pH 7.6

Table 2-2 Substances, enzymes, kits and ready-to-use products

Substances	Distributor
Phalloidin-FITC	Sigma-Aldrich, Deisenhofen, Germany
Chondroitinase ABC	Sigma-Aldrich, Deisenhofen, Germany; and Saikagaku, Tokio, Japan
Quick Start Bradford Protein Assay	BioRad; Munich, Germany
SuperScript™ III First Strand cDNA Synthesis Kit	Invitrogen, Karlsruhe, Germany
SYBR Green® PCR Master Mix Applied	Biosystems, Darmstadt, Germany
TriReagent®	Sigma-Aldrich, Deisenhofen, Germany
Vectashield® Mounting Medium	Vector Laboratories, CA, USA

Table 2-3 Materials and Distributors

Materials	Distributor
Protran™ nitrocellulose membrane for Protein Transfer 0.2 µm	Schleicher & Schuell / Whatmann (GB)
Blot-paper	Whatmann (GB)
LabTek™ CC Chamber slides (8 to 4 chambers)	Nunc, Wiesbaden, Germany
Super Frost™ Slides	Menzel-Gläser, Braunschweig, GErmany

Table 2-4 Primary antibodies and dilutions

Primary andibodies	Distributor	Dilution
Biglycan LF106, polyclonal	Kindly provided by Larry Fisher (NIH, USA)	1:1000
Decorin LF113, polyclonal	Kindly provided by Larry Fisher (NIH, USA)	1:1000
alpha-sm-actin, polyclonal	Abcam, Cambridge, UK	1:50
Anti-fibronectin antibody	Abcam, Cambridge, UK	1:100
Anti-tropoelastin antibody	Abcam, Cambridge, UK	1/250
Anti-TGF-β1, -β2, -β3 monoclonal neutralizing antibody	R&D Systems, Inc. Minneapolis, MN, USA	0.5 µg/ml
Mouse IgG1 Isotype Control	R&D Systems, Inc. Minneapolis, MN, USA	0.5 µg/ml
Anti-dystrophin antibody	Abcam, Cambridge, UK	1:100

Rabbit polyclonal antisera to mouse biglycan (LF-106 and LF 159) and mouse decorin (LF-113) were kindly provided by Larry Fisher (Matrix Biochemistry Section, CSDB, DIR, NIH, Bethesda, Maryland, USA)

Table 2-5 Secondary antibodies

Secondary antibodies	Distributor	Dilution
IRDye 680 goat-anti-Rabbit IgG	LI-COR Biosciences; Lincoln, NE, USA	1:2500 up to 1:10000
IRDye 800CW goat-anti-rabbit IgG		
IRDye 800CW goat-anti-mouse IgG		
IRDye 680 goat-anti-mouse IgG		
goat-anti-rabbit IgG F(ab`)2 Frag. Cy3-conjugated	Sigma-Aldrich, Deisenhofen, Germany	1:600
goat-anti-mouse IgG F(ab`)2 Frag. Cy3-conjugated	Sigma-Aldrich, Deisenhofen, Germany	1:600
goat-anti-rat IgG, rhodamine-red X conjugated, pre-adsorbed,	Dianova, Hamburg, Germany	1:400
sheep-anti-rabbit Cy3	Sigma-Aldrich, Deisenhofen, Germany	1:200
goat anti-rabbit horseradish-peroxidase conjugated (HRP)	Santa Cruz, USA	1:100

Table 2-6 Laboratory Equipment

Equipment		Distributor
spectralphotometer	Nanodrop-1000	Peqlab, Erlangen, Germany
rotary microtom	Leica RM 2255	Leica Microsystems, Wetzlar, Germany
cryostat	Leica CM1850	Leica Microsystems, Wetzlar, Germany
RT-qPCR	Applied Biosystems 7300 Real-Time PCR System	Applied Biosystems, Darmstadt, Germany
Stereo-microscope	Leica DM2000	Leica Microsystems, Wetzlar, Germany
Mini-PROTEAN3 electrophoresis chamber	Mini-PROTEAN3 Electrophoresis cell	BioRad, Munich, Germany
powersupply	Power-Pac 200 +300	BioRad, Munich,

		Germany
protein-transfer	PerfectBlue Semi-Dry Elektroblotter	Peqlab, Erlangen, Germany
PCR-cycler	Mastercycler Gradient	Eppendorf, Hamburg, Germany
realtime-PCR-cycler	Applied Biosystems 7300 Real-Time PCR System	Applied Biosystems, Darmstadt,Germany
centrifuge	Centrifuge 5415R	Eppendorf, Hamburg, Germany
Odyssey	Odyssey Near Infrared Imaging	LI-COR Biosciences Lincoln, NE, USA

Table 2-7 Real Time PCR Primer

Gene	primer-sequences
gapdh	5'-TGGCAAAGTGGAGATTGTTGCC-3' 5'-AAGATGGTGATGGGCTTCCCG-3'
α-sma	5'-CAGGCATGGATGGCATCAATCAC-3' 5'-ACTCTAGCTGTGAAGTCAGTGTCG-3'
TGF-β 1	5 –CCGCAACAACGCCATCTATG-3' 5'-CTCTGCACGGGACAGCAAT-3'
TGF-β receptor type II	5' -CAAGTCGGATGTGGAAATGG-3' 5'–AAATGTTTCAGTGGATGGATGG-3'
cd44	5'-AGG ATG ACT CCT TCT TTA TCC G-3' 5'-CTT GAG TGT CCA GCT AAT TCG-3'
dystrophin	5'-GCCATAGCACGAGAAAAAGC-3' 5'-CGGCTGTTCAGTTGTTCTGA-3'
syntrophin	5'-CCTCAAGAAGACAGGCAAGG-3' 5'-GAGGTCCCTCCAGCAGAAT-3'
nos2	5'-GAAGAAAACCCCTTGTGCTG-3' 5'-TTCTGTGCTGTCCCAGTGAG-3'
plod1	5'-GAGCCTTGGATGAAGTTGTG-3' 5'-TAGTTGCCCAGGTAGTTCAG-3'
plod2	5'-AGTGGCAATTAATGGAAATGGG-3' 5'-CTTGGGAGGGACATCTACTG-3'
tgm 1	5'-CCTCAGATGGATCTTCAATGGT-3' 5'-CCATTGTGCCTTATATTGCAGAG-3'
tgm 2	5'-AAGAGCGAAGGGACATACTG-3' 5'-TGCATCATACTTGGTACTCAGG-3'

Table 2-8 Sequencing primers

Bgn-sequencing primer	*primer-sequences*
Exon 3 to Exon 1	5'-CCTGGTGGAGATTCCTCCCA-3'
Exon 4 to Exon 1	5'-AATGACATTTCTGAGCTTCG-3'
Exon 4 to Exon 8	5'-CTACGAATCCATGACAACCGT-3'
Exon 8 to End	5'-ACTGACCGCCTGGCCATCCAA-3'

2.2 Methods

2.2.1 Mice

All procedures were performed in accordance with the AAALAC guidelines and Guide for the Care and Use of Laboratory Animals (Department of Health and Human Services, National Institutes of Health, Publication No. 86-23) and were approved by the ethical and research board of the University of Duisburg-Essen and the county of Essen.

2.2.2 Isolation of primary murine cardiac fibroblasts

Mice at the age of 4 up to 8 weeks were used for isolation of murine fibroblasts. Mice were euthanized by CO_2 inhalation. Skin was removed and the chest was opened with sterile instruments. The heart was freed from pericardium and atria were removed. Ventricles and septum were transferred into sterile pre-warmed phosphate buffered saline (PBS) immediately. Hearts were washed twice in sterile pre-warmed PBS and cut into small pieces. Heart pieces were explanted into six-well culture plates using cardiomyocyte-plating medium containing 60 % FCS and 8 ng/ml basal fibroblast growth factor (bFGF). Culture plates were pre-coated with 5 µg collagen type I /well. After 24 h at 37℃ the plating medium was changed to DMEM containing 20 % FCS and 8 ng/ml bFGF. The medium was changed every second day for a period of two weeks. Afterwards fibroblasts were washed twice with PBS and treated with Trypsin for ten minutes at 37℃ and separated from the heart pieces. Two da ys later the medium was changed to DMEM containing 10 % FCS and cells were used for experiments after achieving confluence. Only the first three passages of fibroblasts were used.

2.2.3 Cell growth and proliferation assays

For cell growth experiments cells were treated with trypsin and counted in a hematocytometer upon addition of trypan blue to differentiate viable from dead cells.

For assaying proliferation, the incorporation of [^{3}H]-methyl-thymidine into new synthesised DNA was measured. Fibroblasts were plated at 5000 cells /cm² and either serum depleted or treated with media containing 2 or 5 % FCS. After the desired incubation time (24-48 h) the fibroblasts were washed with PBS and lysed by treatment with perchloracid and 1M NaOH for 45 min at 37℃. These lysates were analysed after addition of Rotiszint® eco plus in a scintillation counter.

All experiments including stimulations were performed in DMEM-media containing at least 2 % FCS because bgn$^{-/0}$-fibroblasts showed to be very sensitive towards serum depletion. Fibroblasts were assayed without previous serum depletion. Fibroblasts were synchronized by means of the plating procedure using trypsin for 10 min at RT, and resolving pelleted cells in DMEM containing 2 % FCS and plating a defined cell density by counting cells using a hematocytometer.

2.2.4 Proliferation on cell-derived ECM from WT- or bgn$^{-/0}$-fibroblasts

To determine influence of extracellular matrix (ECM) on proliferation cells were plated on cell culture plates and fed with DMEM containing 10 % FCS and 56 µg/ml ascorbate to stimulate collagen production. After a feeding period of 20 days, ECM was visible on the plate macroscopically. Cells were washed twice with PBS and lysed by 30 min incubation at RT using 2.5 µM ammoniumhydroxide. After lysis of the cells, the ECM was washed three times with sterile distilled water and stored at 4℃ over night.

Fibroblasts were plated on these ECM at a density of 10^3 cells per cm^2. The cells were allowed to settle and grow for 48 h. Afterwards cells were trypsin treated and counted as described above.

2.2.5 Immunocytochemistry

To assess morphological differences and determine states of differentiation fibroblasts were plated on LabTek cell culture micro slides plus minus the indicated stimuli. After incubation under standard conditions the cells where washed and fixed by 3.7 % saline-phosphate-buffered paraformaldehyde for 20 min at RT. Afterwards the cells were incubated with the primary antibody in the recommended dilution for one hour at RT and washed again five times before the fluorochrome conjugated secondary antibody was added for one hour at RT. Cells were washed again to remove unbound antibody. Afterwards nuclei were stained by DNA binding HOECHST Dye (1:10000) for 5 min in the dark and embedded with Vectashield Mounting Medium.

2.2.6 Oil supported collagen Retraction Assay

Oil-supported collagen gel retraction assay was performed as described by Vernon and Gooden (59). This assay visualizes the abilities of cells to contract collagen matrices that are free of adhesion. Trypsin treated cells were mixed with PureCol collagen solution, 10 x DMEM saturated with Na_2CO_3, thus achieving a total concentration of 1.25 mg collagen per gel. Each gel contained 15 x 10^3 cells. 12-well cell culture plates were prepared with 1.4 ml sterile mineral oil and a polyethylene (PE) ring and a Teflon® disk that secured the adhesion-free polymerization of collagen gels. The cell suspension was pipeted into the inner circle of the PE ring. To expand the gel to fill out the whole inner

ring, the same volume of mineral oil was removed. Gels were polymerized for 2 h at 37℃ and 5 % CO_2.
After incubation period of 24 h gel images were recorded under dark field illumination and analysed by NIH freeware ImageJ. Contraction was calculated as percentage of unpopulated control collagen gels.

2.2.7 Protein Analysis

To analyse protein expression and the phosphorylation status of signal-transducing proteins, fibroblasts were lysed by 10 min incubation in HIDE-buffer containing protease and phosphatase inhibitors at 4℃ and rigid scratching of cell culture dishes. Lysates were mixed with SDS-containing 2 fold loading buffer and run on 10 % polyacrylamide-SDS-gels, afterwards the proteins were transferred onto nitrocellulose membrane by electroblotting for 2 h at 1000 mA. Membranes were blocked in 2 % BSA/TBST for 1 h at RT and incubated in primary antibody-solution overnight. Removal of unbound primary antibody was achieved by repeated washing with TBST and followed by one hour of incubation in a solution containing the appropriate near-infrared- fluorochrome conjugated secondary antibody.
The resulting fluorescent signal was detected with Odyssey Near Infrared System (Licor)

2.2.8 Protein concentration

For normalisation of proliferation assay and western blots the protein concentration of samples was measured via Bradford assay. Therefore 5 µl of each sample was mixed with 200 µl of Bradford Reagent (BioRAD) and absorption was measured with a plate reader at 595 nm. Concentration was calculated by standard curve of BSA.

2.2.9 Proteoglycan isolation from culture supernatants

Proteoglycans were isolated according to standard procedures (60). Equal volumes of conditioned medium were collected and applied to Sephacel® - DEAE-chromatography. Proteoglycans were eluted from the column with 3 M NaCl containing urea DEAE-buffer. The samples were precipitated three times in a row by 96 % ethanol containing 1.3 % potassium acetate in order to remove urea and salt. Salt free pellets were resuspended in a 20 µl of distilled water and digested with chondroitinase ABC for 3 h at 37℃, to remove glycosaminoglycan chains from the core proteins of the proteoglycans. One third of the digestions were analysed by 10 % SDS-PAGE followed by standard western-blot procedure.

2.2.10 RNA-extraction and quantitative Real-Time RT-PCR

Total RNA was extracted from cell cultures using TRIzol® reagent (Invitrogen, Carlsbad, CA) according to the manufacturer's instructions. Quality and concentration were determined using the NanoDrop® ND-100 (Wilmington, DE) spectrophotometer. The synthesis of cDNA by reverse transcriptase (RT) using random hexamer primers was performed with 1µg of total RNA using the quantitect reverse transcription kit (Qiagen, Hilden).

Relative quantitation of mRNA expression levels were determined by qPCR with ABI 7300 real time system (Applied Biosystems, Darmstadt) using Platinum SYBR green qPCR SuperMix-UDG kit (Invitrogen, Karlsruhe). The reaction volume of 20 µl contained 10 µl of Platinum SYBR green qPCR SuperMix-UDG, 5 µl cDNA and 2.5 µl of each primer with a final concentration of 10 pmol for every primer. The glyceraldehyde- 3-phosphate dehydrogenase (gapdh) gene is constitutively expressed and was chosen as the endogenous control. The PCR amplification was performed at initially 50℃ for 2 min, followed by 95℃ for 2 min and 40 cycles at 95℃ for 30 s and terminated by 60 ℃ for 30 s. During the last steps, a temperature gradient between 95℃ and 60℃ was created for the

analysis of the DNA dissociation curves. These dissociation curves can be used to monitor the PCR quality. The expression of each target gene was calculated in relation to the housekeeping gene, GAPDH, using the $2^{-\Delta\Delta C}{}_t$ method as described before (61).

2.2.11 Lentiviral overexpression of biglycan

Briefly, cDNA of murine biglycan was obtained by RT-PCR using the whole RNA extracts from C57BL/6J WT mouse hearts. Amplification was achieved by using the following primers XhoI-mBGN-F 5'-CTCGAGATGTGTCCCCTGTGGCTACTC-3' and EcoRI-mBGN-R 5'-GAATTCCTACTTCTTATAATTTCCAAA-3'. The cDNA was cloned into the pCL1mcs vector using XhoI and EcoRI restriction sites. The production of lentivirus, harvest of recombinant lentiviral particles, and transduction of primary murine cardiac fibroblasts were performed as previously described (61). In this lentiviral vector, the CMV promoter drives the overexpression of biglycan. The pCL1 vector expressing only EGFP was used as mock control. Cells were used at day seven after transfection. For transfection cells were incubated with viruses at a dilution 1:20 for 24 h.

The biglycan overexpression vector was sequenced to exclude any point mutations, especially in the extreme N-terminus where the GAG-chains would be attached to the core protein. For sequencing 100 ng of vector DNA were used. Sequencing was performed at GATC Biotech (Konstanz, Germany) and primers are presented in table 2-8).

2.2.12 Experimental myocardial infarction

At the age of 12 weeks WT- and $bgn^{-/0}$-mice were anesthetized by *i.p*. injection of pentobarbital (100 mg/kg). A 2 cm long PE-90 catheter attached to the hub of

a needle was inserted into the trachea. In order to numb the throat and reduce gag reflex a drop of 1 % lidocaine was put on the tip of the tube. Mice were subjected to permanent left anterior descending artery (LAD)-occlusion followed by recovery for 3, 7 or 21 days. Infarcted left ventricles were freed from right ventricle tissue. RNA was isolated from a 1 mm thick section of the *apex cordis*. Hearts were immediately placed in cryomolds filled with OCT-Medium and frozen in liquid isopentan at 40°C without pre-fixation. All procedures were carried out as recently described in detail (62).

2.2.13 Cryomicrotomy and immunohistochemistry

Cross-sections of infracted left ventricles were prepared from un-fixed tissue. Cryomolds were stored at -80°C and brought to -25°C two hours before sectioning. Sections were cut at -25°C at a thickness of 10 µm using a Leica cryostat. Frozen sections were allowed to acclimate to room temperature for two hours before staining.

Sections were fixed for ten minutes in absolute ethanol at 4°C and rehydrated by 5 min in 70° ethanol at 4°C. Sections were washed with PBS three times and incubated for 1 h at RT in histoblock. Incubation with primary antibody followed at 4°C over night. Primary antibody was removed by three times washing with PBS. Blocking of endogenous peroxidases was carried out in 3 % H_2O_2 in PBS for 20 min at RT. Secondary antibody was pipetted on every section and incubated for 1 hour at RT. Excess antibody was removed by washing with PBS. Adjusting the pH was achieved with trisbuffer for 10 min at RT.

Detection with DAB solution was performed for 10 min at RT. Counter staining of nuclei was performed with Mayer's Hematoxylin.

2.2.14 Statistical Analysis

Quantitative results are presented as mean values plus minus the standard error of the mean (SEM). Data sets were compared by unpaired student's T-test, when only two groups of values were compared. For analysis of two groups under two or more conditions two way ANOWA had been applied to the data using the software PRISM Graphpad 4.0. Over all a p-value below 0.05 was considered as statistically significant. The statistical significance between WT and $bgn^{-/0}$ is signatured by asterisk (*) while statistical significance between treatment within one group or genotype is signatured by hash key (#).

3 Results

During cardiac remodelling fibroblasts, which represent 70 % of the non-myocyte cells within the myocardium, proliferate and secrete high amounts of ECM (ECM) to adapt to physiological challenges such as hypertension, myocardial infarction and inflammation (6). Biglycan-deficiency in mice leads to a higher incidence of ventricular rupture following experimental myocardial infarction and a dramatic increase in mortality of the $bgn^{-/0}$-mice.

Cardiac remodelling post infarction is a crucial process characterized by ECM production, cross linkage and degradation, thus leading to a stable scar tissue. As this healing process, mainly accomplished by myofibroblasts, is disturbed in $bgn^{-/0}$-mice, it may be hypothesised that cardiac fibroblasts and their differentiation into myofibroblasts are influenced by the genetic knock out of biglycan. To explore these questions, isolated fibroblasts from either WT-mice or biglycan deficient mice were analysed *ex vivo* in explant cultures.

3.1 Morphology of $bgn^{-/0}$-fibroblasts revealed a distinct phenotype

Fibroblasts from WT-explants grew out of explants during the first week. In comparison biglycan deficient ($bgn^{-/0}$) -fibroblasts grew out already during the first three days after explantation. Fibroblasts were separated from explants by passaging and visualized by microscopy. The morphologies of the two different genotypes were of distinct differences. $Bgn^{-/0}$-fibroblasts were smaller and had a round cell body with many lamelopodia, giving them a spider like shape, compared to WT-fibroblasts which were flat, evenly shaped and showed broad and fewer filopodia (figure 3-1).

By measuring the cell-area from 50 cells per isolation, it became obvious that $bgn^{-/0}$-fibroblasts were significantly smaller than the WT-fibroblasts (fig. 3-2).

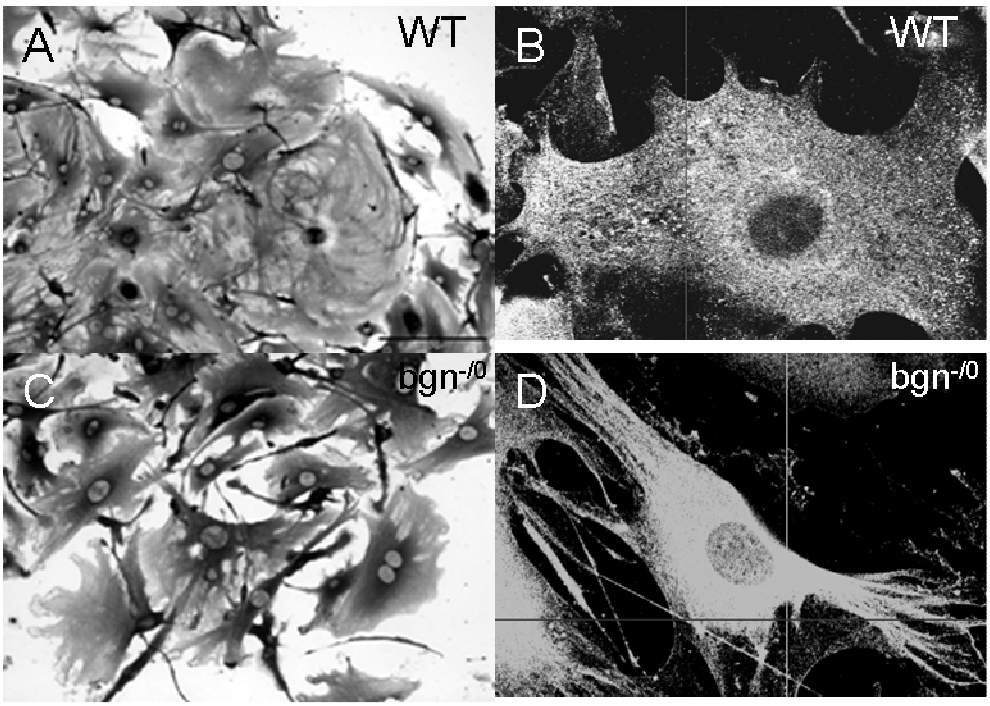

Figure 3-1 Morphologic differences of bgn$^{-/0}$-fibroblasts from WT-fibroblasts

Microscopic images of WT- (**A, B**) and a bgn$^{-/0}$-fibroblasts (**C, D**) taken at 200 (**A, C**) and 400 x magnification. (**B, D**) show smaller cell size of bgn$^{-/0}$-fibroblasts exhibit smaller and more dynamic shape compared to WT.

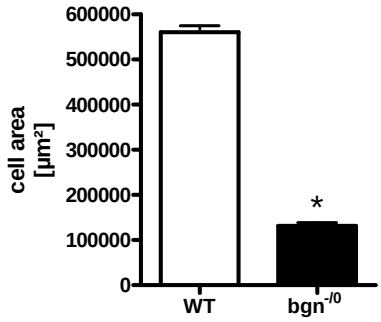

Figure 3-2 Cell size of bgn$^{-/0}$-fibroblasts is reduced in comparison to WT-fibroblasts

50 cells of three independent explant cultures were documented. The cell size was determined. WT-fibroblasts (white bar) were significantly larger than bgn$^{-/0}$-fibroblasts (black bar). *means ± SEM; n=3 *; p<0.05*

The secretion of proteoglycans into conditioned media of the primary cardiac fibroblasts was analysed at 24 and 48 hours (figure 3-3). The results showed that media taken from bgn$^{-/0}$-fibroblasts did not contain biglycan protein.

Surprisingly, the media taken from bgn$^{-/0}$-fibroblasts contained less decorin compared to the WT cell media. This outcome demonstrated that bgn$^{-/0}$ -fibroblasts do not compensate the lack of biglycan by over expressing decorin.

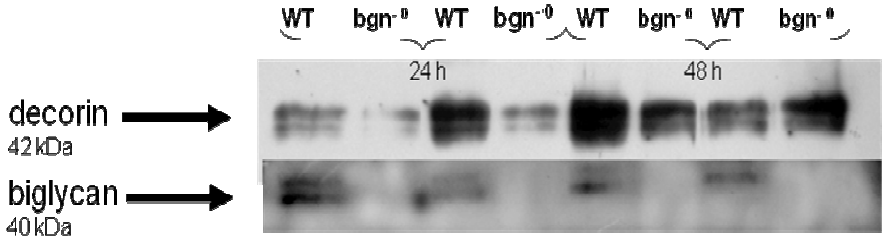

Figure 3-3 Representative western blots of proteoglycans secreted by WT- and bgn$^{-/0}$-fibroblasts during 24 and 48 h

Representative western blots of DEAE-isolated chondroitinase ABC digested proteoglycans from 1 ml conditioned cell culture supernatants, detected with anti-decorin LF113 (upper panel) and anti-biglycan LF106. Alternating order of WT and bgn$^{-/0}$ samples taken from two independent explant-cultures of each genotype. This control experiment shows signals for biglycan only in lanes with media conditioned by WT-fibroblast.

Additionally it was shown that bgn$^{-/0}$-fibroblasts keep a comparable or even lower expression level of decorin even after 48 hour in culture.

3.2 Bgn$^{-/0}$-fibroblasts showed a pro-proliferative phenotype

Cell numbers were determined after separating cells from heart pieces 14 days after explantation. During this time explants were treated with 8 ng/ml basal fibroblast growth factor (bFGF), while medium was refreshed every second day. The number of bgn$^{-/0}$ cells was 1.8 fold higher than cell numbers from WT hearts (fig. 3-4).

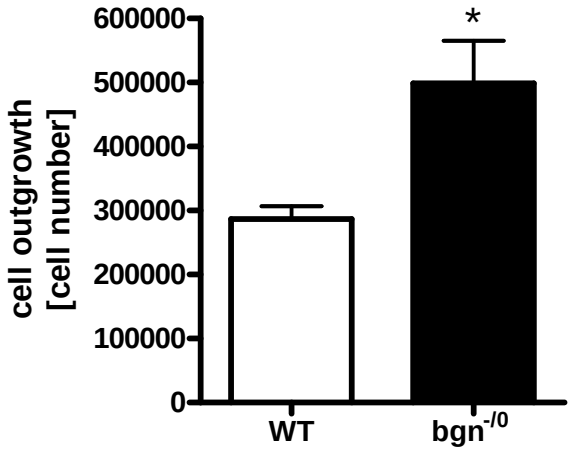

Figure 3-4 Outgrowth from bgn$^{-/0}$-hearts was significantly higher

Fibroblasts cultured in 20% serum containing DMEM in the presence of 8 ng/ml of basal fibroblast growth factor for 14 days. Fibroblasts were then trypsin treated and counted in a hematocytometer (WT white bar; bgn$^{-/0}$ black bar). *mean ± SEM; n = 5;*, p<0.05*

In order to find out whether the increased cell numbers were due to enhanced proliferation of biglycan$^{-/0}$-fibroblasts, several assays to analyse proliferative responses of fibroblasts were performed.

According to standard proliferation assay protocols, cells have to be synchronized by serum depletion for 24 up to 48 hours before stimulation. But serum depletion led to a total loss of bgn$^{-/0}$-fibroblast proliferation. Even the following stimulation with either PDGF-BB or 10 % FCS could not restore proliferation in bgn$^{-/0}$-fibroblasts as shown in fig. 3-5.

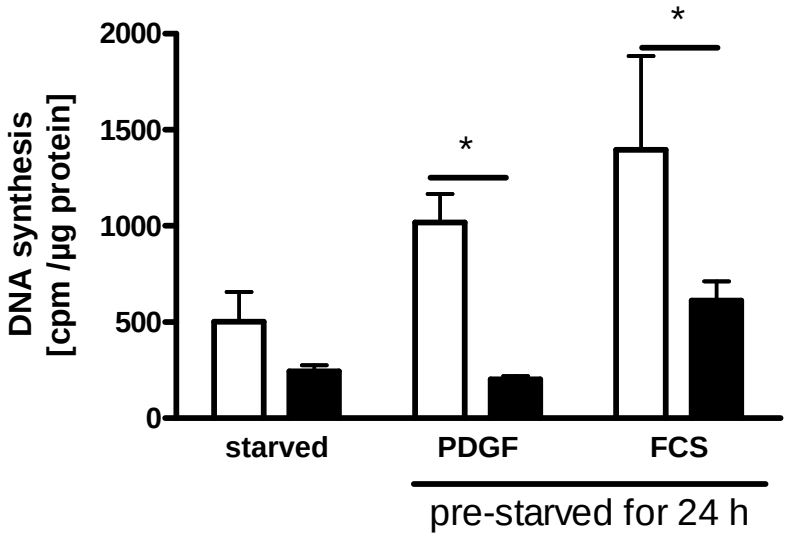

Figure 3-5 Serum-depletion irreversibly abolished proliferation benefit of bgn$^{-/0}$-fibroblasts.

Fibroblasts were serum depleted for 24 hours followed by additional starving or treatment with either 10 ng/ml PDGF-BB or 10 % FCS for another 24 hours. Afterwards [H³]-thymidine incorporation was measured in a scintillation counter (Beckmann Coulter). Protein concentration of cell lysates was measured by Bradford assay for normalization. *mean ± SEM; n = 5;*, p<0.05*

Bgn$^{-/0}$-fibroblasts were highly sensitive to serum depletion in cell culture. Therefore, serum depletion was avoided as synchronising method in the following experiments. Due to the problems of bgn$^{-/0}$-fibroblasts to survive under conditions of serum depletion, cells were routinely analysed at 12, 24 or 48 h after plating, assuming that plating is a synchronising process as well.

[³H]-thymidine incorporation and cell counting experiments were performed to analyse proliferative responses of fibroblasts from bgn$^{-/0}$-mice in comparison to WT-fibroblasts. Bgn$^{-/0}$-fibroblasts showed increased proliferation under standard conditions independent of high or normal serum conditions, as long as the serum concentration was above 2 % serum. The proliferation benefit was determined by cell counting at 48 and 72 hours after plating (Figure 3-6). It was shown that the number of bgn$^{-/0}$-fibroblast was 1.7 fold higher than proliferation of WT-fibroblasts at both time points.

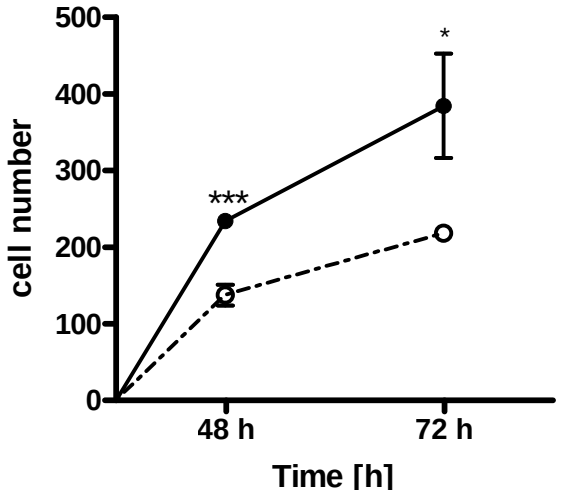

Figure 3-6 Growth of bgn$^{-/0}$-fibroblasts was significantly increased over time in comparison to WT-fibroblasts.

Fibroblasts were plated and grown in 10 % serum. Fibroblasts were trypsin treated and counted after 48 and 72 h. Data represents independent experiments performed in quadruplets. *mean ± SEM; n = 4 and 6; *, p<0.05; ***,p<0.001*

Determining cell numbers is a basal method, which does not exclude that the changes in cell numbers are due to differences in proliferation or survival. Therefore DNA-synthesis of WT- and bgn$^{-/0}$-fibroblasts was compared after 24 h in 20 % serum by [^{3}H]-thymidine incorporation.

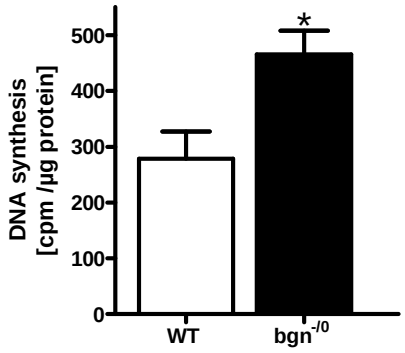

Figure 3-7 DNA synthesis measured by [^{3}H]-thymidine incorporation was increased in bgn$^{-/0}$-fibroblasts

DNA synthesis was measured by [^{3}H]-thymidine incorporation 24 h after plating cells in 20 % DMEM. Experiments were performed in triplicates. *mean ± SEM; n = 4;*, p<0.05*

3.2.1 Proliferation on cell-derived ECM from either WT- or bgn$^{-/0}$-fibroblasts

To investigate if the proliferation benefit of bgn$^{-/0}$-fibroblasts was attributed to the lack of biglycan in the extracellular matrix, a proliferation assay using cell-derived ECM as growth substrate was performed. For this purpose, fibroblasts from WT- and bgn$^{-/0}$-mice were treated with 56 µg/ml ascorbate, which is described to achieve an increased production of collagen. After a feeding period of 20 days with refreshing the ascorbate-containing medium every second day, the ECM was visible macroscopically. Afterwards ECM-producing cells were lysed with ammoniumhydroxide and cell debris was removed by washing with distilled water. ECMs were stored at 4℃ for 24 h. The prepared ECM was repopulated with freshly isolated cells for 48 h.

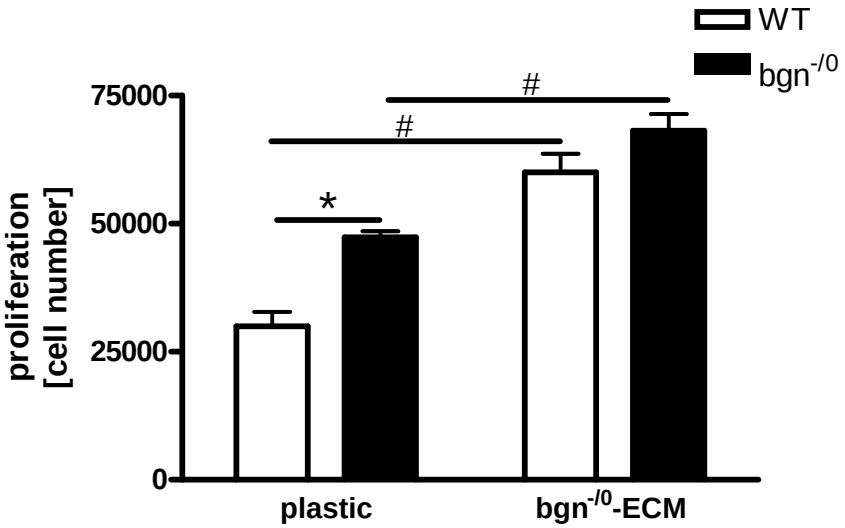

Figure 3-8 ECM derived from bgn$^{-/0}$-fibroblasts enhances proliferation of WT and bgn$^{-/0}$-fibroblasts

Proliferation on bgn$^{-/0}$-cell derived ECM enhanced WT-cell growth two fold over control on plastic and diminished the difference between bgn$^{-/0}$-fibroblasts and WT. *mean ± SEM; n =4; *, p<0.05 WT- versus bgn$^{-/0}$-fibroblasts ; # p<0.05 plastic versus bgn$^{-/0}$-ECM*

As shown in figure 3-8, pre-coating culture dishes with bgn$^{-/0}$-fibroblast derived ECM as growth substrate, enhanced proliferation remarkably 48 h after plating. For these experiments two different explant isolations per genotype were used

for ECM production and each ECM was populated with two independent explant isolations per genotype. ECM produced by bgn$^{-/0}$-fibroblasts enhanced proliferation of WT-fibroblasts 2.1 fold higher as compared to WT-control on plastic. The ECM produced by bgn$^{-/0}$-fibroblasts induced proliferation of bgn$^{-/0}$-fibroblasts only 1.4 fold higher compared to proliferation on plastic. The WT-ECM lacking biglycan diminished the difference in proliferation between the two genotypes, by increasing WT proliferation.

To investigate if increased proliferation on bgn$^{-/0}$-fibroblast derived ECM was due to a lack of biglycan, the proliferation on WT-derived ECM was analyzed in an identical approach. In this set of experiments, using WT cell-derived ECM, the proliferation of WT-fibroblasts was induced 1.8 fold over WT proliferation on plastic. Of note, WT-ECM inhibited the proliferation of bgn$^{-/0}$-fibroblasts, suggesting that the lack of biglycan was indeed responsible for the proliferative phenotype. On WT-ECM bgn$^{-/0}$-fibroblasts grew slower than on plastic and even slower than WT -fibroblasts that were stimulated by the pre-existing ECM.

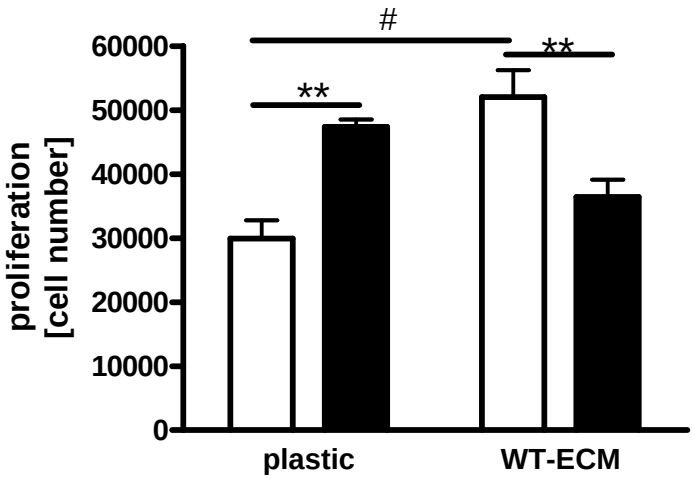

Figure 3-9 WT-ECM enhances WT-fibroblasts but inhibits bgn$^{-/0}$-fibroblasts

WT-ECM enhanced the proliferation of WT-fibroblasts to a higher degree than that of bgn$^{-/0}$-fibroblasts. *mean ± SEM; n =4; *, p<0.05 WT- versus bgn$^{-/0}$-fibroblasts ; # p<0.05 plastic versus WT-ECM*

These experiments using a cell-derived ECM as growth substrate revealed that a WT-ECM increased the proliferation of WT-fibroblasts and abolished the proliferation benefit of bgn$^{-/0}$-fibroblasts. Interestingly, the WT-ECM did not

stimulate WT-fibroblasts to the same extent as the bgn$^{-/0}$-ECM. These data support the hypothesis that a bgn$^{-/0}$-ECM provide a strong pro-proliferative benefit.

3.2.2 Overexpression of murine biglycan protein reverts pro-proliferative phenotype of bgn$^{-/0}$-fibroblasts

To rescue the phenotype by restoring biglycan expression, a lentivirus leading to biglycan overexpression was used. Therefore the murine biglycan mRNA was used as template from C57BL/6J WT mice. The construct was sequenced and reached 100 % sequence homology with the database sequence on NCBI Gene (NM_007542.4).

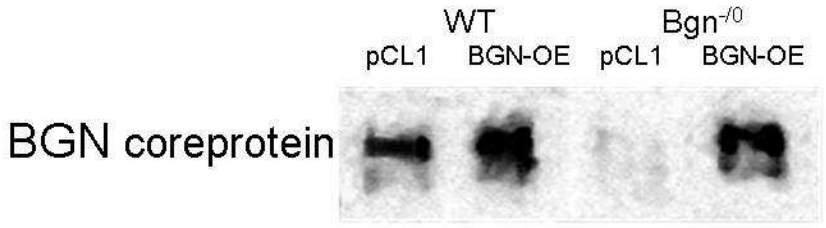

Figure 3-10 Lentiviral restoration of biglycan expression in bgn$^{-/0}$-fibroblasts
DEAE isolated proteoglycans from 1 ml of 4 days conditioned cell culture supernatants were subjected to chondroitinase ABC digestion to remove GAG chains from core protein. BGN-overexpression vector increased biglycan protein in supernatant conditioned by WT-fibroblasts. No core protein was detected in pCL1 mock transfected bgn$^{-/0}$-fibroblasts. Overexpression vector restored biglycan expression in bgn$^{-/0}$-fibroblasts.

Transfected fibroblasts were plated at 5000 cells / cm² and grown in 10 % serum for 72 hours. Afterwards cells were counted in a hematocytometer. The virus treatment slowed down cell growth but the proliferative benefit of bgn$^{-/0}$-fibroblasts remained constant. Over expressing biglycan protein in the bgn$^{-/0}$-fibroblasts abrogated the proliferation benefit.

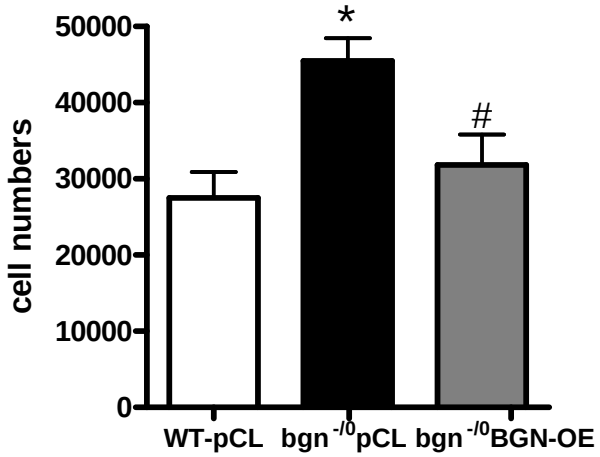

Figure 3-11 Lentiviral overexpression of biglycan protein abrogates the pro-proliferative phenotype of the bgn$^{-/0}$-fibroblasts.

Fibroblasts separated from explant cultures were transfected with lentiviral vectors. After seven days, fibroblasts were plated on new culture plates and the cell growth was determined 72 h after plating. WT -fibroblasts transfected with the empty mock vector pCL1 grew more slowly than bgn$^{-/0}$-fibroblasts transduced with pCL1 control vector (black bar). Bgn$^{-/0}$-fibroblasts transfected with biglycan (BGN-OE) vector were inhibited compared to bgn$^{-/0}$pCL1 and resembled to WT pCL1. *mean ± SEM; n = 5;* ,p<0.05 WT- versus bgn$^{-/0}$-fibroblasts both pCL1 transfected #; p<0.05 bgn$^{-/0}$pCL1 versus bgn$^{-/0}$BGN-OE*

3.3 Oil-supported collagen retraction (OSCR) assay revealed strong contractile phenotype of bgn$^{-/0}$-fibroblasts

The ability of cells to interact with and contract a collagen ECM is part of a physiological process referred to as traction. In addition, it is well known that myofibroblasts are a more contractile cell type than normal fibroblasts. We performed the oil-supported collagen retraction (OSCR) -assay according to Vernon and Gooden with some adaptations. The gels contained 1.25 mg/ml collagen and 15 x 10^3 cells per gel and were allowed to polymerize for two hours at 37℃. The gel contraction was documented 24 hours afterwards. Unpopulated control gels were used as standard for polymerization. The contraction of gels populated with WT- or bgn$^{-/0}$-fibroblasts was calculated as

percentage of the cell-free unpopulated control gels.Gels populated with WT-fibroblasts showed a contraction of 55.4 %. Bgn$^{-/0}$-fibroblasts showed a significantly stronger contraction of 68.6%.

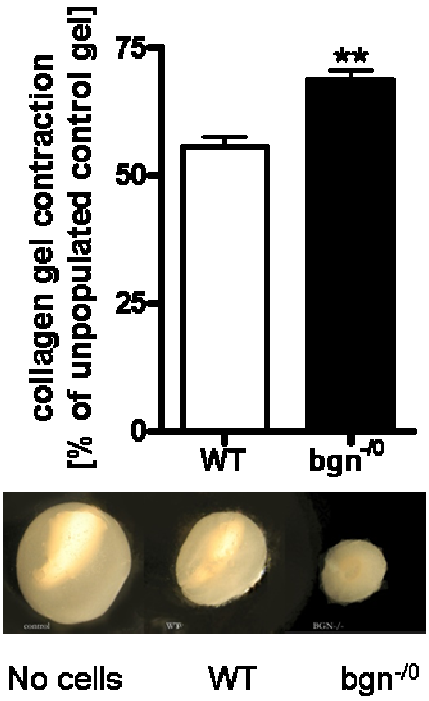

Figure 3-12 OSCR-assay revealed significantly stronger contractile abilities of bgn$^{-/0}$-fibroblasts.

Statistical analysis of OSCR-assay showed significantly increased contraction of collagen gels by bgn$^{-/0}$-fibroblasts (black bar, last image of contracted gels) compared to WT-fibroblasts (white bar second gel in the middle of original images), *mean ± SEM *;p<0.05; n=4*

Because stronger contractile abilities of myofibroblasts are a characteristic distinguishing these specialized cells from normal fibroblasts (20), the hypothesis was developed that bgn$^{-/0}$-fibroblasts undergo un-stimulated spontaneous differentiation into myofibroblasts.

3.4 Immunocytochemical analysis of bgn$^{-/0}$-fibroblasts phenotype

To investigate the differences that cause the varying behaviour of the bgn$^{-/0}$-fibroblasts as compared to WT-fibroblasts, the expression of ECM molecules and components of cytoskeleton as well as focal adhesions were visualized by immunocytochemical staining with specific antibodies. Actin stress fibres are commonly stained with fluorochrome-conjugated phalloidin that binds directly to F-actin fibres in the cytoplasm.

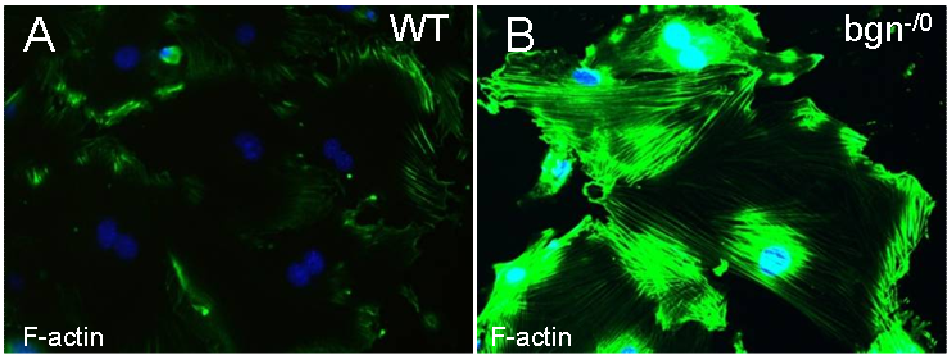

Figure 3-13 F-actin staining shows dramatic differences in the cytoskeleton of bgn$^{-/0}$-fibroblasts.

Fibroblasts of the first passage from both genotypes (WT and bgn$^{-/0}$) were stained for F-actin using phalloidin-FITC 24 h after plating. (**A**) In WT-fibroblasts fluorescent signal from phalloidin-FITC (in green) was limited to cortical sites at the plasmamembrane where actin-filaments are connected to membrane complexes like for example focal adhesions and cadherin clusters. Nuclear counterstaining was performed using Hoechst 3320 dye. (**B**) In bgn$^{-/0}$-fibroblasts F-actin stress fibres are thicker and stretch through the whole cell. Representative images are shown at 200 fold magnification.

It became obvious that bgn$^{-/0}$-fibroblasts had a denser F-actin cytoskeleton than WT-fibroblasts. In WT-fibroblasts the phalloidin signal mostly came from areas close to the cell membrane, where actin filaments end up close to focal adhesions. These so called cortical complexes at the plasma membrane serve as cell-matrix connecting points or more precisely as link between cytoskeleton and the ECM. In contrast to WT-fibroblasts, bgn$^{-/0}$-fibroblasts exhibit strong signals from filaments that were stretched through the whole cell, accumulating to dense bundles at the membrane. These findings suggested that differences

in the differentiation grade of bgn$^{-/0}$-fibroblasts could be responsible for the increased proliferation response.

The most common differentiation for fibroblasts is the transition into myofibroblasts, which is well characterized by incorporation of *de novo* synthesized α-smooth muscle actin (α-SMA) into stress fibres. This differentiation correlates with a higher expression of ECM components like collagens (e.g. collagen type I and collagen type VI), tropoelastin, the fibronectin fragment ED-A, focal adhesions, cadherins and stronger contractile abilities.

The analysed marker proteins, α-SMA, fibronectin ED-A and tropoelastin were increased in bgn$^{-/0}$-fibroblasts as shown in figure 3-13. This confirmed the hypothesis that bgn$^{-/0}$-fibroblasts might directly differentiate into myofibroblasts in cell culture.

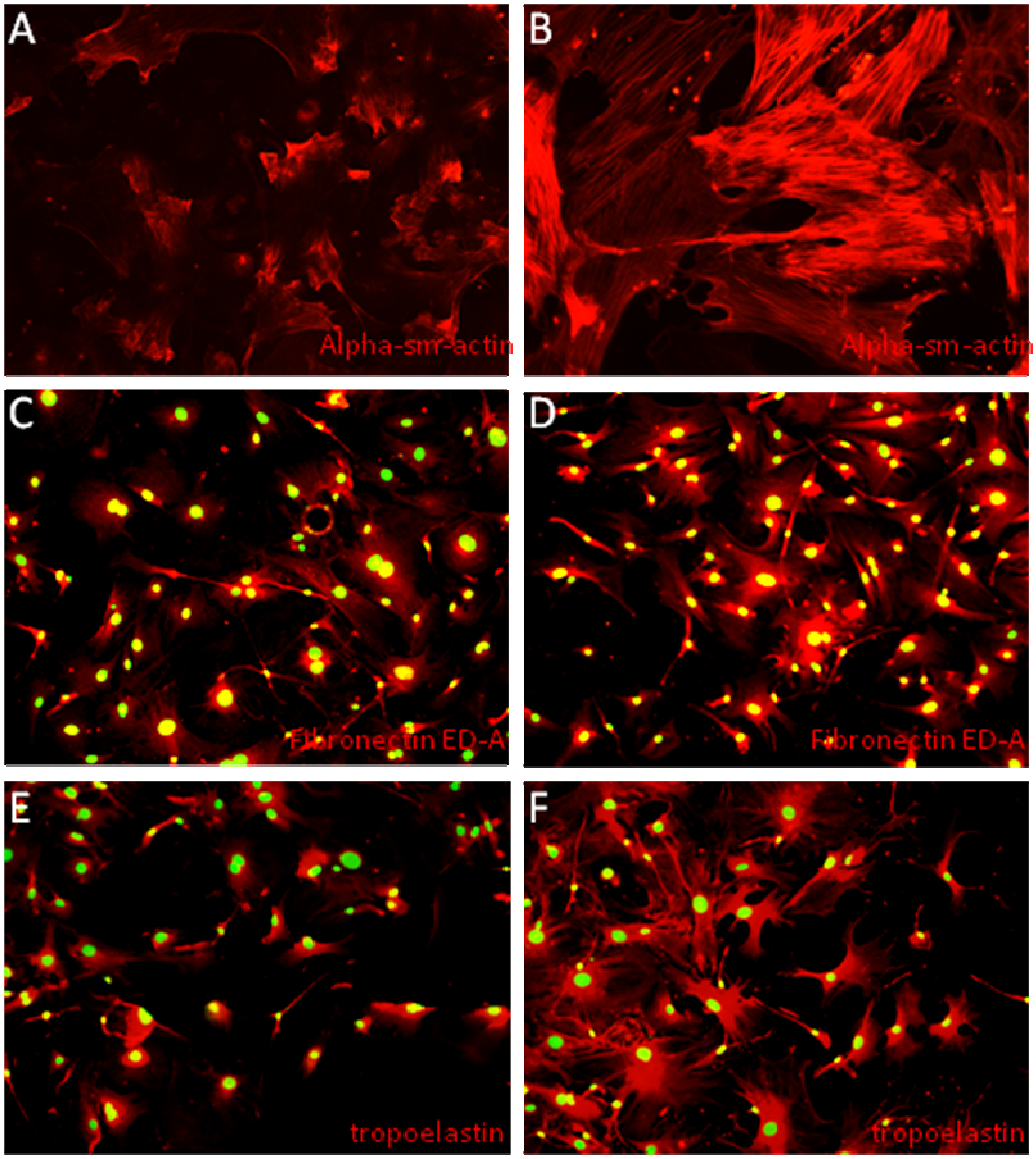

Figure 3-14 Immunocytochemical staining of differentiation marker α-SMA and differentiation-associated fibronectin fragment ED-A and tropoelastin.

Immunocytochemical characterization of WT-fibroblasts (**A**, **C**, **E**) compared to bgn$^{-/0}$-fibroblasts (**B**, **D**, **F**). Shown are representative images of staining for α-SMA (**A** and **B**), fibronectin ED-A (**C**, **D**) and tropoelastin (**E**, **F**) 24 h after plating. Bgn$^{-/0}$-fibroblasts show strong accumulation of myofibroblast markers, as WT-fibroblasts only show basal expression of these proteins. (**A**, **B**) are at 200 x and (**C**-**F**) 100 x magnification.

To further validate this thesis focal adhesion protein paxillin was stained immunocytochemically. This revealed another characteristic feature of myofibroblast differentiation in bgn$^{-/0}$-fibroblasts, which had more signals from

anti-paxillin staining than WT-fibroblasts, representing increased establishment of focal adhesions.

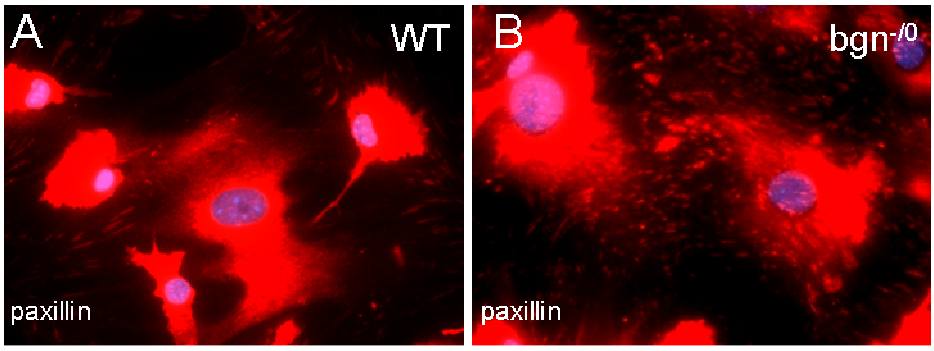

Figure 3-15 Representative Images of immunocytochemical staining for paxillin

Anti-paxillin staining showed less signals for paxillin in WT (***A***) compared to bgn$^{-/0}$-fibroblasts (***B***). More paxillin signals in immunolocalisation indicate increased numbers of focal adhesion complexes in bgn$^{-/0}$-fibroblasts. 200 x magnification

There are three filament systems in eukaryotic cells, the microfilaments which contain actins, the intermediate filaments (vimentin, desmin, lamin) and the microtubules composed of tubulins. While increased and differential expression of microfilaments and intermediate filaments mark the differentiation towards myofibroblast, the physiological role of microtubules during differentiation is largely unknown.

The immunohistochemical analysis of bgn$^{-/0}$-fibroblasts showed that microtubules are differentially regulated as well between the two genotypes.

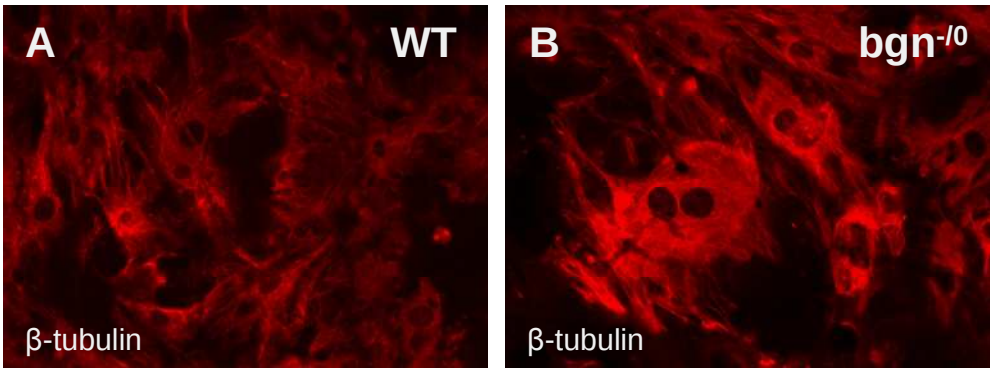

Figure 3-16 Representative images of immunocytochemical staining for β-tubulin

Anti-β-tubulin immunodetection showed stronger signals for β-tubulin in bgn$^{-/0}$-fibroblasts as compared to WT-fibroblasts. The microtubules in bgn$^{-/0}$-fibroblasts are considerable thicker and more prominent compared to microtubules in WT-fibroblasts. 200 x magnification.

3.5 Biochemical and molecular comparison of bgn$^{-/0}$-fibroblasts to WT-fibroblasts

Furthermore, protein expression and mRNA levels of certain markers of myofibroblast differentiation were analysed, to characterize the differences between bgn$^{-/0}$-fibroblasts and WT-fibroblasts more precisely.

A detailed analysis of protein expression and mRNA expression was performed to further prove the differentiation into myofibroblasts and point out the different aspects of the phenotype caused by the absence of biglycan. First, the hypothesis that bgn$^{-/0}$-fibroblasts differentiate into myofibroblasts was verified by α-SMA expression analysis.

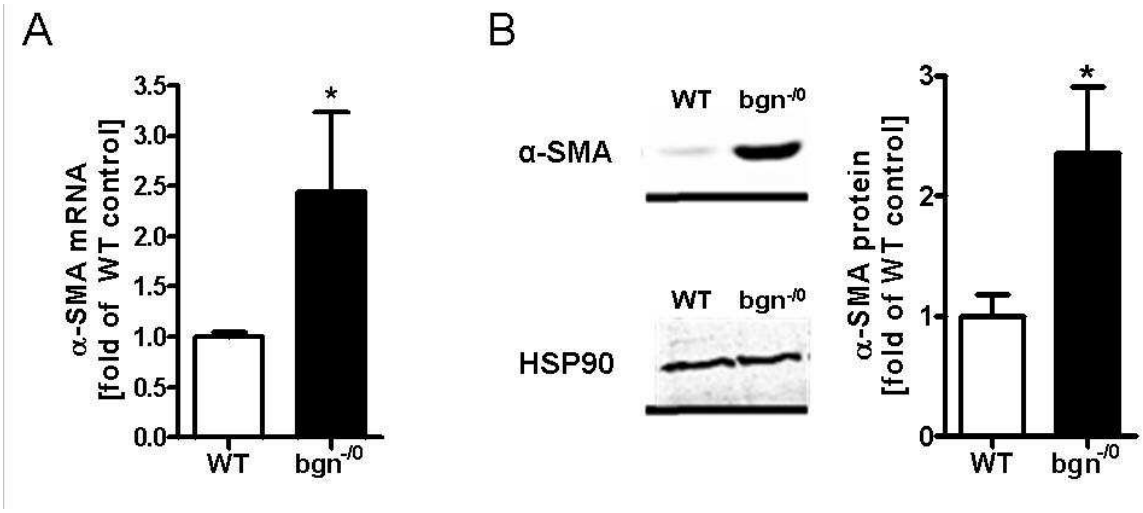

Figure 3-17 α-SMA mRNA and protein are increased in bgn$^{-/0}$-fibroblasts.

(**A**) The mRNA expression as well as (**B**) protein of α-SMA determined by real-time-RT-PCR and western blotting, are elevated in bgn$^{-/0}$-fibroblasts. (**B**) upper panel HSP90 as loading control and lower panel α-SMA protein in bgn$^{-/0}$- and WT-fibroblasts; *mean ± SEM; *, p<0.05; n=5*

The analysis of α-SMA revealed that WT-fibroblasts only express little amounts of α-SMA mRNA and protein, while both m-RNA and protein of α-SMA are increased of about 2.5 fold in bgn$^{-/0}$-fibroblasts, proving a differentiation into active myofibroblasts. It was demonstrated that the pro-proliferative phenotype of bgn$^{-/0}$-fibroblasts could be rescued by lentiviral-mediated restoration of

biglycan expression. To analyse if the high expression of α-SMA in bgn$^{-/0}$-fibroblasts could be reversed by overexpression of biglycan protein too, the protein level of α-SMA in pCL1 and BGN-OE transduced cells was analysed by western blotting.

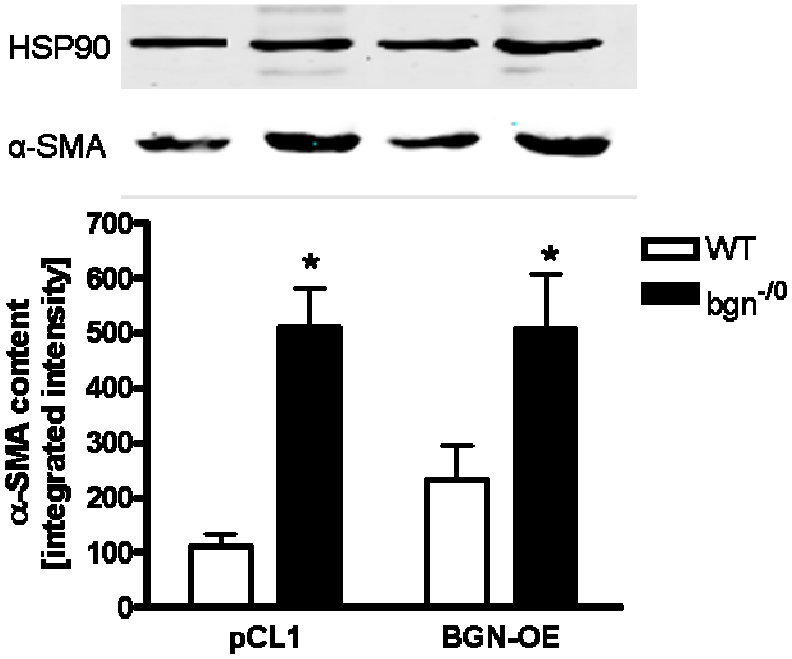

Figure 3-18 Overexpression of bgn does not reduce α-SMA protein in bgn$^{-/0}$fibroblasts

The protein level for α-SMA in WT and bgn$^{-/0}$-fibroblasts 7 days after transfection with pCL1 mock vector, or BGN-overexpression (OE) vector was determined by western blot. In the upper panel HSP90 is shown as loading control. α-SMA protein in WT- and bgn$^{-/0}$fibroblsts is shown in the lower panel. α-SMA protein was quantified for statistical analysis using a Two-Way-ANOVA of variances; *mean ± SEM; *, p<0.05 WT- versus bgn$^{-/0}$-fibroblasts; n=3*

Figure 3-18 shows that restoring the expression of biglycan in bgn$^{-/0}$-fibroblasts did not reduce the amount of α-SMA in these cells. Thus the differentiation phenotype caused by biglycan deficiency was not rescued by lentiviral biglycan expression as was the proliferative phenotype.

The accumulation of α-SMA is characteristic of the differentiation into myofibroblasts. Differentiated myofibroblasts are capable of remodelling the surrounding matrix. This remodelling of ECM is accompanied by expression of high levels of structural ECM molecules, but also by high expression of crosslinking and ECM degrading enzymes. Therefore, a small set of crosslinking and ECM degrading enzymes was analysed.

3.5.1 ECM crosslinking and degrading enzymes are differentially regulated in bgn$^{-/0}$-fibroblasts compared to WT-fibroblasts

ECM crosslinking enzymes like the pro-collagen-prolyl-oxidases (PLOD) are directed to different epitopes in structural components of the ECM such as collagen. These enzymes oxidate specific amino acids and facilitate bindings between aligned molecules, but their function is not limited to ECM stabilization. The tissue transglutaminases (tgm) 1 and 2 are supposed to play a role during apoptosis and cellular differentiation for example .

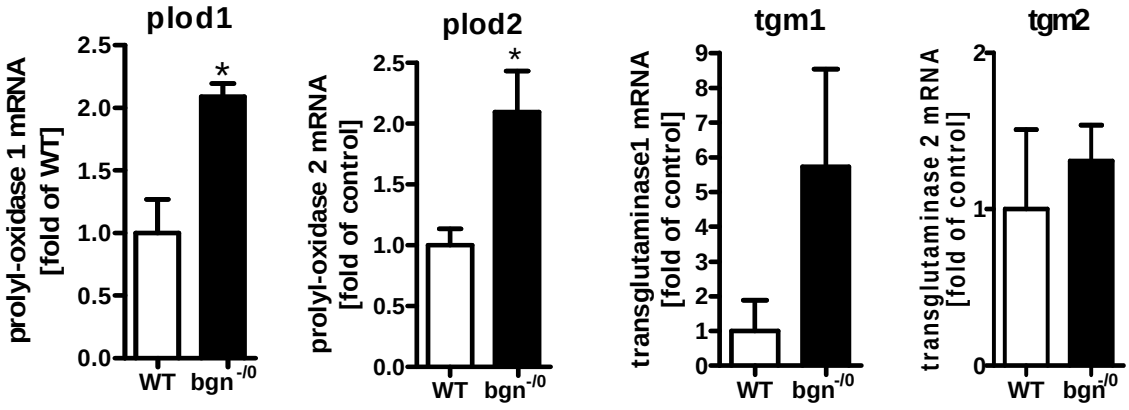

Figure 3-19 Expression of ECM crosslinking enzymes was altered in bgn$^{-/0}$-fibroblasts.
The total mRNA from 10000 cells/cm² were collected 24 h after plating. The mRNA was transcribed into cDNA and used for real-time-RT-qPCR for pro-collagen prolyloxidase isoforms 1 and 2 and tissue transglutaminase isoforms 1 and 2. *mean ± SEM; n = 3; *, p<0.05 WT- versus bgn$^{-/0}$-fibroblasts*

During cardiac remodelling *de novo* synthesis and crosslinking of ECM mark only one part of the process, degradation of ECM is the other part. As already mentioned crosslinking of ECM molecules stabilizes the ECM. But in order to establish a stable ECM after injury, the previously disrupted ECM has at least in part to be removed. ECM degradation is an important process that generates fragments that are capable of inducing signalling for example via integrins. Post infarct remodelling is characterised by production of ECM or scar tissue that has to adapt to a stronger wall pressure and a loss of cardiomyocytes. To achieve this both processes crosslinking and degradation have to take place.

ECM breakdown is mostly executed by matrix metalloproteinases. This family of enzymes includes far more than thirty members by now. In charge for collagen breakdown and fibronectin degradation only a small subset was analysed by real time RT-PCR to display the ECM degradation abilities of the primary cardiac fibroblasts, in the absence of biglycan. Only trends towards of different expressions were detectable, but the discovery that MMP1a is down while MMP9 and 13 are likely to be up-regulated, may hint towards different profiles of ECM degrading enzymes caused by these two different genotypes.

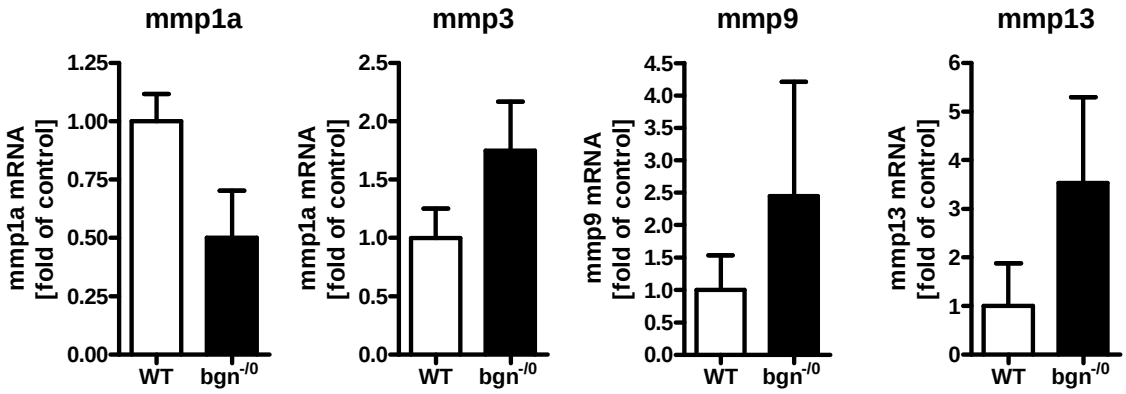

Figure 3-20 Expression of matrix metalloproteinases 1a, 3, 9 and 13 showed a trend towards differential regulation and in bgn$^{-/0}$-fibroblasts compared to WT.

The total mRNA from 10000 cells/cm² were collected 24 h after plating. The mRNA was transcribed into cDNA and used for realtime-RT-qPCR for matrix metalloproteinases 1a, mmp3, mmp9 and mmp13. *mean ± SEM; n = 3; *, p<0.05 WT- versus bgn$^{-/0}$-fibroblasts*

3.5.2 Induction of matrix receptors and cytoskeleton-membrane-anchoring complex in bgn$^{-/0}$-fibroblasts

Molecules like the CD44 receptor (30) and the dystrophin associated protein complex (DAPC) (32) have been shown to interact with biglycan. CD44 is known to be involved and up-regulated in cardiac remodelling and myofibroblast differentiation (31,63), while the DAPC is expressed in cardiomyocytes and

myofibroblasts, but hardly detectable in normal fibroblasts (22,33). CD44 is also involved in focal adhesion establishment and influences the motility of fibroblasts. CD44 is discussed as a factor that is necessary for the recruitment of fibroblasts to sites of injury (39).

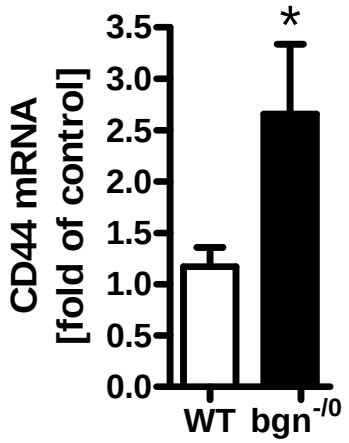

Figure 3-21 The expression of CD44 was significantly increased in bgn$^{-/0}$-fibroblasts.
The total mRNA from 10000 cells/cm² were collected 24 h after plating. And CD44 expression was analysed by realtime RT-PCR. *mean ± SEM; n = 7- 5; *, p<0.05 WT- versus bgn$^{-/0}$-fibroblasts.*

It is well documented that CD44 is able to activate TGF-β signalling by MMP activation, which leads to TGF-β release from the ECM, where it is sequestered by biglycan and decorin (64). Furthermore, it is known that TGF-β is the most familiar inducer of myofibroblast differentiation (65). Up to now it has never been described that biglycan influences the expression of CD44.

The DAPC is a mechano-transduction complex that connects the ECM and the cytoskeleton using integrins (66). Via this linkage the DAPC transduces mechanical force or traction from the cytoskeleton to the ECM. Furthermore the DAPC-integrin complex is involved in recognition of tension that is applied to the ECM. As myofibroblasts exhibit strong traction forces on the ECM as shown in figure 3-11, it was tested whether bgn$^{-/0}$-fibroblasts express higher levels of DAPC. It is shown here for the first time that biglycan deficiency upregulated dystrophin as part of the DAPC.

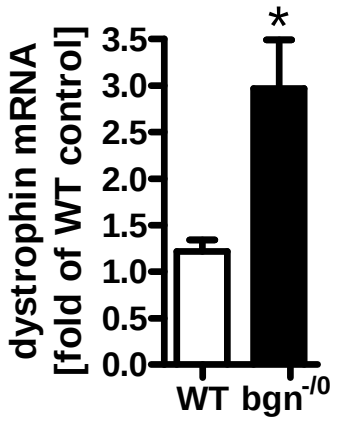

Figure 3-22 The mRNA expression of dystrophin was significantly increased in bgn$^{-/0}$-fibroblasts

The total mRNA from 10000 cells/cm² were collected 24 h after plating. And dystrophin expression was analysed by real-time RT-PCR. mean ± SEM; n = 7- 5; *, p<0.05 WT- versus bgn$^{-/0}$-fibroblasts.

3.5.3 Characterization of TGF-β system in bgn$^{-/0}$-fibroblasts

TGF-β activity is regulated by several mechanisms. Firstly the expression of TGF-β and its receptors can be regulated, secondly TGF-β is secreted as a pro-peptide that has to be modified and dimerize to the mature TGF-β form. TGF-β when secreted can bind to a latency complex and this complex as well as the mature TGF-β can be sequestered into the ECM, for example upon binding to biglycan. Due to the variety of possible pathways to regulate TGF-β neither protein nor mRNA levels alone give sufficient information concerning the activity of TGF-β signalling system. Nevertheless unbound, free secreted TGF-β was analysed in cell culture supernatants by TGF-β ELISA, as well as the mRNA or TGF-β1 and TGF-βRII.

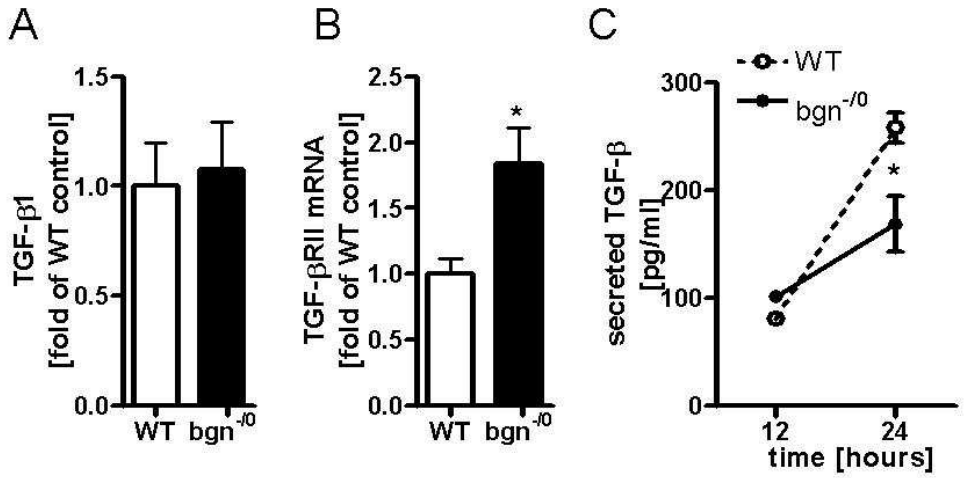

Figure 3-23 TGF-β receptor type II is strongly up-regulated, while TGF-β itself remains unchanged.

(**A**) TGF-β 1 and (**B**) TGF-β Receptor Type II mRNA were analyzed by real-time RT-qPCR. (**C**)Endogenously secreted TGF-β of cell culture supernatants was analyzed by TGF-β ELISA. Supernatants were collected at 12 and 24 h after plating. *Mean ± SEM; n = 3; *, p<0.05 WT-versus bgn$^{-/0}$-fibroblasts. Mean ± SEM; n = 6-7; *, p<0.05 WT- versus bgn$^{-/0}$-fibroblasts.*

The reduced levels of free TGF-β detected after 24 hours are possibly due to diminished secretion or enhanced sequestration to the ECM, more likely is the alternative that TGF-β may have been bound to its surface receptor in a higher extent. Consequently these early results encouraged the further investigation of the role of TGF-β in the bgn$^{-/0}$-fibroblasts.

3.6 The neutralization of TGF-β rescues the pro-proliferative phenotype and differentiation of bgn$^{-/0}$-fibroblasts

To facilitate the role of intrinsic TGF-β in the pro-proliferative, differentiated phenotype of bgn$^{-/0}$-fibroblasts, the cells were grown in the presence of TGF-β neutralizing antibody.

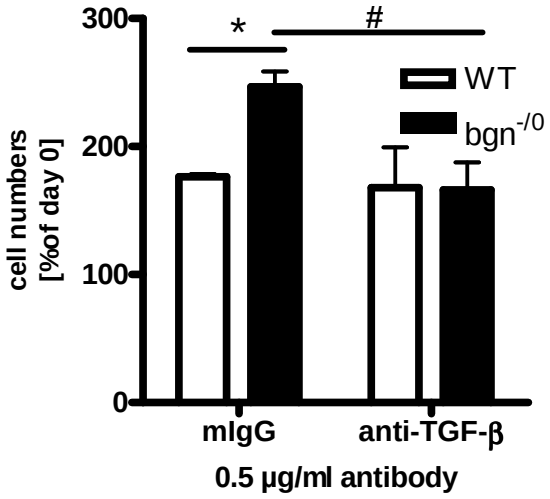

Figure 3-24 The proliferation benefit of bgn$^{-/0}$-fibroblasts was abolished by neutralizing endogenous TGF-β signalling

Proliferation in response to treatment with a neutralizing antibody to TGF-β (0.5 µg/ml) or isotype IgG was determined 48 h after plating in the presence of the antibodies by counting cells in a hematocytometer. *Mean ± SEM; n = 3; *, p<0.05 WT- versus bgn$^{-/0}$-fibroblasts; #, p<0.05 bgn$^{-/0}$anti-TGF-β versus bgn$^{-/0}$IgG treated*

These experiments clearly showed that the pro-proliferative phenotype of bgn$^{-/0}$-fibroblasts was due to endogenous TGF-β signalling, as neutralisation of endogenous TGF-β completely abolished the proliferation benefit of bgn$^{-/0}$-fibroblasts while the WT -fibroblasts were not affected at all.

To analyse if the contractile phenotype and the alterations of the cytoskeleton were also caused by the endogenous TGF-β signalling the neutralizing antibody was also used in the OSCR-Assay and treated cells were analysed by immunocytochemistry with respect to α-SMA incorporation into stress fibres.

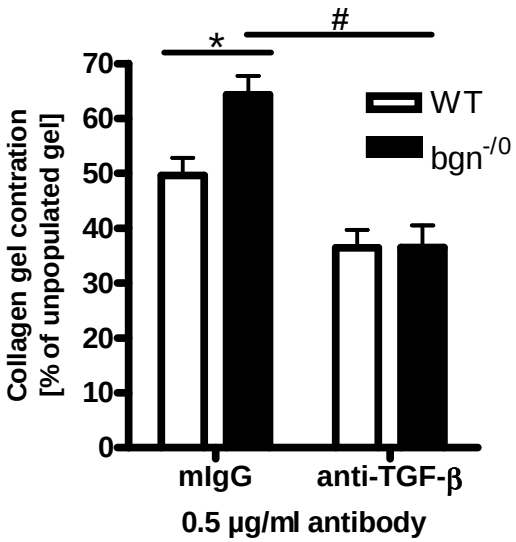

Figure 3-25 Contraction of collagen matrix is inhibited in the presence of neutralizing antibody to TGF-β

Contraction after 24 h treatment with a neutralizing antibody to TGF-β (0.5 µg/ml) or isotype IgG was determined by image analysis. *Mean ± SEM; n = 3; *, p<0.05 WT- versus bgn$^{-/0}$-fibroblasts; #, p<0.05 bgn$^{-/0}$anti-TGF-β versus bgn$^{-/0}$IgG treated*

The contractile abilities of both genotypes were completely blocked in the OSCR-assay by TGF-β neutralisation, which shows that neutralising endogenous TGF-β not only abolishes the proliferation benefit, but the differentiation into myofibroblasts as well.

This was also confirmed by immunocytochemical analysis shown in figure 3-25, which clearly showed that due to the neutralisation of endogenous TGF-β, bgn$^{-/0}$-fibroblasts lost their ability to incorporate α-SMA into stress fibres.

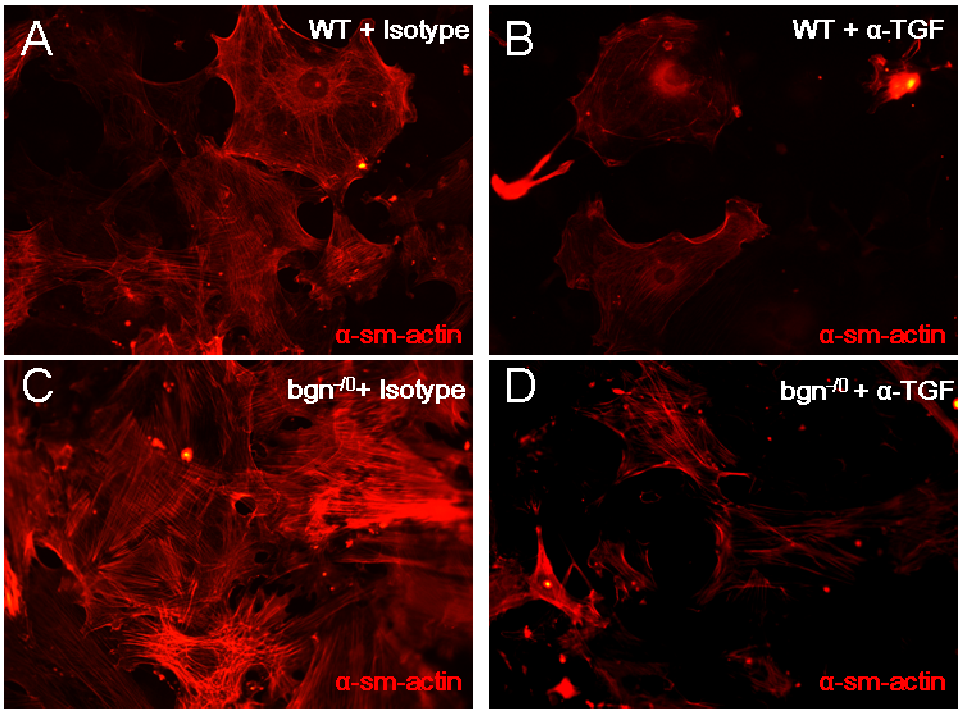

Figure 3-26 bgn$^{-/0}$-myofibroblast phenotype reverses by neutralizing endogenous TGF-β signalling.

Representative images of immunocytochemical staining of α-SMA showing a slight reduction of cortical α-SMA in WT-fibroblasts (***A, B***) after 24 h treatment with the neutralizing anti TGF-β antibody (0.5 µg/ml; ***B, D***) compared to the IgG isotype control (***A, C***). In bgn$^{-/0}$-fibroblasts (***C, D***) treatment with the TGF-β neutralizing antibody led to a phenotypical reversion of myofibroblast characteristics by strong reduction of α-SMA (***D***). *Representative images of n=4 experiments 200 x magnification.*

3.7 TGF-β signalling in bgn$^{-/0}$-fibroblasts

TGF-β signalling is not limited to the canonical pathway of SMAD signalling. TGF-β can interact directly or indirectly by transactivation with various cell surface receptors that still have not been identified in total. TGF-β beside the canonical way can activate several cascades that include different signalling molecules and consequently lead to different cellular outcomes. It is commonly agreed that TGF-β signalling shows cross talk with WNT signalling, MAPK pathway including p38, the SAPK/JNK pathway and ERK. The classical canonical pathway involves the SMAD proteins. SMAD 2 and 3 are receptor-

activated SMADs that become phosphorylated upon receptor activation and build a complex with the common SMAD4. This complex translocates into the nucleus and acts as a transcription factor. There was no difference in SMAD3 phosphorylation, while SMAD2 was significantly stronger phosphorylated in bgn$^{-/0}$-fibroblasts under normal conditions compared to WT-fibroblasts (fig. 3-26).

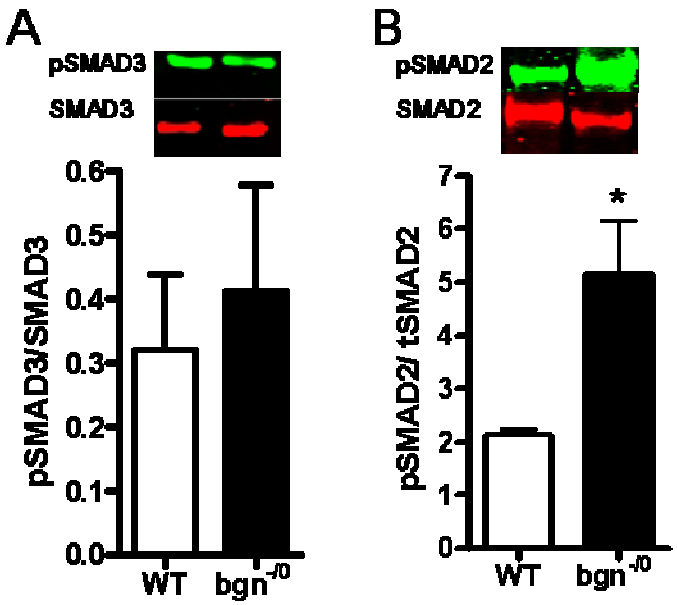

Figure 3-27 SMAD signalling shows over-activity of TGF-β in the absence of biglycan limited to SMAD2 phosphorylation

The phosphorylation of SMAD3 and SMAD2 (pSMAD) was detected in total lysates from 10000 cells/cm² 24 h after plating under standard conditions. Phosphorylation was calculated as the quotient of the integrated intensity of total SMAD and phosphorylated SMAD. *Mean ± SEM; n = 5; 3; *, p<0.05 WT- versus bgn$^{-/0}$-fibroblasts*.

These results demonstrate that despite missing differences in the TGF-β expression (fig.3-22), TGF-β signalling is highly activated and mediates signalling by enhanced phosphorylation of Smad2, which nicely correlates with increased expression of TGF-βRII in bgn$^{-/0}$-fibroblasts and the myofibroblast phenotype.

These western blots also showed that phosphorylated SMAD2 was degraded because multiple cleavage fragments that were absent in the WT protein lysates appeared during these experiments in bgn$^{-/0}$-fibroblasts.

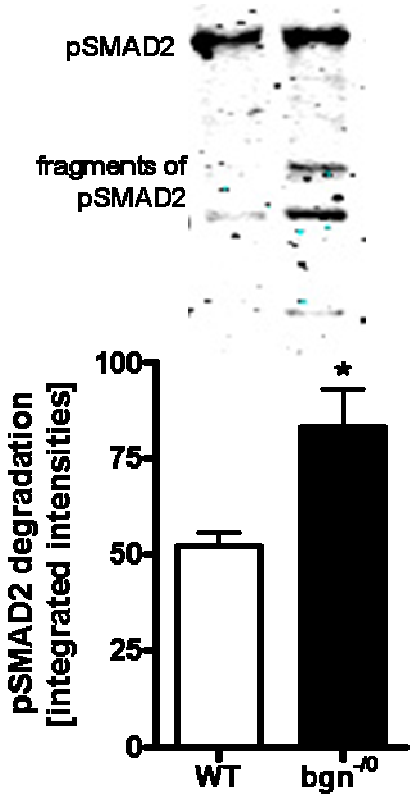

Figure 3-28 Additional bands detected by anti-phosphoSMAD2 antibody in lysates from bgn$^{-/0}$-fibroblasts reflect increased phosphoSMAD2 degradation.

In total lysates from WT- (white bar) and bgn$^{-/0}$-fibroblasts (black bar) 24 hours after plating, phospho-SMAD2 antibody detects fragments of phosphorylated SMAD2, which are predominantly present in samples collected from bgn$^{-/0}$-fibroblasts. *Mean ± SEM; n = 4-5; *, p<0.05 WT- versus bgn$^{-/0}$-fibroblasts*.

Smad2 is degraded as a negative feedback of TGF-β signalling. This degradation of SMAD2 by the proteasome is initiated by ubiquitinilation of SMAD2 by E2-ubquitin ligase SMURF2. But it is also reported that Smurf2 upon binding to phosphorylated Smad2 first recruits transcription repressors like SNoN and Ski for degradation (40). To analyse this additional possibility by which the complex of Smurf2 and phospho-SMAD2 might actively induce signalling, the expression of SMURF2 was analysed by western blotting.

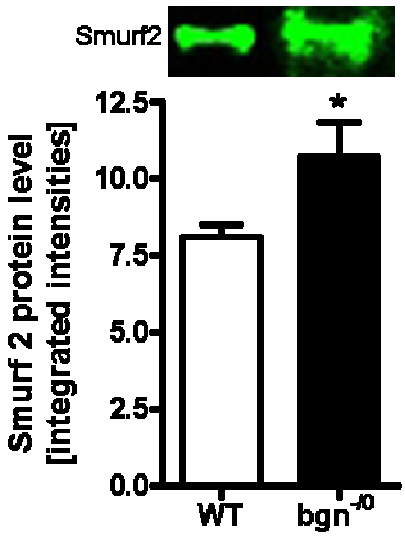

Figure 3-29 SMURF 2 protein is significantly increased in bgn$^{-/0}$-fibroblasts.
SMURF2 was detected in total lysates from fibroblasts grown at a density of 10000 cells/cm² under standard conditions 24 h after plating. *Mean ± SEM; n = 7; *, p<0.05 WT- versus bgn$^{-/0}$-fibroblasts*.

Another crucial factor that is induced by TGF-β signalling is SMAD7, which is a so called inhibitory SMAD protein. SMAD7 represses most of the TGF-β regulated cellular responses like proliferation and ECM production, but SMAD 7 is required for TGF-β induced apoptosis, through its interaction with β-catenin. It stabilizes β-catenin in the cadherin complex. Furthermore, high levels of β-catenin and SMAD7 can cause an increase in c-myc. Together with p53 those two are postulated to induce apoptosis (42).

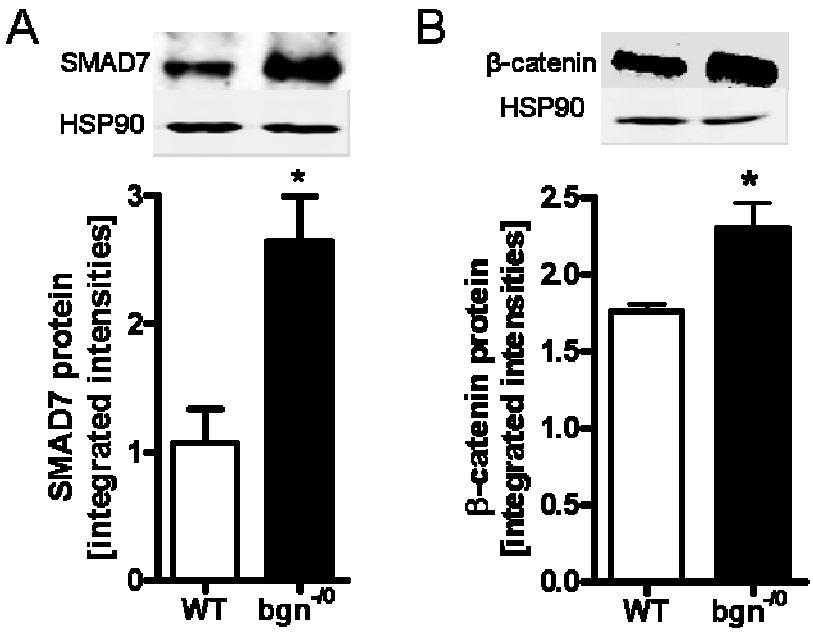

Figure 3-30 SMAD 7 and β-catenin protein are increased in bgn$^{-/0}$-fibroblasts.

SMAD7 (**A**) and β-catenin (**B**) were detected in total lysates from fibroblasts grown at a density of 10000 cells/cm² under standard conditions 24 h after plating. Loading of equal protein amounts was visualized by detection of HSP90. *Mean ± SEM; n =3-6; *, p<0.05 WT- versus bgn$^{-/0}$-fibroblasts.*

According to literature TGF-β induced apoptosis is mediated via high expression levels of SMAD7 and β-catenin, which induce the expression of c-myc and p53. Because both molecules are increased in bgn$^{-/0}$-fibroblasts it was examined if bgn$^{-/0}$-fibroblasts undergo apoptosis under standard conditions.

Indeed it was detected that PARP 1 cleavage as well as Caspase3 cleavage were increased in bgn$^{-/0}$-fibroblasts.

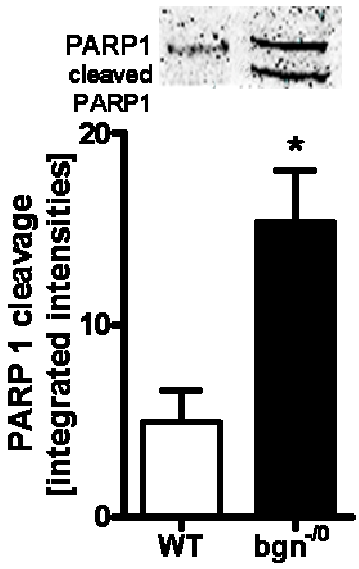

Figure 3-31 Increased cleavage of PARP 1 points towards pro-apoptotic phenotype of bgn$^{-/0}$-fibroblasts in response to over-active TGF-β signalling.

PARP1 and cleavage of PARP1 was detected in total lysates from fibroblasts grown at a density of 10000 cells/cm² under standard conditions 24 h after plating. *Mean ± SEM; n =9; *, p<0.05 WT- versus bgn$^{-/0}$-fibroblasts*.

Therefore the current data may suggest that the enhanced endogenous TGF-β signalling that leads to differentiation of cardiac fibroblasts into myofibroblasts is in turn subsequently accompanied by increased apoptosis of myofibroblasts.

3.8 Translation of *in vitro* results to post infarct remodelling *in vivo*.

In vitro findings often do not correlate with the *in vivo* situation. To verify the relevance of this *in vitro* data it was a necessity to analyse if the biglycan knock out leads to enhanced myofibroblast differentiation after myocardial infarction *in vivo* as well. In post infarction remodelling TGF-β and biglycan are both up-regulated. While TGF-β is an early phase responding gene, biglycan expression is induced at the late phase after myocardial infarction (52,67).

The basal mRNA expression of α-SMA in heart was contributed by smooth muscle cells of coronary arteries and a few active interstitial myofibroblasts. It is of note, that the basal expression of α-SMA in bgn$^{-/0}$-fibroblasts was already

elevated, which points towards already active myofibroblasts, because bgn$^{-/0}$-mice show no increased vascularisation of the heart.

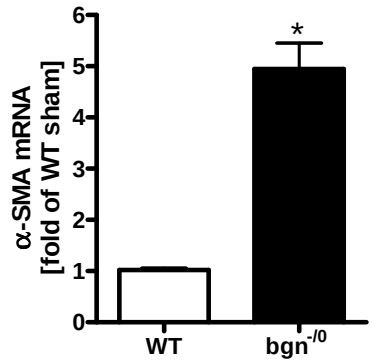

Figure 3-32 Basal α-SMA mRNA expression in cardiac *apex cordis* of bgn$^{-/0}$-mice is significantly increased.

The mRNA of α-SMA is dramatically increased in 1 mm cardiac *apex cordis* samples from sham bgn$^{-/0}$-mice compared to age matched littermate WT-mice. *Mean ± SEM; n =5; *, p<0.05 WT-versus bgn$^{-/0}$-mice.*

After myocardial infarction the expression of α-SMA increases, this is caused by increasing myofibroblast differentiation. This effect can be a first approach to examine myofibroblast differentiation and the amount of these cells. The basal levels of α-SMA mRNA was quantified in the cardiac *apex cordis* of twelve weeks old sham mice. The result shown in fig. 3-31 demonstrates that in bgn$^{-/0}$-hearts the expression of α-SMA is already increased, which suggests that fibroblasts are spontaneously differentiated into myofibroblasts in uninjured bgn$^{-/0}$-hearts as well.

Subsequently the expression of α-SMA mRNA in infarcted hearts was analysed.

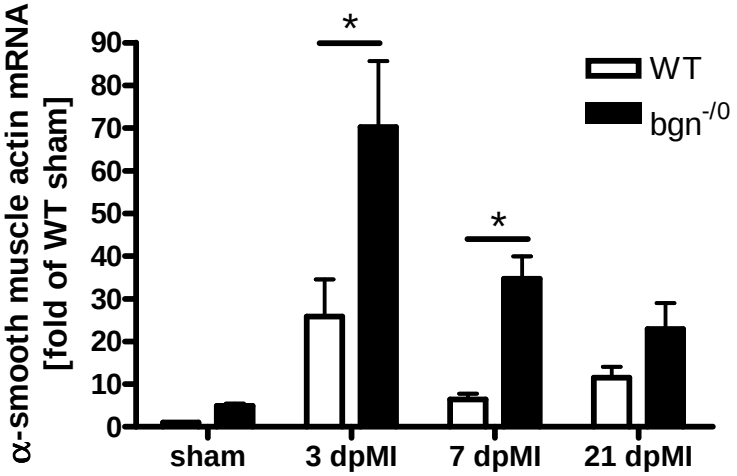

Figure 3-33 In response to experimental myocardial infarction the α-SMA mRNA expression in cardiac *apex cordis* was increased and remained elevated in bgn$^{-/0}$-hearts at days 3 and 7 after MI.

Apex cordis from sham and post infarction hearts were lysed for total RNA extraction. mRNA was transcribed into cDNA and analyzed in real time RT-PCR for quantification of α-SMA expression. *Mean ± SEM; n = 4-9; *, p<0.05 WT- versus bgn$^{-/0}$-fibroblasts.*

The mRNA expression of α-SMA increased in response to MI. At day three after MI the signal in WT hearts was most prominent. The amount of α-SMA mRNA decreased thereafter but persisted elevated towards the late time point of 21 days after infarction. In WT-hearts the amount of myofibroblasts at day 21 was already decreased by nearly 40 % of the amount at day 3. In bgn$^{-/0}$-hearts the presence of myofibroblasts from day 3 declines by about 32 % to day 21 after MI. Therefore the rate of myofibroblast clearance seemed to be unaffected

The increase of the mRNA always precedes the appearance of the protein. Immunohistochemical staining of α-SMA in murine MI was performed to answer the question if myofibroblasts or angiogenesis induce the high levels of α-SMA mRNA. At day 3 after MI only a few positive cells were detected as can be seen in figure 3-33. The immunolocalization of α-SMA within the infarct showed a distinct localization of α-SMA positive cells in coronary vessels and non-myocyte cells.

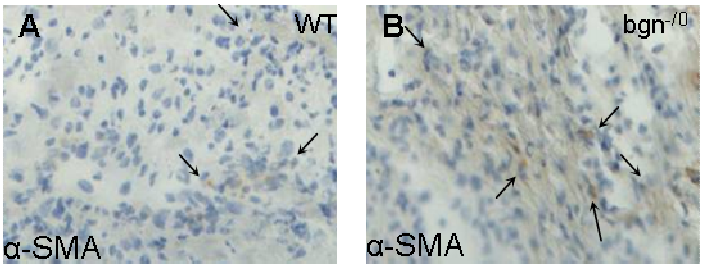

Figure 3-34 Immunohistochemical staining showed higher accumulation of α-SMA positive fibroblasts in the peri-infarct zone 3 days after MI

Representative images of immunohistochemical staining of α-SMA demonstrating the appearance of myofibroblasts in the peri-infarct zone 3 days post MI with more α-SMA positive cells not located to vessels in bgn$^{-/0}$-hearts compared to WT littermates. Arrows indicate α-SMA positive myofibroblasts.

For day 7 after experimental MI these α-SMA positive cells were quantified in a defined area of 90000 µm², beginning at the fibrotic border to the infarct. Vessels were excluded from analysis.

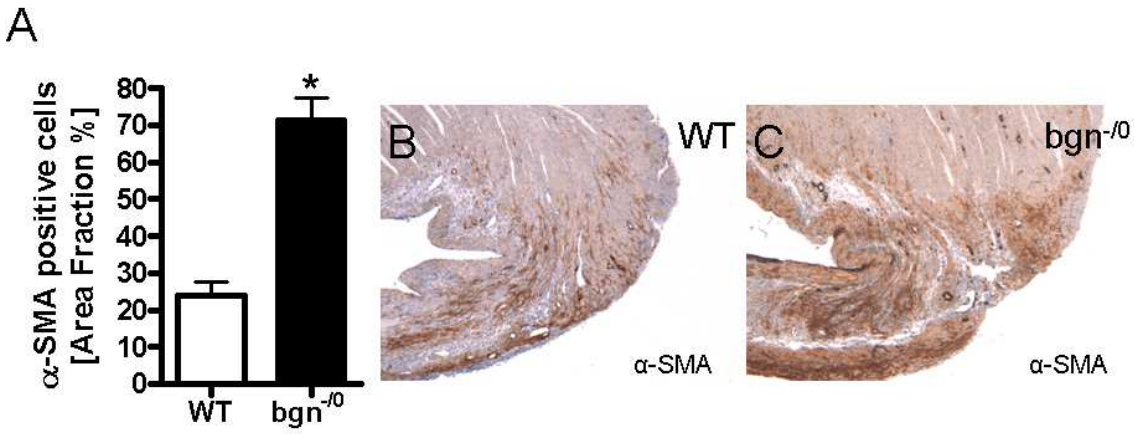

Figure 3-35 Immunohistochemical staining showed increased accumulation of α-SMA positive fibroblasts in the peri-infarct zone at 7 days post MI

(**A**) Quantification of positively stained cells within 90000 µm² of the infarct border. *Mean ± SEM; n =4-9; *, p<0.05 WT- versus bgn$^{-/0}$-fibroblasts.* (**B, C**) Representative images of immunohistochemical staining of α-SMA displaying active myofibroblasts in the peri-infarct zone 7 days post MI with more positive cells in bgn$^{-/0}$-hearts (**C**) as compared to WT-hearts (**B**).

The analysis of the infarcted hearts revealed that there were more α-SMA positive myofibroblasts at day 7 after MI than at day 3. Furthermore it became

obvious that there were significantly increased amounts of α-SMA positive cells in infarcts from bgn$^{-/0}$-mice at both time points. These data suggest that the *in vitro* results may be relevant for the post infarct remodelling *in vivo*, revealing that due to biglycan-deficiency more fibroblasts differentiate into myofibroblasts in the scar. As this may lead to extra tensions within the scar, this might contribute to rupture of the infarcted ventricle as described before (52).

3.8.1 Bgn$^{-/0}$-myofibroblasts fail to activate nNOS despite DAPC up-regulation *in vivo* after experimental MI

The question remains, if there is a link between biglycan and a possible characteristic functional marker for myofibroblasts in *vivo*. The detection of increased dystrophin expression in bgn$^{-/0}$-fibroblasts is described here as one hallmark for the differentiation *in vitro*. Immunohistochemical staining for dystrophin in post infarct hearts of WT and bgn$^{-/0}$-mice revealed a surprising result. In the heart of bgn$^{-/0}$-mice, cardiomyocytes showed stronger signals for dystrophin in their plasma membrane. In addition cardiac myofibroblasts in the infarct express dystrophin too.

These dystrophin positive fibroblasts appear in the same amount as the α-SMA positive myofibroblast. In direct comparison it became obvious that in bgn$^{-/0}$-mice the signal for dystrophin-positive fibroblasts was dramatically increased showing a similar pattern as the α-SMA positive myofibroblasts.

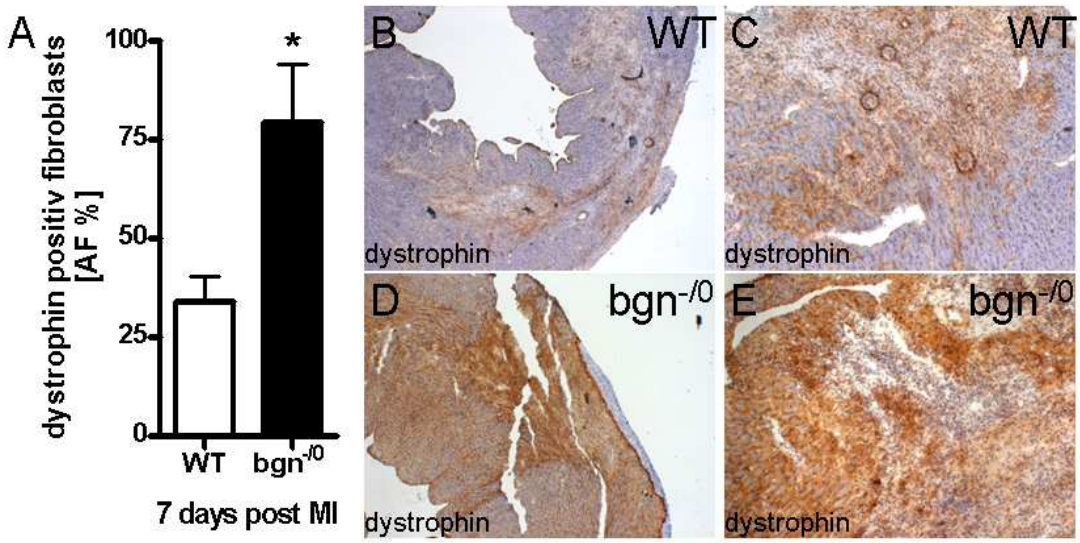

Figure 3-36 The immunolocalization of dystrophin in the infarcted area shows dramatically increased numbers of dystrophin in bgn$^{-/0}$-hearts after experimental myocardial infarction

(**A**) Quantification of 90000 µm² of the infarct border. Positively stained cells were determined as percentage of total area and given as area fraction. *Mean ± SEM; n =4-9; *, p<0.05 WT- versus bgn$^{-/0}$-mice.* Representative images of immunohistochemical staining of dystrophin demonstrate stronger signals in bgn$^{-/0}$-fibroblasts compared to WT littermates. (**B, D**)Pictures were taken at 40 x magnification and (**C, E**) 100 x magnification.

To verify these immunohistochemical results the mRNA expression of dystrophin in *apex cordis* samples from mice that were subjected to experimental MI was analysed. It could be shown that, while dystrophin mRNA was elevated in response to the infarction in WT-mice, it was even more increased in bgn$^{-/0}$-mice.

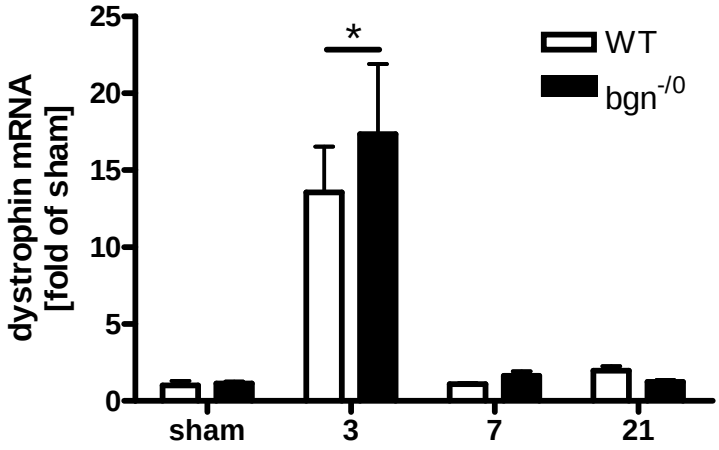

Figure 3-37 Dystrophin mRNA was increased in response to myocardial infarction and even more elevated to in bgn$^{-/0}$-mice comp

Apex cordis from sham and post infarct hearts were lysed for RNA extraction. RNA was transcribed into cDNA and analyzed by real time RT-PCR for quantification of dystrophin mRNA expression. *Mean ± SEM; n =4-9; *, p<0.05 WT- versus bgn$^{-/0}$--mice.*

It has been reported that biglycan influences the expression of syntrophins which represent the cytosolic components of the DAPC (32). Among the biglycan regulated proteins is α-syntrophin, which is up-regulated in bgn$^{-/0}$-mice (fig. 3-37). Syntrophin is a linking protein that binds physically to dystrophin and the inducible nNOS.

This link is important for mechanic tension response and the activation of nNOS. NO leads to vasodilatation NO that secures sufficient blood and oxygen supply of muscle. Correlating with the increased α-SMA and the dystrophin mRNA in the absence of biglycan the expression of α-syntrophin are up-regulated too, in response to MI. However, α-syntrophin mRNA declines after day 3 and decreases to the same level that was detected in WT-hearts.

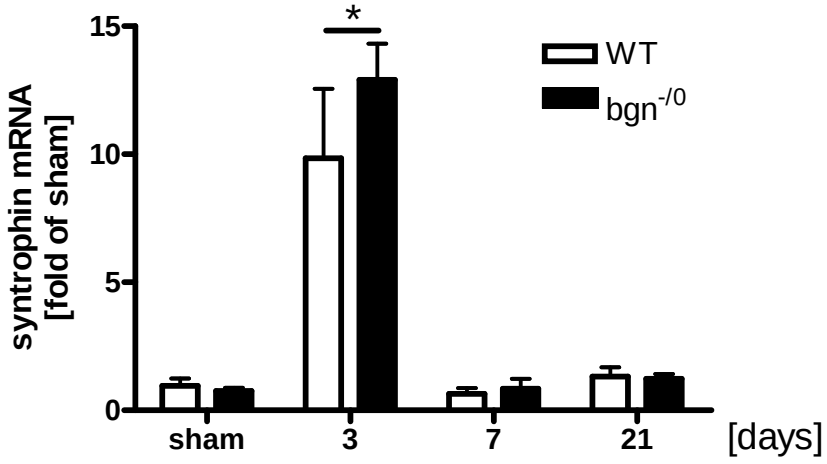

Figure 3-38 Syntrophin mRNA was increased in response to myocardial infarction and even more elevated in bgn$^{-/0}$-mice compared to WT littermates.

Apex cordis from sham and post-infarct hearts were lysed for total RNA extraction. The mRNA was transcribed into cDNA and analyzed by real time RT-PCR for the quantification of α-syntrophin mRNA *expression*. *Mean ± SEM; n =4-9; *, p<0.05 WT- versus bgn$^{-/0}$-mice.*

To analyse the nNOS expression in response to MI may give information about the functionality of the DAPC. The inducible isoform nNOS is highly up-regulated in response to MI in WT-hearts at day 3. However the induction of nNOS expression in bgn$^{-/0}$-hearts is significantly.

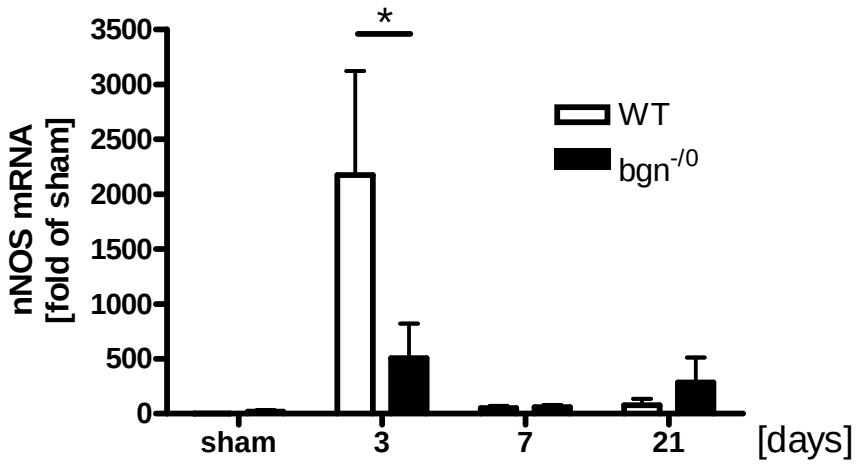

Figure 3-39 Post infarction induction of nNOS mRNA is significantly reduced in bgn$^{-/0}$-mice.

Apex cordis from sham and post infarct hearts were lysed for total RNA extraction. The mRNA was transcribed into cDNA and analysed by real time RT-PCR for the expression of nNOS mRNA. *Mean ± SEM; n = 4-9; *, p<0.05 WT- versus bgn$^{-/0}$-mice.*

These data may suggest that in bgn$^{-/0}$-mice nNOS activation fails, at day three after MI. The physiological consequence of less vasodilatory NO in the infarcted heart may lead to critically reduced supply of oxygen. This may subsequently support impaired hemodynamics and infarct healing as seen in bgn$^{-/0}$-mice after experimental myocardial infarction. Further functional analysis of infarcted hearts would be necessary to prove these mechanistic details.

4 Discussion

Fibroblasts are cells of mesenchymal origin that produce a variety of ECM molecules including multiple collagens and fibronectin. To identify fibroblasts the examination of the morphology is still the gold standard. But the morphology can vary depending on the tissue origin or even with the location within the same organ. Fibroblasts are the main non-myocyte cell type in the heart, along with endothelial and vascular smooth muscle cells. Morphologically fibroblasts are flat and spindle shaped. A defining characteristic is that fibroblasts lack a basement membrane and this attribute can be used to distinguish fibroblasts from all other permanent cell types in the heart. Fibroblasts are source and target of different stimuli, with the task to coordinate chemical, mechanical and electrical signals between the cellular components and the ECM within the heart. It has been shown that upon stimulation cardiac fibroblasts secrete high amounts of ECM molecules including the small leucine-rich repeat proteoglycan biglycan (54,68). Biglycan is involved in collagen and elastin fibrillogenesis (34-36).

Furthermore in response to myocardial infarction biglycan (bgn) as well as the highly homologous decorin have been shown to be regulated differently. The genetic deletion of decorin led to increased scar size, higher remote hypertrophy and ventricular dilation. This phenotype was marked by collagen fibril disorder and a depressed ventricular function and suggested a role of decorin in proper fibrotic evolution of myocardial infarctions (51). The genetic deletion of biglycan caused an even more pronounced cardiac phenotype, characterized by dramatically increased mortality of $bgn^{-/0}$-mice after experimental myocardial infarction, accompanied by perturbed scar remodelling and hemodynamic insufficiency (52). Mechanistically it was demonstrated that the collagen network of the infarct scars was distorted explaining the rupture phenotype. In the present study it was examined whether the loss of biglycan might affect the phenotype of cardiac fibroblasts *in vitro* which could cause the phenotype after MI *in vivo*.

4.1 Morphological differences between WT and bgn$^{-/0}$-fibroblasts

Primary cardiac fibroblasts from WT-mice show a uniform morphology of flat even shaped cells that remained constant through five passages in cell culture. These WT cells were relatively robust also with respect to the. During a two week period of treatment with high serum and bFGF cardiac fibroblast grew out from heart piece explants. To compare WT-fibroblasts to bgn$^{-/0}$-fibroblasts, explants of both genotypes were isolated simultaneously. Bgn$^{-/0}$-fibroblasts were smaller in size and showed a more rounded cell shape with thin protrusions (fig.3-1). Bgn$^{-/0}$-fibroblasts grew out in considerable numbers already three days after explantation and could be harvested in higher numbers compared to WT-fibroblasts (fig. 3-4).

4.2 Pro-proliferative phenotype of cardiac fibroblasts in the absence of biglycan

In the first set of experiments a pro-proliferative phenotype of biglycan deficient (bgn$^{-/0}$) -fibroblasts was be detected. Bgn$^{-/0}$-fibroblasts grew out from explant culture of hearts in significantly larger numbers compared to WT-fibroblasts. This period may represent a mixture of migratory and proliferative response. The pro-proliferative phenotype of the bgn$^{-/0}$-fibroblasts was confirmed by thymidine incorporation and cell counting experiments (fig. 3-6, 3-7).

The pro-proliferative phenotype was rescued either by providing fibroblasts with biglycan containing ECM as growth substrate or by lentiviral restoration of biglycan expression. In contrast to the presented data it was shown before that biglycan overexpression increases proliferation of smooth muscle cells in the aortic wall and in renal arterioles, proven by large numbers of PCNA-positive cells in these vessels and accompanied by an increase in the medial thickness of the vessels. As mechanisms were explained by an increased expression of cyclin dependent kinase (cdk) 2 and a reduction of cdk-inhibitor p27 (55) was proposed.

Some studies on proliferative responses to biglycan were executed by treatment with soluble biglycan. It is of interest, that soluble biglycan has different functions than ECM bound biglycan. Nevertheless, these studies showed that biglycan stimulates proliferation of microglial cells (69) and of rat osteoblasts from calvaria but not of human osteoblasts from the knee (70). It was published that biglycan inhibits proliferation and migration of endothelial cells, osteogenic precursors and pancreatic cancer cells (71). Apart from that, it was demonstrated that biglycan increases the expression of a cdk-inhibitor, namely p21.

These studies show that biglycan has cell type specific effects on proliferation response. Additionally, it was published that biglycan has anti-proliferative effects in mesangial *cells*, that are dependent on PDGF-BB treatment (72).

Therefore it is believed that biglycan has a regulatory function with respect to the cyclin- dependent kinases and their inhibitors and might thereby control cell cycle progression. Furthermore biglycan and the class II SLRP lumican inhibit the expression of cyclin A and elevate the cell cycle inhibitors p21/p27 (47,73).

Another pathway how biglycan regulates cell growth is the physical interaction with growth factors. It has been shown that growth factors that activate biglycan expression afterwards are targets of biglycan mediated inhibition such as TGF-β. Furthermore, biglycan acts also as an important part of regulatory feedback loops for PDGF-BB as well as for TNF-α and TGF-β (72,74).

4.3 Differentiation in the absence of biglycan

The morphological analysis of $bgn^{-/0}$-fibroblasts revealed distinct differences to WT-fibroblasts. The detailed immunohistochemical analysis of the fibroblasts proved that these differences already appear in the cytoskeleton. $Bgn^{-/0}$-fibroblasts were smaller in size and showed a dense α-SMA positive cytoskeleton, which is a characteristic feature of differentiated myofibroblasts (20). The restoration of biglycan expression by the lentivirally mediated overexpression rescued only the proliferative phenotype but did not rescue the

differentiation, as verified by α-SMA protein expression. Furthermore $bgn^{-/0}$-fibroblasts show stronger signals for the fibronectin ED-A fragment. This fibronectin splice variant is a ligand at $\alpha_4\beta_7$-integrin and thereby connects cell membranes to ECM. Fibronectin ED-A is upregulated in various healing responses and disease states such as in skin granulation tissue and hepatic fibrosis (75). It was shown that this fibronectin ED-A domain is necessary for TGF-β triggered α-SMA expression and the differentiation into myofibroblasts (76). These results point towards multiple but in part independent actions of biglycan with affecting proliferation and myofibroblast differentiation. Both proliferation and differentiation come along with differences in the expression of the TGF-β receptor type II, which was increased in the absence of biglycan. Moreover the neutralisation of endogenous TGF-β resulted in the inhibition of proliferation and differentiation too.

It is generally acknowledged that TGF-β is the priming factor that activates myofibroblasts. TGF-β is a growth factor that supports differentiation rather than proliferation. Upon activation of TGF-β, PDGF and connective tissue growth factor (CTGF, (77,78)) which are predominantly responsible for proliferation of myofibroblasts are induced. It was shown in vascular endothelial cells that by supporting an anti-proliferative effect of biglycan, CTGF suppresses its synthesis (79). Other soluble factors that have been shown to promote myofibroblast activation are angiotensin II, aldosterone, thrombin and endothelin (54,68,80-83). Angiotensin II stimulates TGF-β and also the expression of biglycan (68). After MI angiotensin II induces fibroblast proliferation in rats. Angiotensin II is detectable in every ventricle in the early phase from day 2 until day 4 after MI. It is also located at sites of myocyte necrosis and in the widespread peri-vascular area. Through the induction of TGF- β angiotensin II induces the appearance of myofibroblasts from day 2 until week 6 after angiotensin II treatment (81).

However, a variety of factors are involved in myofibroblast differentiation as well and these factors also affect biglycan expression even if only partly. Aldosterone infusion inhibits fibroblast proliferation after MI and leads to a deferred myofibroblast appearance. However it has not been investigated yet if

aldosterone has any effects on biglycan expression (81). Thrombin stimulates the biglycan expression in cardiac fibroblasts as well as in vascular smooth muscle cells and it also induces the differentiation of lung fibroblasts into myofibroblasts (54,80). Endothelin induces the differentiation of skin fibroblasts and keratinocytes into myofibroblasts (83). It has been published, that endothelin induces biglycan expression in vascular smooth muscle cells by endothelin receptor transactivation of TGF-βRI (82). The mentioned studies agree that a factor that induces myofibroblast differentiation induces biglycan too. In summary many of the regulators of the myofibroblast phenotype involve effects on biglycan expression and TGF-β activity. The role of TGF-β in differentiation is not an on/off mechanism but a delicately regulated process and depends on the cellular response to ECM remodelling (84).

It has been shown that biglycan is involved in bone marrow stromal cell (BMSC) differentiation. In BMSC biglycan -deficiency represses the differentiation into osteogenic cells. In the same study it has also been shown that biglycan expression inhibits the proliferation of BMSC. This phenotype can be rescued by WISP 1, a growth factor of the CCN family administration to the cells (71).

Biglycan-deficiency resulted in a higher phosphorylation of SMAD2 a regulatory SMAD.

The presented data demonstrates that in the absence of biglycan, cardiac fibroblasts express higher levels of the TGF-βRII and that they show increased phosphorylation of the TGF-β signalling mediator SMAD2. The canonical pathway of TGF-β includes the activation of both r-SMADs, SMAD2 and SMAD3. As SMAD 3 phosphorylation was not increased in $bgn^{-/0}$-fibroblasts, it was likely that TGF-β signalling was mediated by other signalling cascades. The increased phosphorylation of SMAD2 comes along with an increased expression of SMURF2. This coincidence of an increased phosphorylation of SMAD2 and an increased expression of SMURF2 suggests additional signalling pathways. Ubiquitin ligase SMURF 2 recruits SMAD2 for proteasomal degradation and it has also been described to build a complex with phosphorylated SMAD2 leading to the degradation of transcription inhibitors like SnoN and c-Ski (40). It has been shown recently that upon TGF-β treatment c-

Ski translocates into the nucleus in the long term. Overexpression of c-Ski in cardiac myofibroblasts leads to the loss of α-SMA and contractility and to the induction of apoptosis. Hence c-Ski is an example of a TGF-β responding factor that is involved in reversion of the myofibroblast phenotype. Additionally the expression of the inhibitory SMAD7 is increased in $bgn^{-/0}$-fibroblasts. The inhibitory SMAD 7 is localized in the nucleus. Due to active TGF-β signalling SMAD7 translocates from the nucleus into the cytosol where it interacts with the kinases TAK1, MKK3 and p38. The activation of this pathway can also lead to the induction of the transcription factor nuclear factor kappa B (NFκB), a pro-proliferative and pro-migratory factor, which is also increased in the absence of biglycan. Specific inhibitors to the single kinases could be used to verify their involvement in the signal transduction. Additionally the β-catenin expression was increased in $bgn^{-/0}$-fibroblasts. An increased accumulation of β-catenin in the cytosol is well documented upon TGF-β stimulation. It was demonstrated that in the course of myofibroblast differentiation β-catenin interacts physically with SMAD2 during $\alpha_3\beta_1$ integrin signalling. Due to its interaction with E-cadherin/ β-catenin complex, $\alpha_3\beta_1$ integrin locates at cell-cell contact sites. Cadherins are transmembrane proteins with extracellular calcium binding domains; these molecules connect cells at their surfaces by homodimerization of the extracellular domain following calcium binding. Cadherins bind to actin filaments and α- and β-catenin at the intracellular part. The loss of cadherins is an established diagnostic feature in pathological conditions, as it promotes tissue instability and invasiveness of for example tumor cells (85,86).

Another linkage between TGF-β induced SMAD proteins and β-catenin is that β-catenin is stabilized by SMAD7 at cadherin cell-cell adhesion sites. SMAD7 prevents the ubiquitinylation and degradation of β-catenin. The accumulation of β-catenin can lead to active signalling, as β-catenin translocates into the nucleus and induces the transcription of genes associated with apoptosis. Furthermore SMAD7 interaction with β-catenin is required for TGF-β induced apoptosis (42-44).

Additionally, it has been demonstrated that biglycan and fibromodulin double deficient mandibular condylar chondrocytes have an overactive TGF-β signalling, resulting in chondrogenesis and ECM turnover. The loss of biglycan

and fibromodulin leads to a reduced sequestration of TGF-β that causes an over activity of TGF-β (64). The effect of biglycan seems to be tissue- and cell type-specific. Biglycan as a calcium modifying molecule supposedly plays a different role in the heart than it does in bone marrow.

The characteristic of ECM remodelling during infarct healing is the accumulation of collagen. The deposition of collagen is accompanied by increased pyridinoline cross-links, which are derived from hydroxylated lysine residues. The increase in pyridinoline crosslinks is likely to be the result of an increased activity of the enzyme that is responsible for the hydroxylation of the lysine residues in collagen peptides which are catalyzed by the procollagen-lysine, 2-oxoglutarate 5-dioxygenases (PLOD) 1 and 2. The resulting hydroxylysyl groups in collagen are attachment sites for carbohydrates and glycosaminoglycans and thus are crucial for the stability of intermolecular crosslinks. Collagen crosslinking is supposed to determine the miscellaneous relations that exists between accumulation of cardiac collagen and either myocardial stiffness or ventricular remodelling in hypertension (87). Thus the expression of collagen crosslinking enzymes gives information about the remodelling capacity within a tissue. In $bgn^{-/0}$-fibroblasts PLOD1, PLOD2 were induced significantly as compared to WT-fibroblasts.

Another group of crosslinking enzymes is respresented by the tissue transglutaminase (tgm) 1 and 2. While tgm1 is not influenced by the genetic loss of biglycan in cardiac fibroblasts, the tgm2 expression shows a strong trend towards induction. Numerous studies over the last two decades revealed multiple functions of tissue transglutaminase 2 (tgm2). It is of note that like biglycan, tgm2 has Ca^{2+}-dependent functions leading to the transamidation of proteins and the formation of protein polymers via protease-resistant covalent isopeptide bonds. But Ca^{2+} binding happens at concentrations usually in the supraphysiological, not the physiological range that is associated with most intracellular processes. This *means* that they are virtually inactive under normal conditions and only activated following major disruptions in physiological homoeostatic mechanisms (88). Tgm2 also possesses GTPase enzymatic activity which connects this enzyme to intracellular signalling pathways.

Moreover, in addition to the cytoplasmic and nuclear localization, a significant part of tgm2 is present on the cell surface. A number of recent findings indicate that surface tgm2 is involved in the interactions of cells with the surrounding ECM. In epithelial cell attachment and cell spreading tgm2 appears to be concentrated at cell adhesion sites that are enriched with β_1 integrin. In densely spread cell-layers tgm2 appears to be more diffusely distributed along the basal membrane, with dense localizations at sites of cell-cell and cell-substratum contacts (89,90). Tgm2 modifies the stability of ECM proteins and renders the ECM resistance to degradation. In addition, tgm2 also activates TGF-β. Both actions of tgm2 modulate the infiltration by macrophages and myofibroblasts (91). It has been shown that in rats the ectopic expression of tgm2 increased the caspase-3 activity and calcium overload in cardiomyocytes (92). The induction of crosslinking enzymes in $bgn^{-/0}$-fibroblasts was not confirmed *in vivo*, where only a trend towards induction could be detected (52).

ECM remodelling is not only composed of ECM production and crosslinking, ECM degradation is also of major importance. The key players in this process of degradation are the matrix metalloproteinases.

Interstitial collagenase (MMP-1), neutrophil collagenase (MMP-8), and collagenase-3 (MMP-13) possess high substrate specificities for fibrillar collagens, as well as other ECM proteins such as proteoglycans, including biglycan, perlecan and versican. Biglycan has shown to protect collagen fibres from MMP mediated degradation, while biglycan itself is degraded by MMP13 during cartilage degradation (27). The gelatinases (MMP-2 and MMP-9) demonstrate a substrate affinity for denatured fibrillar collagen, basement membrane proteins such as collagen type IV, fibronectin, and laminin, but they exhibit a proteolytic activity against elastin and proteoglycans as well. The substrate selection for stromelysin-1 (MMP-3) includes proteoglycans, all basement membrane proteins and elastin. The expression and activity of MMPs after myocardial infarction influences the cardiac outcome as deletion of MMPs improves infarct healing and deletion of tissue inhibitors of MMPs (TIMPs) accelerate cardiac remodelling and exacerbates cardiac remodelling and heart failure (93-95). It was shown that the collagenases MMP8 and MMP13 are rigorously upregulated during the first five days following acute MI (96).

The induction of both ECM crosslinking and degrading enzymes is characteristic for the myofibroblastic phenotype and supports the thesis that bgn$^{-/0}$-fibroblasts show distinct differences to WT-fibroblasts in respect to cardiac remodelling after MI. As reported before (52) these findings correlate with the increased expression of MMP13 in bgn$^{-/0}$-mice after experimental MI *in vivo*. The discrepancy in the expression of crosslinking and degrading enzymes between *in vitro* and *in vivo* data might be due to the time point at which the data was collected. The *in vivo* data was collected at day 7 after experimental MI, when the scar is established and the myofibroblasts already start to disappear. However, the *in vitro* data mirrors a proceeding a situation where myofibroblasts are still highly active.

The induction of CD44 expression in the absence of biglycan draws attention on new aspects, as CD44 is also involved in focal adhesion establishment and influences the motility of fibroblasts. CD44 is also supposed to be a factor that is necessary for the recruitment of fibroblasts to sites of injury (39). Interestingly CD44 activates TGF-β signalling by modulating MMP activation. This activation of MMPs leads to TGF-β release from the ECM, where it is sequestered by biglycan and decorin (64). The two gelatinases MMP-2 and MMP-9 proteolytically cleave latent TGF-β, providing an important mechanism for TGF-β activation. It has been published that CD44 recruits MMP-9 which then localizes to the surface of normal keratinocytes where it activates latent TGF-β. Therefore it may be suggested that coordinated CD44, MMP-9, and TGF-β function may provide a physiological mechanism of tissue remodelling in response to disease (97). In CD44 null mice fibroblast infiltration and matrix production in the infarct zone are markedly reduced, both supports the role of CD44 as a regulatory receptor for myofibroblast differentiation and infiltration (63). The up-regulation of CD44 in the absence of biglycan matches the differentiated phenotype of the bgn$^{-/0}$-fibroblasts. Analysing bgn$^{-/0}$-fibroblasts proliferation and differentiation under treatment with either a knock down by short-hairpin RNA to CD44 and MMP inhibitors could be utilized to prove this concept. In summary the absence of biglycan affects the TGF-β system

involving TGF-β sequestration, receptor expression, cytosolic signalling mediators as well as the cross talking between TGF-β and ECM receptors.

Another surprising finding was the change in the expression of components of the dystrophin associated protein complex (DAPC) in $bgn^{-/0}$-fibroblasts. For skeletal muscle, it was shown that biglycan physically interacts with the DAPC and regulates the expression of important components of this complex. It was also shown that biglycan is up-regulated in the dystrophic mdx (x-related muscular dystrophy) muscle. This brings up the idea that biglycan might also influence the DAPC in cardiac muscle in response to hypertrophy and fibrosis (98).

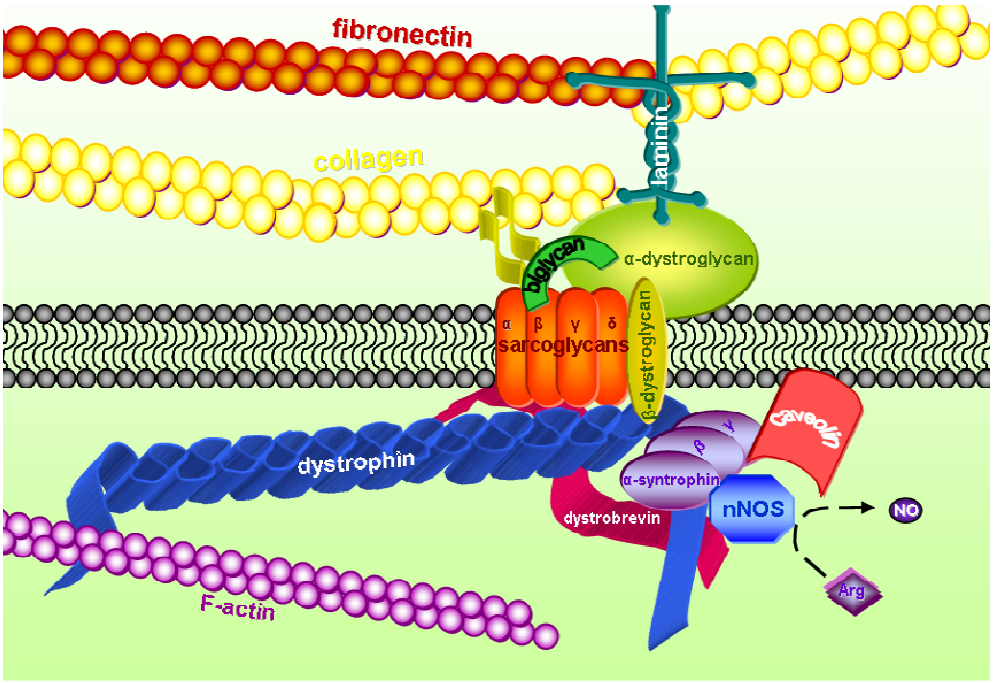

Figure 4-1 The dystrophin associated protein complex induces NO release upon muscle contraction to provide muscle perfusion by blood vessel dilation.

The dystrophin associated protein complex (DAPC) links the cytoskeleton to the structural components of the ECM. Tension and contraction are transduced by this multi-component complex.

In this light, it is important to investigate the effects of biglycan deficiency on the DAPC in cardiac fibroblasts. This multi-component complex recruits the nNOS to the sarcolemma where the enzyme binds to syntrophins. The muscle

contraction is coupled to calcium influx which is directly associated with NO synthesis. The formation of NO at the muscle cell membrane by nNOS facilitates the directed diffusion of NO towards vascular smooth muscle cells. In vascular smooth muscle cells NO targets the guanylyl cyclase, whose activity is elevated about 100-fold due to the binding of NO. The resulting increase of cGMP mediates the vessel dilation and increases the perfusion of the contracting muscle.

Biglycan regulates the expression of DAPC proteins like dystrobrevins, syntrophins and nNOS (32). The activation of nNOS leads to the secretion of vasodilatory NO which has been shown to induce the biglycan expression in the cardiac system (54) providing a regulatory feedback loop.

It may be hypothesized that the induction of biglycan expression functions as a negative regulator of myofibroblast differentiation that is partly lost in $bgn^{-/0}$-fibroblasts due to enhanced TGF-β signalling. Furthermore the lack of biglycan might disturb the biological function of the DAPC, leading to a loss of function in $bgn^{-/0}$-myofibroblasts. Figure 4-2 provides a schematic overview of these two working hypotheses.

4.4 Constitutive rate of apoptosis in the absence of biglycan is part of unleashed TGF-β signalling

Despite its functions concerning the regulation of proliferation and differentiation, biglycan influences apoptosis as well. This is another interesting point supporting the hypothesis that biglycan is critically involved in the regulation of the myofibroblastic response.

Under standard conditions biglycan deficient fibroblasts show a high level of PARP 1 cleavage, which is indicative for increased apoptosis. These specialized cells, disappear from sites of injury after the establishment of healed tissue has been reached, by undergoing apoptosis (20). Therefore the down regulation of biglycan as observed *in vivo* during late phase remodelling of scar healing might contribute to apoptotic removal of fibroblasts. This is in line with

the observation in mesangial cells it has been shown that soluble biglycan inhibited cyclohexamid induced apoptosis (72).

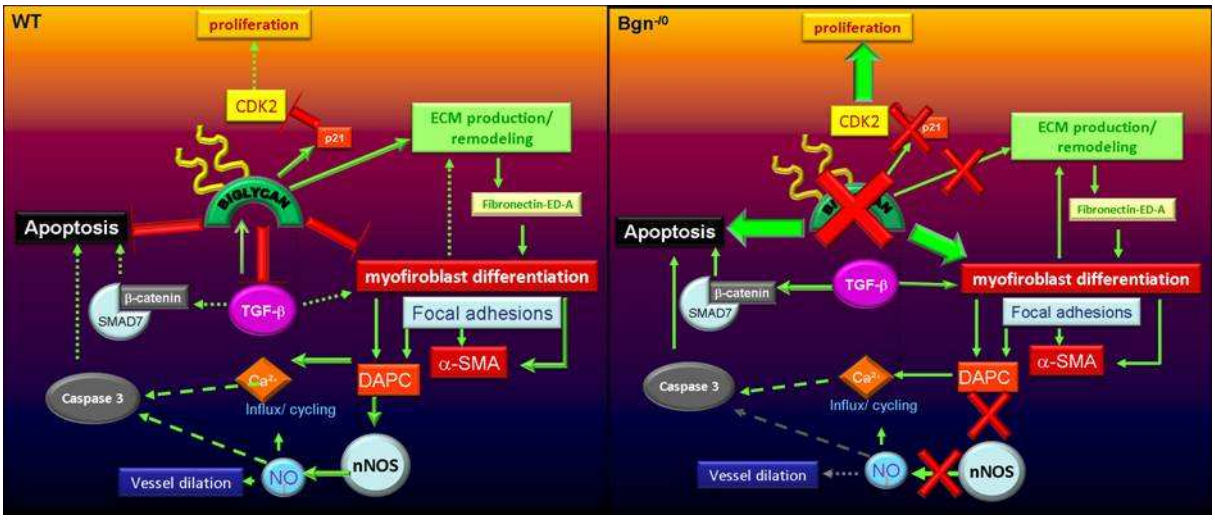

4-2Schematic summary of biglycan functions in WT and bgn$^{-/0}$-fibroblasts

The upper panel presents the WT-fibroblast growth and differentiation regulation in the presence of biglycan. Biglycan induces the cdk-inhibitor p21 and thereby inhibits the proliferation of fibroblasts. Biglycan is involved in the organisation of fibrillogenesis of collagen and elastic fibres and secures ECM integrity. Furthermore biglycan inhibits TGF-β and thus regulates myofibroblast differentiation and apoptosis in response to TGF-β. In the knock out fibroblast (lower panel) the lack of biglycan leads to a pro-proliferative phenotype as the induction of the cdk inhibitors is absent. Additionally the absence of biglycan unleashes TGF-β signalling, leading to spontaneous differentiation into myofibroblasts. Bgn$^{-/0}$-myofibroblasts lack the ability to organize the ECM. Moreover bgn$^{-/0}$-myofibroblasts show deregulation of the DAPC, which might lead to alterations in calcium cycling and production of vasodilatory NO. At the end the lack of biglycan results in TGF-β induced apoptosis mediated by SMAD7 and β-catenin.

In 2003 Young *et al*. firstly showed that biglycan deficient mice have diminished capacity to produce bone marrow stromal cells, and secondly that these cells also show a reduced response to TGF-β, reduced collagen synthesis and comparatively exhibit more apoptosis than cells from normal control littermates. Additionally, it has been demonstrated that biglycan and decorin double deficient BMSCs undergo apoptosis more often than WT BMSCs (99).

Furthermore SMAD 7 interacts with β-catenin to modulate TGF-β-induced apoptosis. Thus SMAD7 acts as positive regulator of the TGF-β activated pathway involving TAK1-MKK3 and p38 mitogen-activated kinases, leading to

induction of c-myc and p53 and subsequently apoptosis (42,43,100,101). Indeed increased apoptosis indicated by PARP cleavage has been detected despite of the proliferative phenotype. These results suggest that biglycan is not only involved in appearance of myofibroblasts, but also in regulation of myofibroblast disappearance

4.5 Translation of bgn function *in vitro* into *in vivo* situation

To understand the complex pathological events after acute myocardial infarction (MI) it is useful to separate these events into functional phases. A useful division would contain the initial phase when the myocardium directly reacts on vessel occlusion induced hypoxia, the early phase subdivided into inflammatory and proliferative phase, when cardiac remodelling is crucial and the late phase when the healing is processed and adaptation to the injury has accomplished (62). The initial phase is also termed evolving phase and is timely restricted. During this phase hydrogen ions accumulate in the myocardium and potassium ions are extruded from the cells into extracellular space. Calcium2^+ is replaced from the sarcoplasmic reticulum by contractile proteins like the DAPC. This leads to cease of contraction. Sodium ion influx leads to swelling of cells. Proteolytic enzymes are released into the ECM space and $Ca2^+$ ultimately invades the mitochondria inducing apoptosis. Additionally necrosis of cardiomyocytes occurs during ischemia. Necrosis of cardiomyocytes leads to release of chemokines and cytokines for recruiting leukocytes to the ischemic area. But also the vasculature is affected, capillaries are compressed collateral vessels are compromised and leakiness of small capillaries convey the risk of haemorrhage (102). The following inflammatory phase is characterized by infiltration of the infarct area by macrophages, granulocytes and monocytes (103,104). During inflammation of the infarct vascular permeability leads to extravasations of plasma proteins leading to fibrin-based provisory scar (105). The accumulation of cytokines, chemokines and growth factors, such as TGF-β, lead to the appearance of activated myofibroblasts (23). During the proliferative phase of

infarct healing the fibrin-based scar is removed by granulation tissue cells and activated myofibroblasts proliferate and produce extensive amounts of ECM, establishing a cellular fibronectin-, hyaluronan- and collagen- based scar. Additionally fibroblasts and myofibroblast reorganize the microvasculature. During this phase of cardiac remodelling the composition of infarct ECM changes rapidly and dramatically alters microenvironment and thereby regulation of cell behaviour. Additionally the changes in ventricular ECM alter the mechanical properties of the ventricle and also modulate the cellular phenotype and gene expression profiles. Subsequently the late phase of infarct healing is characterized by a matured scar. During this phase myofibroblasts disappear from the infarct zone by apoptosis and probably by reversion into resident fibroblasts. If myofibroblasts disappear too early from sites of injury they would leave immature scars, but persistence in high numbers would lead to increasing fibrosis, which would cause a progressive heart failure (14, 16, and 23).

Most importantly the myofibroblast phenotype of bgn$^{-/0}$-fibroblasts appearing *in vitro* was also detected *in vivo.* Namely, increased α–SMA occurred in infarcted hearts of bgn$^{-/0}$-mice at all day 3 and day 7after MI (fig. 3-33).

Furthermore biglycan-deficiency may act pro-fibrotic by causing myofibroblast differentiation and in turn ECM production. Up to now there has been no evidence of a pro-fibrotic phenotype in bgn$^{-/0}$-mice during *in vivo* experiments. Moreover the pro-apoptotic phenotype of the bgn$^{-/0}$-myofibroblasts has to be taken into account too. The more myofibroblasts disappear early, possibly after a shortened life span, the less myofibroblasts are affecting proper tissue remodelling. Apart from that it is also possible that bgn$^{-/0}$-myofibroblasts are physiologically less capable of ECM remodelling. Thus the suggestion that bgn$^{-/0}$-myofibroblasts are not as active concerning their fibrotic response is more likely. Furthermore in WT-mice myofibroblasts disappear at the time point when biglycan massively accumulates in the peri-infarct area (fig.4-1), (52). All data considered this allows the assumption that biglycan acts as a molecular switch to terminate the myofibroblast response.

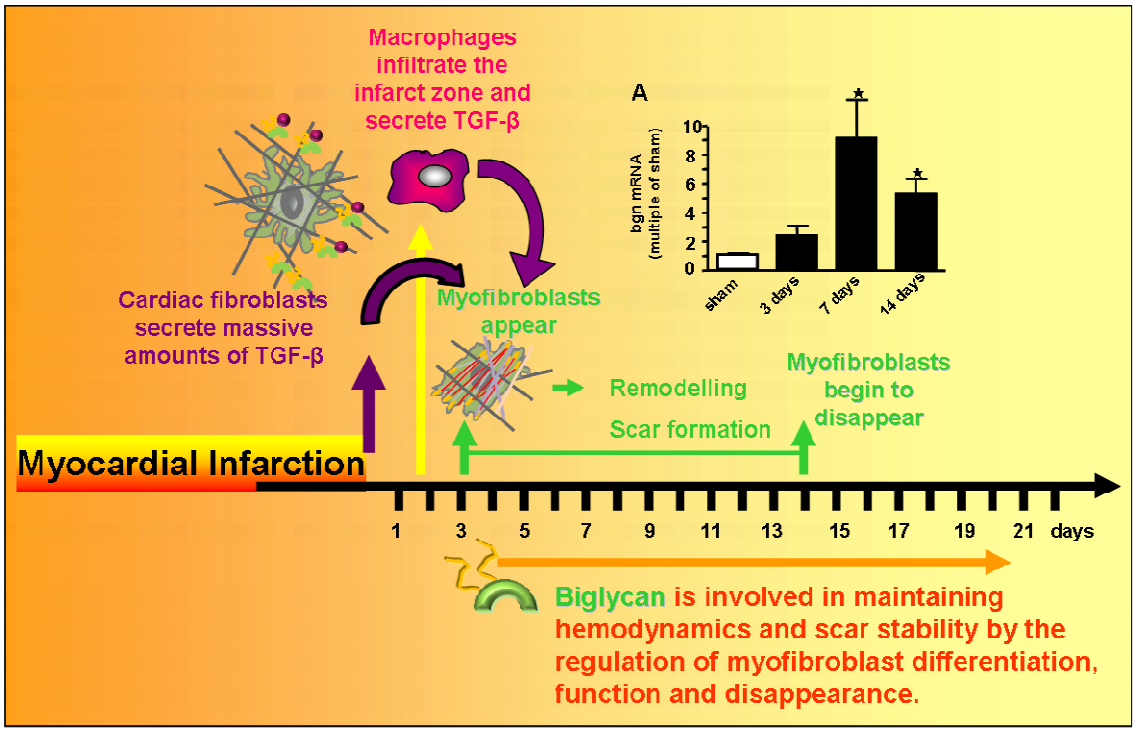

Figure 4-3 Timeline of functional events after myocardial infarction and the role of biglycan

This schematic timeline presents functional events following acute myocardial infarction. Cardiac fibroblasts recruit macrophages to the infarcted tissue. During the first two days macrophages, granulocytes and monocytes infiltrate the infarct. Fibroblasts and macrophages secrete high amounts of cytokines and growth factors like TGF-β, which lead to the activation and differentiation of fibroblasts into myofibroblasts, that peak between day 3 and day 7 after MI. Myofibroblasts contract the infarct tissue and secrete ECM molecules, MMPs and additional enzymes to remodel the ECM. Upon remodelling a stable scar is formed by day 7. Biglycan is known to be involved in collagen and elastin organization and it is up-regulated during remodelling and scar formation, reaching a peak expression at 7 days after MI. At this time point myofibroblasts are already declining.

The up-regulation of dystrophin and syntrophin after MI was apparently not a feature limited to cardiomyocytes, because myofibroblasts are positive for dystrophin too as shown by immunohistochemistry in this thesis. This data shows for the first time, which myofibroblasts express high amounts of dystrophin and syntrophin in the infarcted ventricle, both proteins are only negligibly detectable in normal fibroblasts. The similarity of α-SMA and dystrophin location in the infarct and the strong signal for dystrophin in fibroblastic cells, suggest the possibility that dystrophin might be a functional

marker for myofibroblasts in the heart. The DAPC is required for sarcolemmal localization of nNOS (106) and it is possible that the absence of biglycan the DAPC is deregulated and that thus the activation of the neuronal nitric oxide synthase (nNOS) after experimental MI fails (fig. 3-38). The nNOS knock out mice exhibit relatively normal heart function with a suppressed ionotropic response to β-adrenergic stimulation, which reflects changes in myocyte calcium cycling. As the eNOS/nNOS double deficient mice show a defect in calcium cycling that resembles the one of nNOS-knock out, it is assumed that the nNOS effect is predominant in the heart (107). Furthermore it was shown that $nNOS^{-/-}$-mice exhibit increased mortality and an impaired hemodynamic function after experimental myocardial infarction (108). The hypothesis that biglycan is involved in NO release from myofibroblasts still has to be verified by further experiments.

In conclusion the presented data show that the SLRP biglycan, despite its role in stabilizing the collagen containing ECM and protecting it from cleavage, is involved in the signalling that mediates fibroblast differentiation and proliferation. This is of interest with respect to therapeutic pharmacological intervention since AT1-antagonists inhibit biglycan expression in cardiac fibroblasts and are known to reduce fibrosis (68,109).

5 Summary

After myocardial infarction (MI) extracellular matrix (ECM) remodelling is on the one hand required for the formation of stable scar tissue but on the other hand can turn into pathologic remodelling. The small leucine-rich proteoglycan (SLRP) biglycan (bgn) has been shown to be critically involved in these processes. During post-ischemic remodelling cardiac fibroblasts differentiate into myofibroblasts which are the main cell type mediating ECM remodelling and scar contraction. Aim of the present study was to characterize the role of biglycan for the phenotype of cardiac fibroblasts.

Cardiac fibroblasts were isolated from hearts of wild-type (WT) versus bgn$^{-/0}$-mice. Phenotypical characterization of the bgn$^{-/0}$-fibroblasts revealed increased proliferation that was suppressed to WT-level by WT-cell-derived ECM and by lentiviral restoration of biglycan expression. Characterization of bgn$^{-/0}$-fibroblasts revealed increased expression levels of ECM crosslinking enzymes, as well as CD44 and TGF-βRII. In line with these results the phosphorylation of SMAD2 and ERK1/2 was increased and administration of neutralizing antibodies to TGF-β reversed the pro-proliferative phenotype. Furthermore, bgn$^{-/0}$-fibroblasts were characterized by increased alpha-smooth muscle actin (α-SMA) incorporated into stress fibres, increased expression of focal adhesions and increased contraction of collagen gels, indicative for differentiation into myofibroblasts. Surprisingly, bgn$^{-/0}$-fibroblasts showed increased apoptosis under normal conditions. *In vivo* in WT-hearts the time course of α-SMA expression post MI showed peak levels at 3 days. Of note in bgn$^{-/0}$-mice the increase of α-SMA was markedly enhanced suggesting that biglycan deficiency also promotes myofibroblast proliferation and differentiation *in vivo* post MI. For the first time it was shown that myofibroblast differentiation caused by biglycan deficiency was accompanied by increased expression of the dystrophin associated protein complex *in vitro* and additionally *in vivo*. Importantly an up-regulation of the DAPC did not correlate with an induction of nNOS expression post infarction. This data support the hypothesis that bgn$^{-/0}$-fibroblasts differentiate to myofibroblasts and exhibit characteristic features of this specialized cell type, but fail with respect to key functions, which results in apoptosis, impaired scar formation and disturbed hemodynamic function after

MI. In conclusion these data point to an inhibitory role of biglycan during cardiac myofibroblasts proliferation and differentiation possibly due to increased sensitivity to endogenous TGF-β and SMAD2 signalling.

6 References

1. Cohn, J. N., Ferrari, R., and Sharpe, N. (2000) *J Am Coll Cardiol* **35**, 569-582
2. Zamilpa, R., and Lindsey, M. L. *J Mol Cell Cardiol* **48**, 558-563
3. Welch, M. P., Odland, G. F., and Clark, R. A. (1990) *J Cell Biol* **110**, 133-145
4. Banerjee, I., Fuseler, J. W., Price, R. L., Borg, T. K., and Baudino, T. A. (2007) *Am J Physiol Heart Circ Physiol* **293**, H1883-1891
5. Camelliti, P., Borg, T. K., and Kohl, P. (2005) *Cardiovasc Res* **65**, 40-51
6. Porter, K. E., and Turner, N. A. (2009) *Pharmacol Ther* **123**, 255-278
7. Berschneider, H. M. (1992) *Ann N Y Acad Sci* **664**, 140-147
8. Berschneider, H. M., and Powell, D. W. (1992) *J Clin Invest* **89**, 484-489
9. Hinterleitner, T. A., Saada, J. I., Berschneider, H. M., Powell, D. W., and Valentich, J. D. (1996) *Am J Physiol* **271**, C1262-1268
10. Wilborn, J., Crofford, L. J., Burdick, M. D., Kunkel, S. L., Strieter, R. M., and Peters-Golden, M. (1995) *J Clin Invest* **95**, 1861-1868
11. Wilborn, J., DeWitt, D. L., and Peters-Golden, M. (1995) *Am J Physiol* **268**, L294-301
12. Powell, D. W., Mifflin, R. C., Valentich, J. D., Crowe, S. E., Saada, J. I., and West, A. B. (1999) *Am J Physiol* **277**, C1-9
13. D'Amore, P. A. (1992) *Semin Cancer Biol* **3**, 49-56
14. Desmouliere, A. (1995) *Cell Biol Int* **19**, 471-476
15. Desmouliere, A., and Gabbiani, G. (1995) *Exp Nephrol* **3**, 134-139
16. Desmouliere, A., Redard, M., Darby, I., and Gabbiani, G. (1995) *Am J Pathol* **146**, 56-66
17. Desmouliere, A., Tuchweber, B., and Gabbiani, G. (1995) *J Hepatol* **22**, 61-64
18. Arenberg, D. A., Keane, M. P., DiGiovine, B., Kunkel, S. L., Morris, S. B., Xue, Y. Y., Burdick, M. D., Glass, M. C., Iannettoni, M. D., and Strieter, R. M. (1998) *J Clin Invest* **102**, 465-472
19. Jobson, T. M., Billington, C. K., and Hall, I. P. (1998) *J Clin Invest* **101**, 2650-2657
20. Hinz, B. (2007) *J Invest Dermatol* **127**, 526-537
21. Sun, Y., and Weber, K. T. (1996) *J Mol Cell Cardiol* **28**, 851-858
22. Tomasek, J. J., Gabbiani, G., Hinz, B., Chaponnier, C., and Brown, R. A. (2002) *Nat Rev Mol Cell Biol* **3**, 349-363
23. Sun, Y., and Weber, K. T. (2000) *Cardiovasc Res* **46**, 250-256
24. Young, M. F., Bi, Y., Ameye, L., and Chen, X. D. (2002) *Glycoconj J* **19**, 257-262
25. Roughley, P. J., White, R. J., and Mort, J. S. (1996) *Biochem J* **318 (Pt 3)**, 779-784
26. Scott, I. C., Imamura, Y., Pappano, W. N., Troedel, J. M., Recklies, A. D., Roughley, P. J., and Greenspan, D. S. (2000) *J Biol Chem* **275**, 30504-30511
27. Monfort, J., Tardif, G., Reboul, P., Mineau, F., Roughley, P., Pelletier, J. P., and Martel-Pelletier, J. (2006) *Arthritis Res Ther* **8**, R26
28. Hildebrand, A., Romaris, M., Rasmussen, L. M., Heinegard, D., Twardzik, D. R., Border, W. A., and Ruoslahti, E. (1994) *Biochem J* **302 (Pt 2)**, 527-534
29. Schaefer, L., Babelova, A., Kiss, E., Hausser, H. J., Baliova, M., Krzyzankova, M., Marsche, G., Young, M. F., Mihalik, D., Gotte, M., Malle, E., Schaefer, R. M., and Grone, H. J. (2005) *J Clin Invest* **115**, 2223-2233

30. Kitaya, K., and Yasuo, T. (2009) *J Leukoc Biol* **85**, 391-400
31. Webber, J., Jenkins, R. H., Meran, S., Phillips, A., and Steadman, R. (2009) *Am J Pathol* **175**, 148-160
32. Mercado, M. L., Amenta, A. R., Hagiwara, H., Rafii, M. S., Lechner, B. E., Owens, R. T., McQuillan, D. J., Froehner, S. C., and Fallon, J. R. (2006) *FASEB J* **20**, 1724-1726
33. Kaprielian, R. R., and Severs, N. J. (2000) *Heart Fail Rev* **5**, 221-238
34. Corsi, A., Xu, T., Chen, X. D., Boyde, A., Liang, J., Mankani, M., Sommer, B., Iozzo, R. V., Eichstetter, I., Robey, P. G., Bianco, P., and Young, M. F. (2002) *J Bone Miner Res* **17**, 1180-1189
35. Danielson, K. G., Baribault, H., Holmes, D. F., Graham, H., Kadler, K. E., and Iozzo, R. V. (1997) *J Cell Biol* **136**, 729-743
36. Reinboth, B., Hanssen, E., Cleary, E. G., and Gibson, M. A. (2002) *J Biol Chem* **277**, 3950-3957
37. Geng, Y., McQuillan, D., and Roughley, P. J. (2006) *Matrix Biol* **25**, 484-491
38. Huang, S. S., and Huang, J. S. (2005) *J Cell Biochem* **96**, 447-462
39. Acharya, P. S., Majumdar, S., Jacob, M., Hayden, J., Mrass, P., Weninger, W., Assoian, R. K., and Pure, E. (2008) *J Cell Sci* **121**, 1393-1402
40. Bonni, S., Wang, H. R., Causing, C. G., Kavsak, P., Stroschein, S. L., Luo, K., and Wrana, J. L. (2001) *Nat Cell Biol* **3**, 587-595
41. Edlund, S., Bu, S., Schuster, N., Aspenstrom, P., Heuchel, R., Heldin, N. E., ten Dijke, P., Heldin, C. H., and Landstrom, M. (2003) *Mol Biol Cell* **14**, 529-544
42. Edlund, S., Lee, S. Y., Grimsby, S., Zhang, S., Aspenstrom, P., Heldin, C. H., and Landstrom, M. (2005) *Mol Cell Biol* **25**, 1475-1488
43. Landstrom, M., Heldin, N. E., Bu, S., Hermansson, A., Itoh, S., ten Dijke, P., and Heldin, C. H. (2000) *Curr Biol* **10**, 535-538
44. Mazars, A., Lallemand, F., Prunier, C., Marais, J., Ferrand, N., Pessah, M., Cherqui, G., and Atfi, A. (2001) *J Biol Chem* **276**, 36797-36803
45. Otsuka, G., Agah, R., Frutkin, A. D., Wight, T. N., and Dichek, D. A. (2006) *Arterioscler Thromb Vasc Biol* **26**, 737-743
46. Roberts, A. B., and Sporn, M. B. (1993) *Growth Factors* **8**, 1-9
47. Weber, C. K., Sommer, G., Michl, P., Fensterer, H., Weimer, M., Gansauge, F., Leder, G., Adler, G., and Gress, T. M. (2001) *Gastroenterology* **121**, 657-667
48. Massague, J. (2000) *Nat Rev Mol Cell Biol* **1**, 169-178
49. Colston, J. T., de la Rosa, S. D., Koehler, M., Gonzales, K., Mestril, R., Freeman, G. L., Bailey, S. R., and Chandrasekar, B. (2007) *Am J Physiol Heart Circ Physiol* **293**, H1839-1846
50. Parkes, J. G., Liu, Y., Sirna, J. B., and Templeton, D. M. (2000) *J Mol Cell Cardiol* **32**, 233-246
51. Weis, S. M., Zimmerman, S. D., Shah, M., Covell, J. W., Omens, J. H., Ross, J., Jr., Dalton, N., Jones, Y., Reed, C. C., Iozzo, R. V., and McCulloch, A. D. (2005) *Matrix Biol* **24**, 313-324
52. Westermann, D., Mersmann, J., Melchior, A., Freudenberger, T., Petrik, C., Schaefer, L., Lullmann-Rauch, R., Lettau, O., Jacoby, C., Schrader, J., Brand-Herrmann, S. M., Young, M. F., Schultheiss, H. P., Levkau, B., Baba, H. A., Unger, T., Zacharowski, K., Tschope, C., and Fischer, J. W. (2008) *Circulation* **117**, 1269-1276
53. Campbell, P. H., Hunt, D. L., Jones, Y., Harwood, F., Amiel, D., Omens, J. H., and McCulloch, A. D. (2008) *Mol Cell Biomech* **5**, 27-35

54. Tiede, K., Melchior-Becker, A., and Fischer, J. W. Basal *Res Cardiol* **105**, 99-108
55. Shimizu-Hirota, R., Sasamura, H., Kuroda, M., Kobayashi, E., Hayashi, M., and Saruta, T. (2004) *Circ Res* **94**, 1067-1074
56. Heegaard, A. M., Corsi, A., Danielsen, C. C., Nielsen, K. L., Jorgensen, H. L., Riminucci, M., Young, M. F., and Bianco, P. (2007) *Circulation* **115**, 2731-2738
57. Theocharis, A. D., and Karamanos, N. K. (2002) *Atherosclerosis* **165**, 221-230
58. Ayada, Y., Kusachi, S., Murakami, T., Hirohata, S., Takemoto, S., Komatsubara, I., Hayashi, J., Iwabu, A., Ninomiya, Y., and Tsuji, T. (2001) *Clin Exp Hypertens* **23**, 633-643
59. Vernon, R. B., and Gooden, M. D. (2002) *In Vitro Cell Dev Biol Anim* **38**, 97-101
60. Yanagishita, M. (2001) *Methods Mol Biol* **171**, 3-8
61. Dai, G., Freudenberger, T., Zipper, P., Melchior, A., Grether-Beck, S., Rabausch, B., de Groot, J., Twarock, S., Hanenberg, H., Homey, B., Krutmann, J., Reifenberger, J., and Fischer, J. W. (2007) *Am J Pathol* **171**, 1451-1461
62. Dobaczewski, M., Bujak, M., Zymek, P., Ren, G., Entman, M. L., and Frangogiannis, N. G. (2006) *Cell Tissue Res* **324**, 475-488
63. Huebener, P., Abou-Khamis, T., Zymek, P., Bujak, M., Ying, X., Chatila, K., Haudek, S., Thakker, G., and Frangogiannis, N. G. (2008) *J Immunol* **180**, 2625-2633
64. Embree, M. C., Kilts, T. M., Ono, M., Inkson, C. A., Syed-Picard, F., Karsdal, M. A., Oldberg, A., Bi, Y., and Young, M. F. *Am J Pathol* **176**, 812-826
65. Desmouliere, A., Geinoz, A., Gabbiani, F., and Gabbiani, G. (1993) *J Cell Biol* **122**, 103-111
66. Anastasi, G., Cutroneo, G., Gaeta, R., Di Mauro, D., Arco, A., Consolo, A., Santoro, G., Trimarchi, F., and Favaloro, A. (2009) *Int J Mol Med* **23**, 149-159
67. Deten, A., Holzl, A., Leicht, M., Barth, W., and Zimmer, H. G. (2001) *J Mol Cell Cardiol* **33**, 1191-1207
68. Tiede, K., Stoter, K., Petrik, C., Chen, W. B., Ungefroren, H., Kruse, M. L., Stoll, M., Unger, T., and Fischer, J. W. (2003) *Cardiovasc Res* **60**, 538-546
69. Kikuchi, A., Tomoyasu, H., Kido, I., Takahashi, K., Tanaka, A., Nonaka, I., Iwakami, N., and Kamo, I. (2000) *J Neuroimmunol* **106**, 78-86
70. Douglas, T., Hempel, U., Mietrach, C., Viola, M., Vigetti, D., Heinemann, S., Bierbaum, S., Scharnweber, D., and Worch, H. (2008) *J Biomed Mater Res A* **84**, 805-816
71. Inkson, C. A., Ono, M., Bi, Y., Kuznetsov, S. A., Fisher, L. W., and Young, M. F. (2009) *Cells Tissues Organs* **189**, 153-157
72. Schaefer, L., Beck, K. F., Raslik, I., Walpen, S., Mihalik, D., Micegova, M., Macakova, K., Schonherr, E., Seidler, D. G., Varga, G., Schaefer, R. M., Kresse, H., and Pfeilschifter, J. (2003) *J Biol Chem* **278**, 26227-26237
73. Vuillermoz, B., Khoruzhenko, A., D'Onofrio, M. F., Ramont, L., Venteo, L., Perreau, C., Antonicelli, F., Maquart, F. X., and Wegrowski, Y. (2004) *Exp Cell Res* **296**, 294-306
74. Tufvesson, E., and Westergren-Thorsson, G. (2002) *FEBS Lett* **530**, 124-128
75. Kaneda, K., Ekataksin, W., Sogawa, M., Matsumura, A., Cho, A., and Kawada, N. (1998) *Hepatology* **27**, 735-747
76. Jarnagin, W. R., Rockey, D. C., Koteliansky, V. E., Wang, S. S., and Bissell, D. M. (1994) *J Cell Biol* **127**, 2037-2048

77. Grotendorst, G. R. (1997) *Cytokine Growth Factor Rev* **8**, 171-179
78. Igarashi, A., Okochi, H., Bradham, D. M., and Grotendorst, G. R. (1993) *Mol Biol Cell* **4**, 637-645
79. Kaji, T., Yamamoto, C., Oh-i, M., Nishida, T., and Takigawa, M. (2004) *Biochem Biophys Res Commun* **322**, 22-28
80. Bogatkevich, G. S., Tourkina, E., Silver, R. M., and Ludwicka-Bradley, A. (2001) *J Biol Chem* **276**, 45184-45192
81. Campbell, S. E., Janicki, J. S., and Weber, K. T. (1995) *J Mol Cell Cardiol* **27**, 1545-1560
82. Little, P. J., Burch, M. L., Getachew, R., Al-aryahi, S., and Osman, N. *J Cardiovasc Pharmacol* **56**, 360-368
83. Shephard, P., Hinz, B., Smola-Hess, S., Meister, J. J., Krieg, T., and Smola, H. (2004) *Thromb Haemost* **92**, 262-274
84. Jourdan-Lesaux, C., Zhang, J., and Lindsey, M. L. *Life Sci*
85. Kim, K. K., Wei, Y., Szekeres, C., Kugler, M. C., Wolters, P. J., Hill, M. L., Frank, J. A., Brumwell, A. N., Wheeler, S. E., Kreidberg, J. A., and Chapman, H. A. (2009) *J Clin Invest* **119**, 213-224
86. Kim, Y., Kugler, M. C., Wei, Y., Kim, K. K., Li, X., Brumwell, A. N., and Chapman, H. A. (2009) *J Cell Biol* **184**, 309-322
87. Badenhorst, D., Maseko, M., Tsotetsi, O. J., Naidoo, A., Brooksbank, R., Norton, G. R., and Woodiwiss, A. J. (2003) *Cardiovasc Res* **57**, 632-641
88. Burgoyne, R. D., and Weiss, J. L. (2001) *Biochem J* **353**, 1-12
89. Gaudry, C. A., Verderio, E., Aeschlimann, D., Cox, A., Smith, C., and Griffin, M. (1999) *J Biol Chem* **274**, 30707-30714
90. Gaudry, C. A., Verderio, E., Jones, R. A., Smith, C., and Griffin, M. (1999) *Exp Cell Res* **252**, 104-113
91. Shweke, N., Boulos, N., Jouanneau, C., Vandermeersch, S., Melino, G., Dussaule, J. C., Chatziantoniou, C., Ronco, P., and Boffa, J. J. (2008) *Am J Pathol* **173**, 631-642
92. Song, H., Kim, B. K., Chang, W., Lim, S., Song, B. W., Cha, M. J., Jang, Y., and Hwang, K. C. *J Recept Signal Transduct Res*
93. Lindsey, M. L., Escobar, G. P., Dobrucki, L. W., Goshorn, D. K., Bouges, S., Mingoia, J. T., McClister, D. M., Jr., Su, H., Gannon, J., MacGillivray, C., Lee, R. T., Sinusas, A. J., and Spinale, F. G. (2006) *Am J Physiol Heart Circ Physiol* **290**, H232-239
94. Creemers, E. E., Davis, J. N., Parkhurst, A. M., Leenders, P., Dowdy, K. B., Hapke, E., Hauet, A. M., Escobar, P. G., Cleutjens, J. P., Smits, J. F., Daemen, M. J., Zile, M. R., and Spinale, F. G. (2003) *Am J Physiol Heart Circ Physiol* **284**, H364-371
95. Creemers, E. E., Cleutjens, J. P., Smits, J. F., and Daemen, M. J. (2001) *Circ Res* **89**, 201-210
96. Peterson, J. T., Li, H., Dillon, L., and Bryant, J. W. (2000) *Cardiovasc Res* **46**, 307-315
97. Yu, Q., and Stamenkovic, I. (2000) *Genes Dev* **14**, 163-176
98. Bowe, M. A., Mendis, D. B., and Fallon, J. R. (2000) *J Cell Biol* **148**, 801-810
99. Bi, Y., Stuelten, C. H., Kilts, T., Wadhwa, S., Iozzo, R. V., Robey, P. G., Chen, X. D., and Young, M. F. (2005) *J Biol Chem* **280**, 30481-30489
100. Tang, Y., Liu, Z., Zhao, L., Clemens, T. L., and Cao, X. (2008) *J Biol Chem* **283**, 23956-23963

101. Ebisawa, T., Fukuchi, M., Murakami, G., Chiba, T., Tanaka, K., Imamura, T., and Miyazono, K. (2001) *J Biol Chem* **276**, 12477-12480
102. Pepine, C. J. (1989) *Am J Cardiol* **64**, 2B-8B
103. Shimoni, S., Frangogiannis, N. G., Aggeli, C. J., Shan, K., Quinones, M. A., Espada, R., Letsou, G. V., Lawrie, G. M., Winters, W. L., Reardon, M. J., and Zoghbi, W. A. (2002) *Circulation* **106**, 950-956
104. Gersch, C., Dewald, O., Zoerlein, M., Michael, L. H., Entman, M. L., and Frangogiannis, N. G. (2002) *Histochem Cell Biol* **118**, 41-49
105. Frangogiannis, N. G., Smith, C. W., and Entman, M. L. (2002) *Cardiovasc Res* **53**, 31-47
106. Adams, M. E., Mueller, H. A., and Froehner, S. C. (2001) *J Cell Biol* **155**, 113-122
107. Barouch, L. A., Harrison, R. W., Skaf, M. W., Rosas, G. O., Cappola, T. P., Kobeissi, Z. A., Hobai, I. A., Lemmon, C. A., Burnett, A. L., O'Rourke, B., Rodriguez, E. R., Huang, P. L., Lima, J. A., Berkowitz, D. E., and Hare, J. M. (2002) *Nature* **416**, 337-339
108. Burger, D. E., Lu, X., Lei, M., Xiang, F. L., Hammoud, L., Jiang, M., Wang, H., Jones, D. L., Sims, S. M., and Feng, Q. (2009) *Circulation* **120**, 1345-1354
109. Shimizu-Hirota, R., Sasamura, H., Mifune, M., Nakaya, H., Kuroda, M., Hayashi, M., and Saruta, T. (2001) *J Am Soc Nephrol* **12**, 2609-2615

7 Ciriculum vitae

Der Lebenslauf ist in der Online-Version aus Gründen des Datenschutzes nicht enthalten.

The CV is not included in the online version, for reasons of data protection.

.

8 Original publications:

Deficiency of biglycan causes cardiac fibroblasts to differentiate into a myofibroblast phenotype Melchior-Becker A, Dai G, Ding Z, Schaefer L, Schrader J, Young MF and Fischer JW. ***J. Biol. Chem****. jbc.M110.192682. First Published on March 18, 2011,* [Epub ahead of print]

Inhibition of hyaluronan synthesis accelerates murine atherosclerosis: Novel insights into the role of hyaluronan synthesis. Nagy N, Freudenberger T, Melchior-Becker A, Röck K, Ter Braak M, Jastrow H, Kinzig M, Lucke S, Suvorava T, Kojda G, Weber A-A, Sörgel F, Levkau B, Ergün S, and Fischer JW ***Circulation*** 2010 Nov 30;122(22):2313-22

Transcriptional and posttranscriptional regulators of biglycan in cardiac fibroblasts.Tiede K, Melchior-Becker A, Fischer JW. ***Basic Res Cardiol.*** 2010 Jan;105(1):99-108. Epub 2009

Long-term treatment with the AT1-receptor antagonist telmisartan inhibits biglycan accumulation in murine atherosclerosis. Nagy N, Melchior-Becker A, Fischer JW. Basal ***Res Cardiol.*** 2010 Jan;105(1):29-38. Epub 2009

Small leucine-rich proteoglycans in atherosclerotic lesions: Novel targets of chronic statin treatment? Marzoll A, Melchior-Becker A, Cipollone F, Fischer JW. ***J Cell Mol Med.*** 2009 Dec 8. [Epub ahead of print]

Biglycan is required for adaptive remodelling after myocardial infarction; Westermann D*, Mersmann J*, Melchior A*, Freudenberger T*, Petrik C, Schaefer L, Lüllmann-Rauch R, Lettau O, Jacoby C, Schrader J,Brand-Herrmann SM, Young MF, Schultheiss HP, Levkau B, Baba HA, Unger T, Zacharowski K, Tschöpe C, Fischer JW. ***Circulation***. 2008 Mar 11;117(10):1269-76. * shared first authorship

Effects of fibroblast extracellular matrix calcification on platelet adhesion in vitro. Kwiatkowski JN, Melchior A, Endt-Knauer H, Schrör K, Fischer JW, Weber AA. ***Platelets***. 2008 Sep;19(6):467-70.

Chronic ultraviolet B irradiation causes loss of hyaluronic acid from mouse dermis because of down-regulation of hyaluronic acid synthases. Dai G, Freudenberger T, Zipper P, Melchior A, Grether-Beck S, Rabausch B, de Groot J, Twarock S, Hanenberg H, Homey B, Krutmann J, Reifenberger J, Fischer JW. ***Am J Pathol.*** 2007 Nov;171(5):1451-61.

Published abstracts:

Melchior-Becker A, Schäfer L, Fischer JW Mice Double-Deficient for Apolipoprotein E and Biglycan Show Enhanced Atherosclerosis on Normal Chow ***Circulation***. 2010; 122:A15387

Melchior A., Fischer J.W., Biglycan plays a key role in cardiac remodelling; In: ***Hämostasiologie*** 2008; 28: 1-98; A24

Westermann D, Mersmann, Melchior A, Freudenberger T, Petrik C, Lüllmann-Rauch R, Young MF, Levkau B, Baba H, Unger Th, Zacharowski K, Tschöpe C, Fischer JW. Cardiac dysfunction and decreased survival of biglycan-deficient mice after myocardial infarction; In: *Naunyn-**Schmiedeberg's Archieves of Pharmacology*** Volume 375 Supplement 1 March 2007; 295 p.63

Westermann D., Mersmann J., Melchior A., Young M.F., Levkau B., Baba H., Unger T., Zacharowski K., Tschöpe C., Fischer J.W. Impaired cardiac function and decreased survival of biglycan deficient mice after myocardial infarction; In: ***Hämostasiologie*** 2007;27 (1-84) FV78

Kwiatkowski JN, Melchior A, Endt-Knauer H, Censarek P., Fischer JW, Schrör K, Weber AA. Effects of extracellular matrix calcification on platelets adhesion under flow conditions; In: ***Hämostasiologie*** 2007; 27 (1-84) P066

Westermann D., Mersmann J., Petrik C., Melchior A., Lüllmann Rauch R.; Young MF; Levkau B; Baba H; Zacharowski K; Unger T; Tschöpe C; Fischer JW: Biglycan is Required for Adaptive Remodelling After Myocardial Infarction In: ***Circulation***. 2006;114:II 175-II 176.

Awards:

12/2010	Sientific scholarship from “Der herzkranke Diabetiker” Foundation, Berlin, Germany
10/2007	Posteraward Joint-Symposium of the SFB 612, GRK 1089 (Düsseldorf) and SFB 688 (Würzburg); Düsseldorf, Germany
7/2008	Posteraward at the 13th Gordon Research Conference on Proteoglycans; Andover New Hamshire, USA

9 Acknowledgement

First and foremost, I would like to thank my supervisor Prof. Dr. rer. nat. Jens W. Fischer for his ongoing support and encouragement during the last years. I was very fortunate to have had a supervisor who gave me freedom to explore my own ideas and at the same time the guidance to keep me on course. But I am also grateful for the opportunities to expire science in his Lab and in the scientific community by visiting national and international meetings. I also like to thank for his trust in my skills and my ideas.
I thank Dr. Marian Young for encouraging words and for my mice.
I really owe these mice a lot, giving really everything to expand our knowledge. I learned and expired a lot just by working with these mice! Thanks!
I'd like to acknowledge Dr. Xaoping Ding (Institut für Herz- Kreislaufphysiologie, Heinrich-Heine-Universität Düsseldorf) for the experimental MI.
I am grateful to my friends at the lab, it was a great time, even when it wasn't.
A very special warm thank you to my "Nurse Betty"! Betty for all the hugs, the songs, the fun, the help with writing, for proofreading, genotyping but most of all for keeping my faith, thanks a lot!
I'd like to thank Dr. Nadine Nagy, you became a friend that I don't ever want to miss again, thanks for keeping me swimming when the water got troubled, for getting me laugh when everything was a reason to cry, thanks for being such an honest friend.
I'd like to thank Dr. Andrea Marzoll for her friendship and all the fun and most of all for her support. Thanks to Dr. Berit Rabausch we had a great time in Wiesbaden and I often miss your open heart.
I'd like to thank Dr. Sören Twarock, for sharing his exhaustless knowledge.
I'd like to thank Dr. Gernot Kaber for tremendous discussions over a late night beer.
I thank Dr. Guang Dai for a good time and his help with the overexpression, guess there will never be two dancing elephants in the institute again.
Thanks to Dr. Till Freudenberger for proofreading this thesis and for sharing friendly times on congresses and at the bench.
I thank Katharina Röck and Julia Müller for being my dancing and singing cheers.
Dr. Maria Grandoch, Dr. Michael Ter Braak for the nice working atmosphere and their patience with my explanations, their help on FACS and so many nice conversations.
Dr. Christian Niedworok, I think every lab needs a pirate-postdoc and I really did.
Erika Lohmann, Karin Montag and Gertrud Sieberg for their help and for their protecting assistance with the FAX!
I thank all the technicians that worked hard to help and to support.
Peggy Marra-Mann for her friendship and her help, sometimes I would have been drowning without your help.
I am grateful to my cookie Annika Zimmermann for a special friendship and the wigging. Hey but I'd tried to improve!
Dori Doro for being my breakfast buddy! Barbara, Sylvie, Annette, Kirsten, Sabine, Monika and Tanja … this is definitely the best birdcage and you made work feel like home.
I thank the whole GRK 1089 for teaching and supporting and encouraging, as I learned a lot being a part of a great teaching structure.
I'd like to thank my parents, thanks for your love, your support and thanks for giving me wings to fly.
I'd like to thank my parents in law for their love and their support.
I have to thank my husband Kai for his imperturbable overwhelming love, his unbreakable faith in me and his patience as I know it's never easy with me.
Last but not least I am grateful to my beloved Mighty as I would not have come this far, if he hadn't been there.

10 Affidavit

Hiermit erkläre ich, gem. §6 Abs. 2, Nr. 8 der Promotionsordnung der Math.-Nat.- Fachbereiche
zur Erlangung der Dr. rer. nat., dass ich das Arbeitgebiet, dem das Thema ”Molecular and functional characterization of biglycan during pathologic cardiac remodelling” zuzuordnen ist, in Forschung und Lehre vertrete und den Antrag von Frau Ariane Melchior-Becker befürworte.

Datum Prof. Dr. rer. Nat. J.W. Fischer

Hiermit erkläre ich, gem. §6 Abs. 2, Nr. 6 der Promotionsordnung der Math.-Nat.- Fachbereiche zur Erlangung des Dr. rer. nat., dass ich die vorliegende Dissertation selbstständig verfasst und mich keiner anderen als der angegebenen Hilfsmittel bedient habe.

Datum Ariane Melchior-Becker

Hiermit erkläre ich, gem. §6 Abs. 2, Nr. 7 der Promotionsordnung der Math.-Nat.- Fachbereiche zur Erlangung des Dr. rer. nat., dass ich keine anderen Promotionen bzw. Promotionsversuche in der Vergangenheit durchgeführt habe und dass diese Arbeit von keiner anderen Fakultät abgelehnt worden ist.

Datum Ariane Melchior-Becker